4 FIELD INSPECTION AND DATA ANALYSES

This chapter presents the inspection data for 20 bridges that were built between 1997 and 2001. Section 4.1 presents the list of bridges and the data collection procedure. Data includes crack orientation, length, and width. In addition, Section 4.2 presents the method for processing the collected inspection data that will be used in Section 4.3. Section 4.3 includes analysis of the effect of bridge geometry, and parameters related to design on early-age bridge deck cracking including skew, span type, year built, ADTT, girder type, and inspected lane-span length. Finally, Section 4.4 presents the conclusions made on analysis results.

4.1 FIELD INSPECTION

Twenty existing bridges were randomly selected throughout the state to be included in this task of inspection. In all cases, the deck was at most of five years of age. The purpose was to document the extent of early-age deck cracking. This list was then approved by MDOT and is shown in Table 4-1. All 20 bridges have been inspected.

A sample inspection data sheet is included due to the volume of raw data sheets. Compiled inspection raw data for all the bridges is given in Appendix B. The inspection data obtained for Bridge (S04-82062) in the Metro region is shown in Figure 4-1. Cracks are marked on the sheet as lines. The length and the width are noted along the crack line. Pictures taken of the deck are marked on the inspection sheet. The picture number is given within brackets with an arrow showing the direction from which the picture was taken. Some selected pictures of the inspected bridge deck are shown in Figure 4-2. The bridge carries Scotten over US-12. This deck was placed in 2000, thus is 3 years old. The inspection data shows that there is significant cracking.

Table 4-1. List of Bridge Decks Inspected

Bridge ID	Year Built	Facility Carried	Features Intersected	ADT
S19 of 82023	1997	14th St.	I-94	9172
S11 of 82025	1997	Harper Av.	I-94	9250
S01 of 82111	1997	Monroe Av.	I-375	1000
S09 of 82252	1997	State Fair Av.	I-75	10960
B01 of 06071	1998	M-13	Saganning Creek	6400
B02 of 06071	1998	M-13	S BR Pine River	6400
S27 of 41064	1998	M-6 EB	M-37	16500
S28 of 41064	1998	M-6 WB	M-37	14900
S06 of 82025	1999	Barrett	I-94	1500
S03 of 63022	1999	South Hill Rd	I-96	700
S15 of 25032	1999	M-57	I-75	45000
B01 of 44012	1999	M-24	S BR Flint River	16020
B03 of 73031	2000	M-52	N BR Bad River	14000
S17 of 82112	2000	Oakman	M-10	15170
S04 of 82062	2000	Scotten	US-12	13000
S03 of 82024	2000	Woodward	I-94	16000
S03 of 82192	2001	Fern	M-39	7500
S06 of 82192	2001	Village	M-39	4500
B02 of 64012	2001	US-31 BR	N.BR. Pentwater R.	2278
B03 of 64012	2001	US-31 BR	Bass Lake Creek	3500

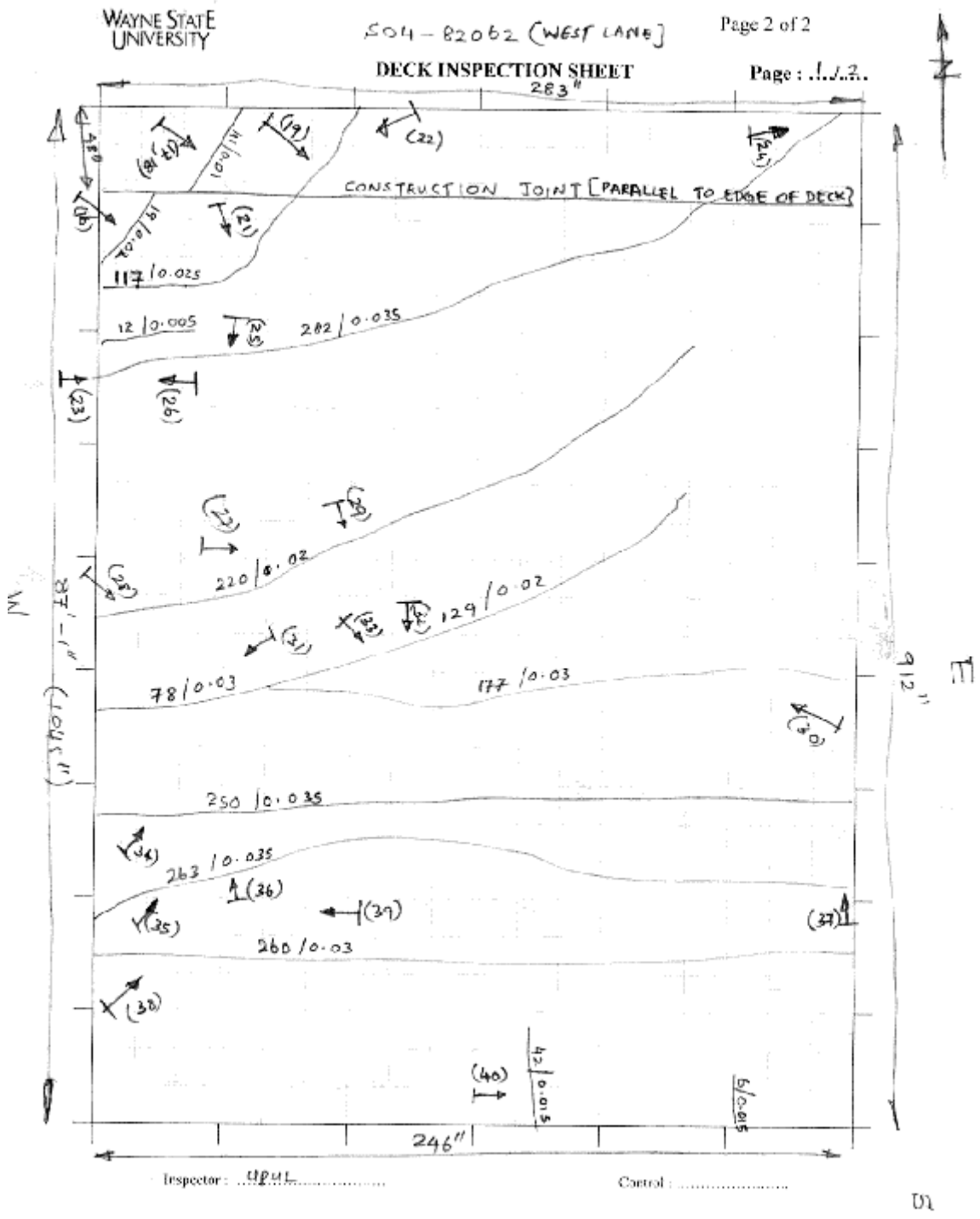

Figure 4-1. Deck inspection template example with sample inspection data

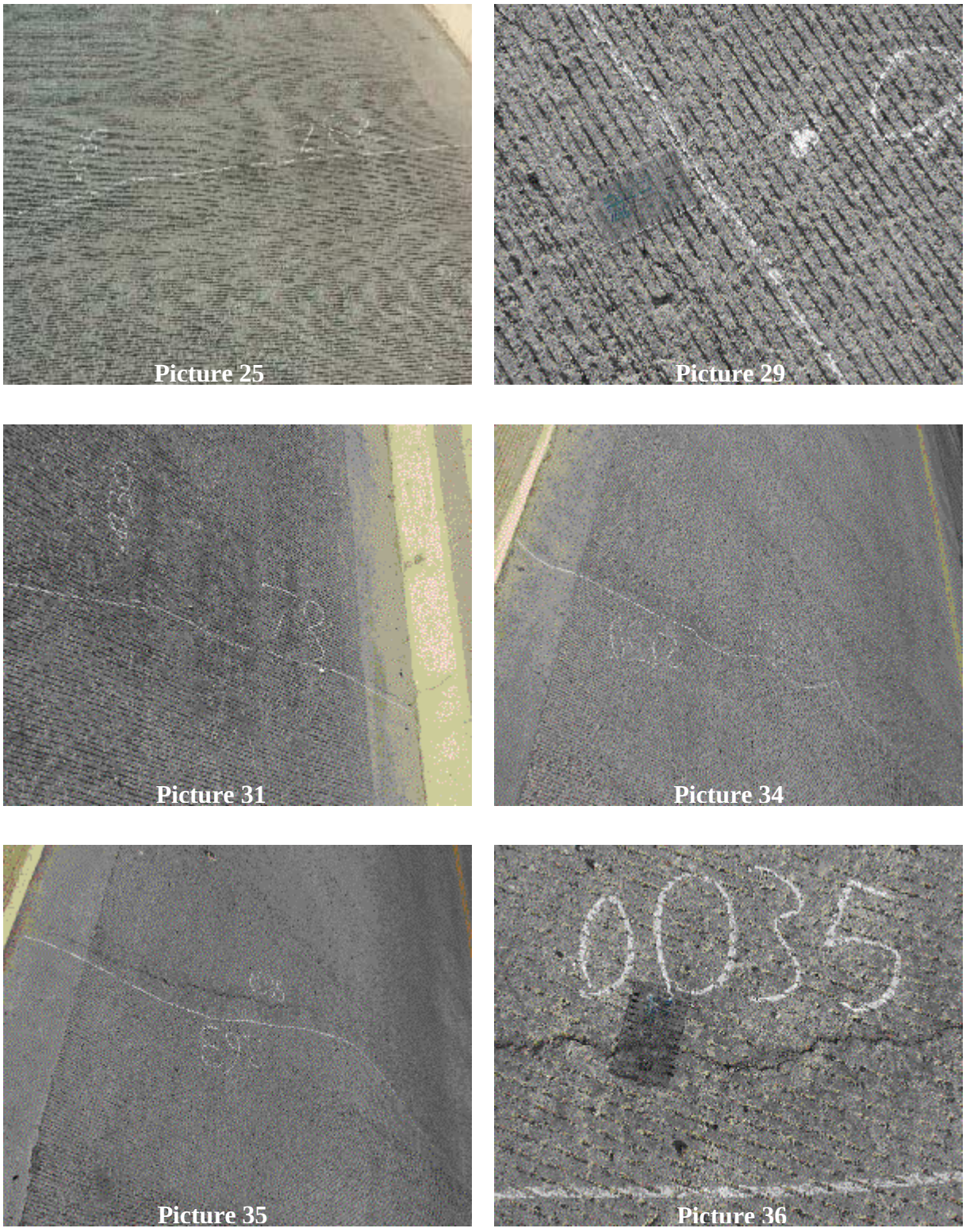

Figure 4-2. Selected photos taken during the deck inspection

4.2 INSPECTION DATA PROCESSING STEPS

From the inspection data sheet, the crack orientation can be categorized into four groups.

1. Longitudinal cracks: cracks that are predominantly parallel to the traffic direction.
2. Transverse cracks: cracks that are predominantly perpendicular to the traffic direction.
3. Diagonal cracks: cracks that are not transverse or longitudinal cracks.
4. Map cracking: a series of cracks that extend only into the upper surface of the deck.

The crack density of groups 1, 2, and 3 was calculated by dividing the sum of the lengths of the cracks for each group by the area of the inspected bridge lane-span. The crack density of group 4, map cracking, was calculated by dividing the sum of cracked area by the area of the inspected bridge lane-span. Table 4-2 summarizes the crack density of each crack group for the 20 inspected bridges and the following controlling parameters: bridge skew, span type, year built, girder type, the inspected lane-span length, and slab thickness.

In order to study the relationship between the crack density and the controlling factors mentioned above, the crack density histogram of groups 1, 2, and 3 is calculated first. Figure 4-3, Figure 4-4, and Figure 4-5 show the crack density histogram for longitudinal, transverse, and diagonal cracks respectively. The map crack density for 14 out of the 20 bridge decks is equal to zero.

In order to have a continuous longitudinal crack density histogram, the last 3 extreme values in Figure 4-3 (3 bridges) are deleted as shown in Figure 4-6. For the transverse deck cracking histogram to be continuous, just one bridge is excluded from the analysis as shown in Figure 4-7. The analysis will consider all the diagonal crack density data, since the histogram is continuous.

Table 4-2. Deck Crack Density of the Inspected Bridges and Controlling Parameters

Bridge ID	Longitudinal crack density (in/in^2)	Transverse crack density (in/in^2)	Diagonal crack density (in/in^2)	Map crack density (in^2/in^2)	Span length (ft)	Span type	Girder type	Slab thickness (in)	Year built	Skew angle (deg)
S01 of 82111	1.37E-02	4.84E-03	1.86E-03	0	27.43	Simple	Spread Box	8.5	1997	5
S09 of 82252	2.51E-02	2.68E-03	2.79E-03	0.11251	24.75	Continuous	Steel	9	1997	0
S11 of 82025	1.70E-02	0.00E+00	7.98E-03	0.002199	39	Simple	Steel	8	1997	50
S19 of 82023	5.00E-02	4.90E-04	2.79E-04	0.059583	28.08	Simple	Steel	8	1997	0
B01 of 06071	1.06E-02	0.00E+00	0.00E+00	0	25	Continuous*	Adj Box	6	1998	0
B02 of 06071	1.13E-02	1.19E-03	0.00E+00	0	32	Continuous	Steel	8	1998	0
S27 of 41064	4.13E-04	0.00E+00	0.00E+00	0	131.56	Simple	PCI	9	1998	19
S28 of 41064	1.88E-03	4.91E-04	6.84E-04	0	131.56	Simple	PCI	9	1998	19
B01 of 44012	6.19E-03	4.92E-03	5.88E-04	0	64.99	Simple	Steel	9	1999	0
S03 of 63022	7.99E-03	3.12E-04	0.00E+00	0	112.5	Simple	Adj Box	6	1999	24
S06 of 82025	5.23E-03	0.00E+00	8.73E-04	0.000245	30.92	Simple	Steel	9	1999	13
S15 of 25032	5.03E-02	2.35E-02	1.43E-02	0	32.81	Simple	Adj Box	6	1999	0
B03 of 73031	3.31E-03	6.66E-03	2.70E-04	0	50	Simple	PCI	8	2000	0
S03 of 82024	5.16E-02	4.39E-03	4.22E-03	0	63.67	Continuous*	Spread Box	9	2000	6
S04 of 82062	2.82E-03	4.36E-03	2.13E-03	0.000661	62.5	Continuous	Steel	8	2000	28
S17 of 82112	1.80E-03	6.47E-03	8.70E-04	0	73.95	Continuous	Steel	9	2000	22
B02 of 64012	3.44E-03	8.14E-04	0.00E+00	0	49	Simple	Spread Box	9	2001	18
B03 of 64012	8.22E-04	0.00E+00	0.00E+00	0	50.98	Simple	Adj Box	6	2001	0
S03 of 82192	6.69E-03	0.00E+00	7.27E-05	0	38	Simple	Steel	9	2001	0
S06 of 82192	1.66E-03	1.02E-04	0.00E+00	0.002839	29.5	Simple	Steel	9	2001	0

* - Simple span with continuous deck

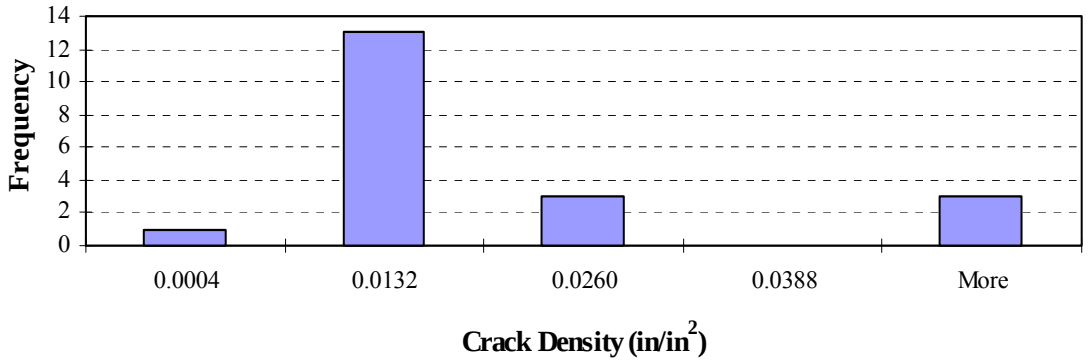

Figure 4-3. Longitudinal crack density histogram (20 Bridges)

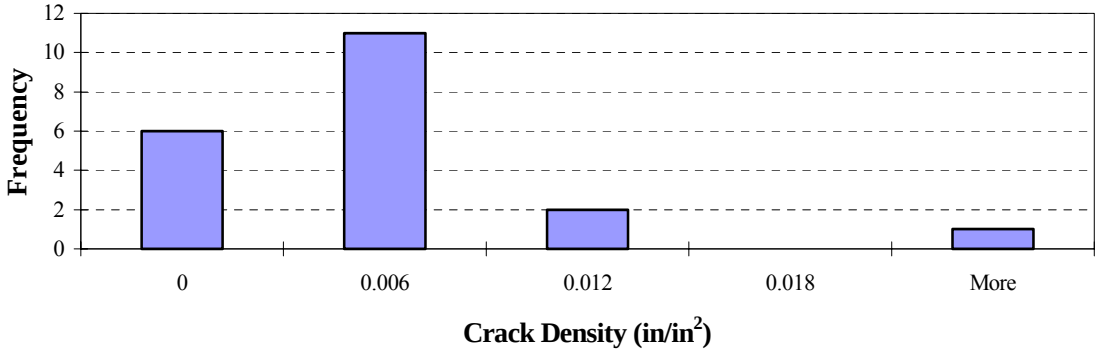

Figure 4-4. Transverse crack density histogram (20 Bridges)

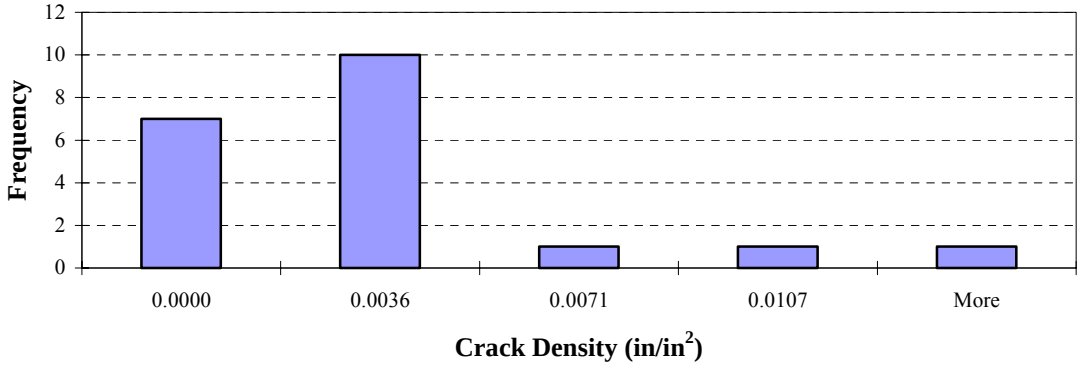

Figure 4-5. Diagonal crack density histogram (20 bridges)

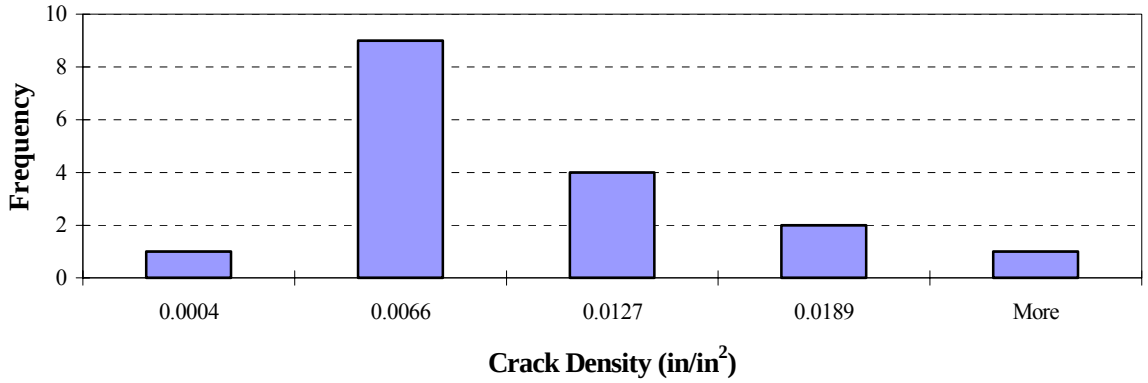

Figure 4-6. Modified longitudinal crack density histogram (17 Bridges)

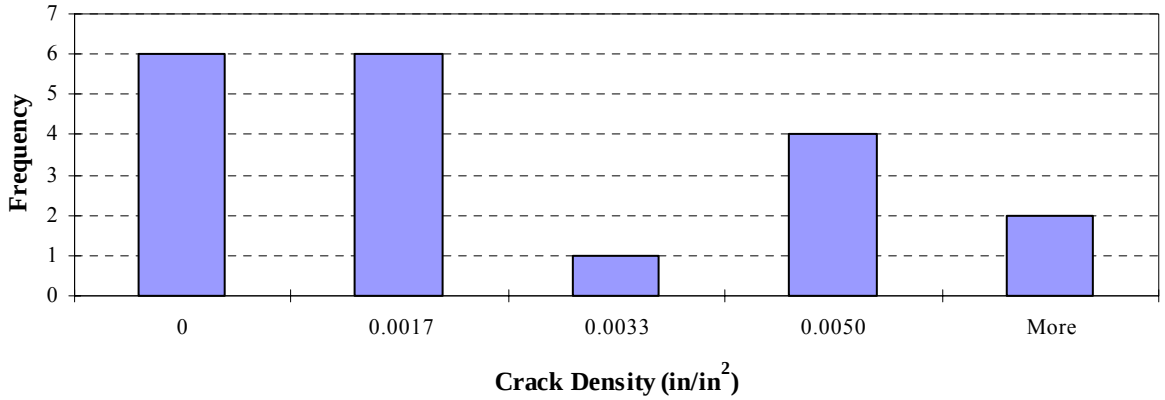

Figure 4-7. Modified transverse crack density histogram (19 Bridges)

4.3 BRIDGE GEOMETRY AND DESIGN EFFECT ON DECK CRACKING

4.3.1 Longitudinal Cracks and Controlling Factors

4.3.1.1 Level I

At this level, only one controlling factor is considered each time in the analysis of the longitudinal crack data. Figure 4-8 through Figure 4-12 show the relationship between the crack density and each of the following parameters: bridge design type, girder type, bridge skew, slab thickness, year built, and the inspected lane-span length.

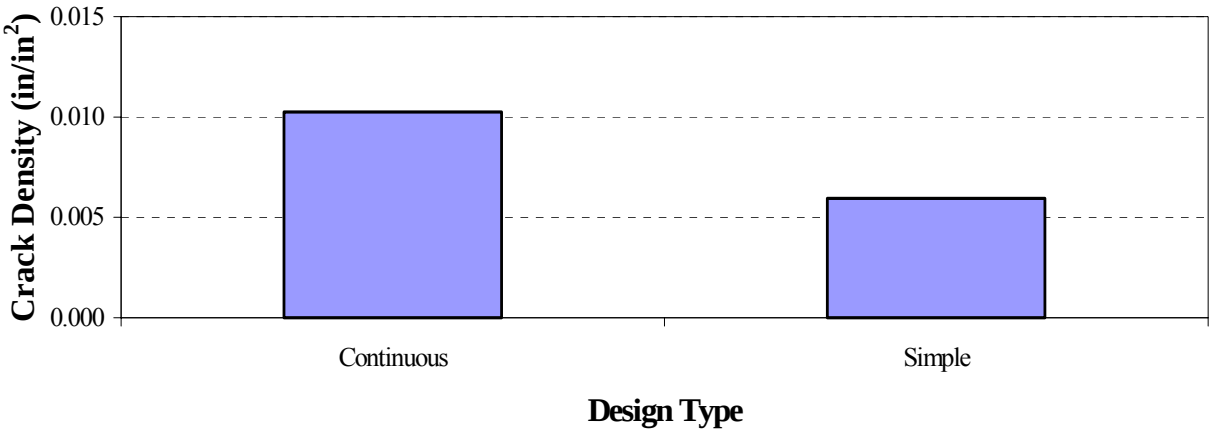

Figure 4-8. Beam structural type vs longitudinal crack density

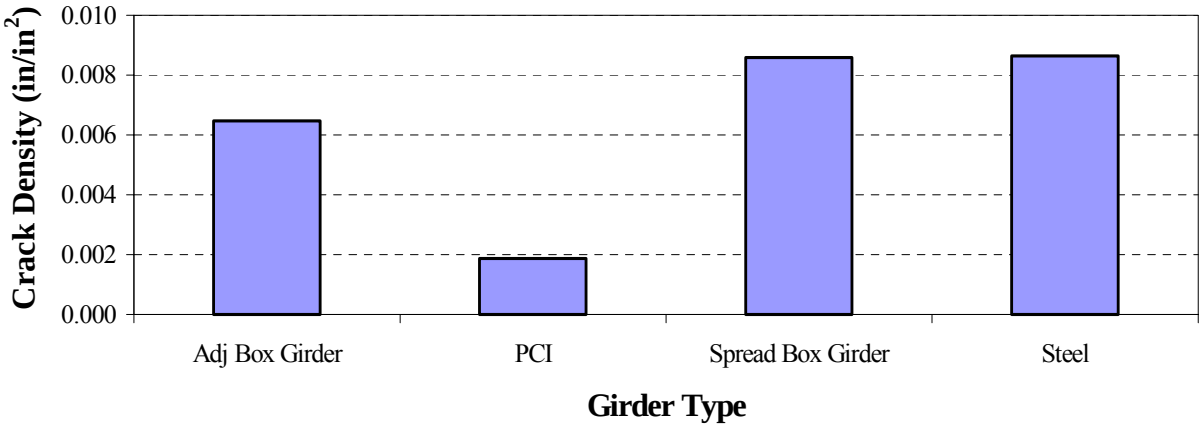

Figure 4-9. Girder type vs longitudinal crack density

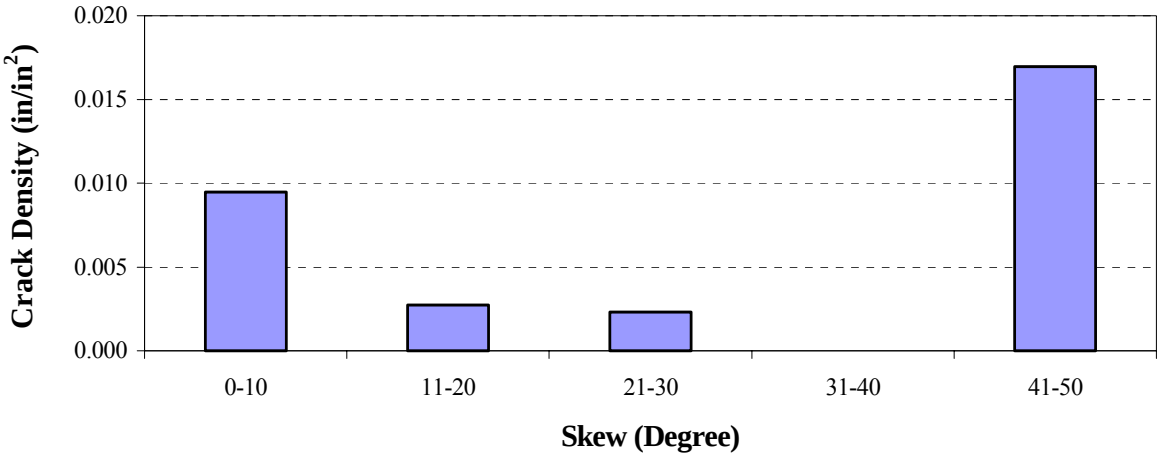

Figure 4-10. Bridge skew vs longitudinal crack density

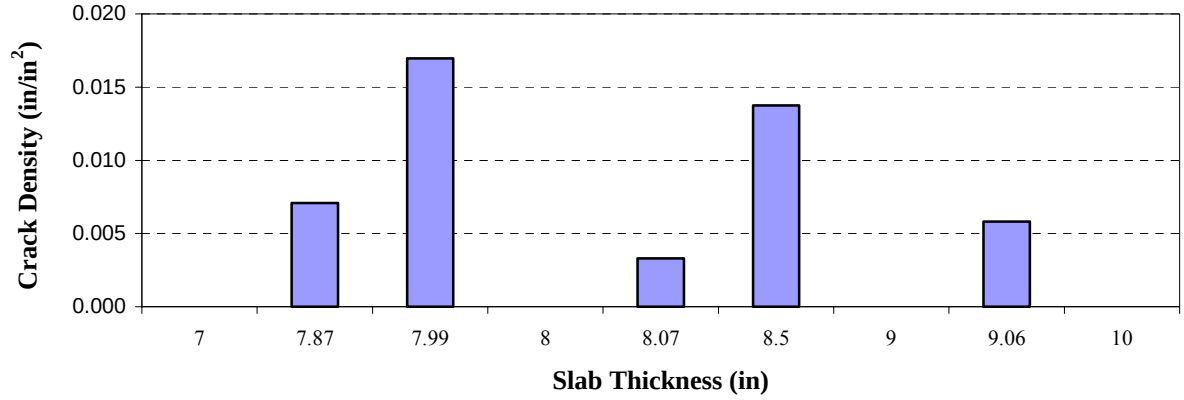

Figure 4-11. Slab thickness vs longitudinal crack density

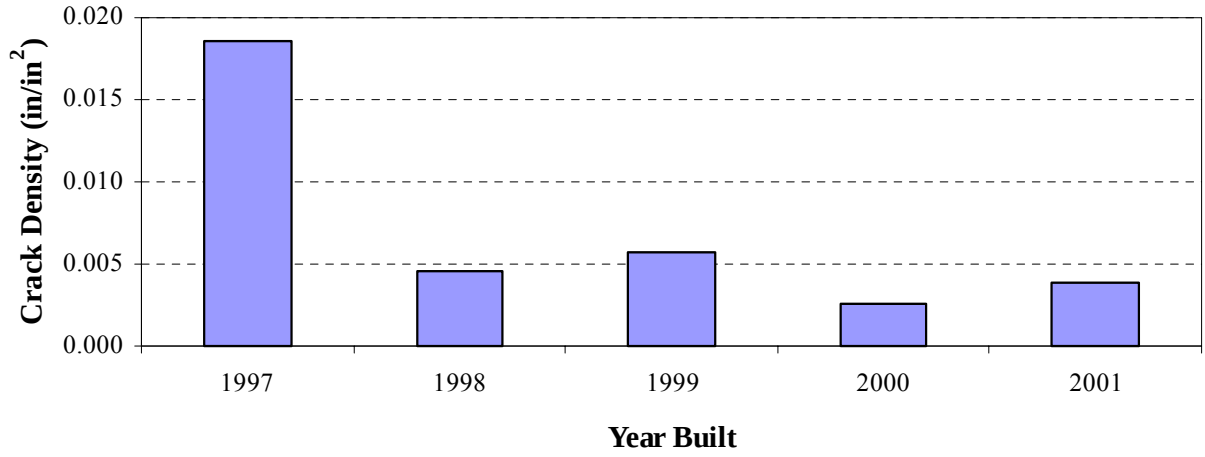

Figure 4-12. Year built vs longitudinal crack density

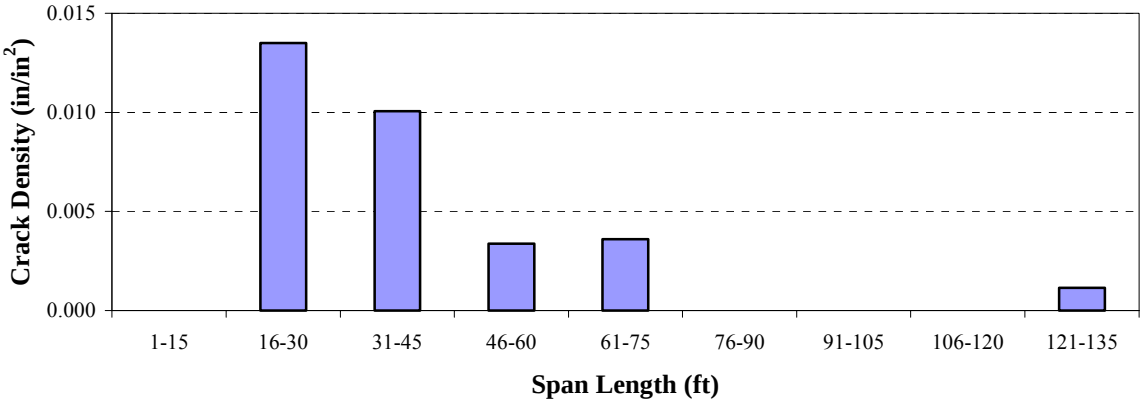

Figure 4-13. Inspected span length vs longitudinal deck cracking

4.3.1.2 Level II

At this level, two controlling factors are considered in the analysis of the longitudinal cracks. Figure 4-14 shows that multi-span continuous steel bridge decks crack more than simple span steel bridge decks. Figure 4-15 shows the relation between the longitudinal crack and the girder type for simple span bridges.

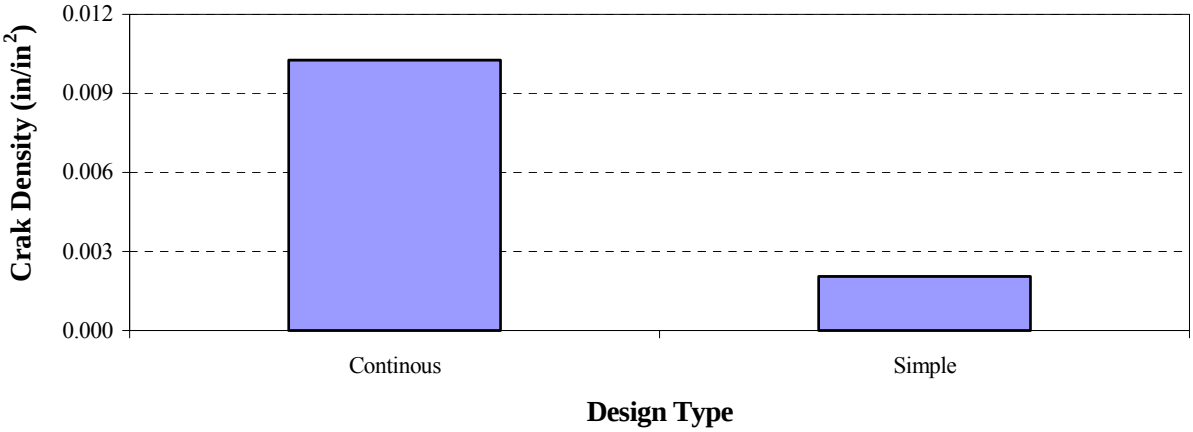

Figure 4-14. Structural type vs longitudinal crack density in steel bridges

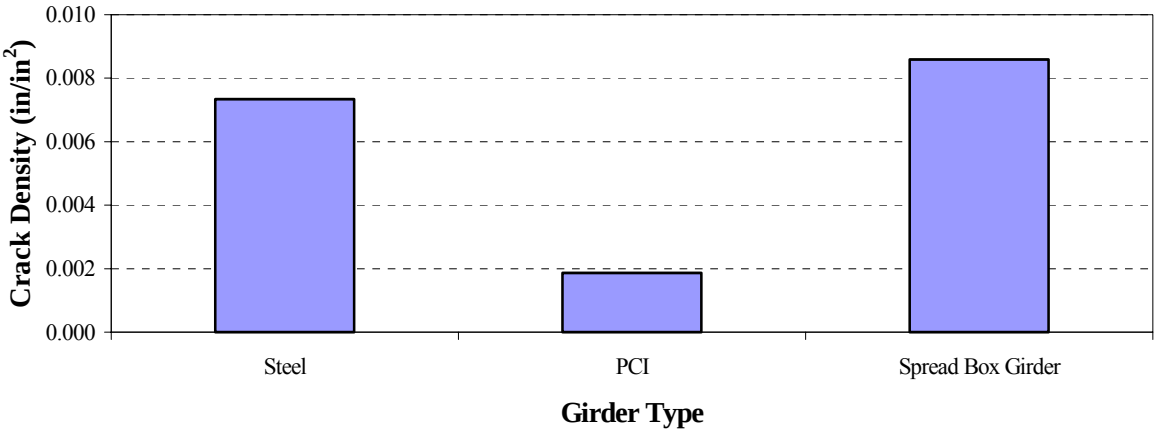

Figure 4-15. Girder type vs longitudinal crack density for simple span bridges

4.3.2 Transverse and Diagonal Cracks and Controlling Factors

4.3.2.1 Level I

At this level, only one controlling factor is considered each time in the analysis of the transverse and diagonal crack data. Figure 4-16 through Figure 4-21 show the relationship between the crack density and each of the following parameters: bridge design type, girder type, bridge skew, slab thickness, year built, and the inspected lane-span length.

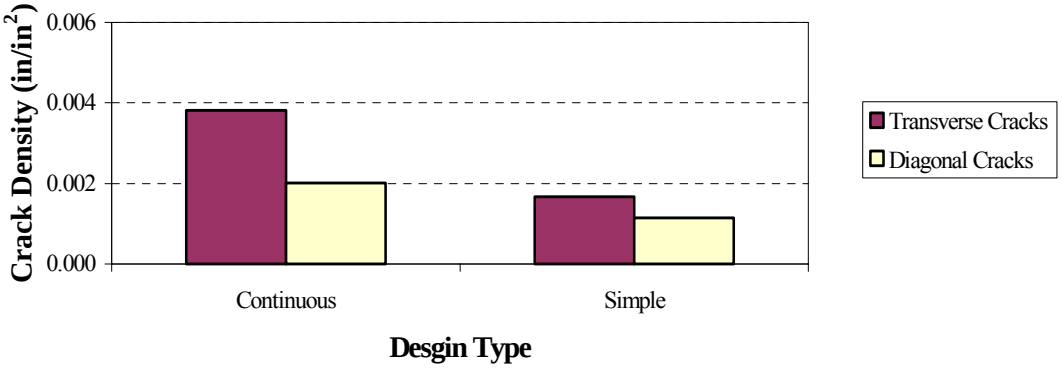

Figure 4-16. Beam structural type vs crack density

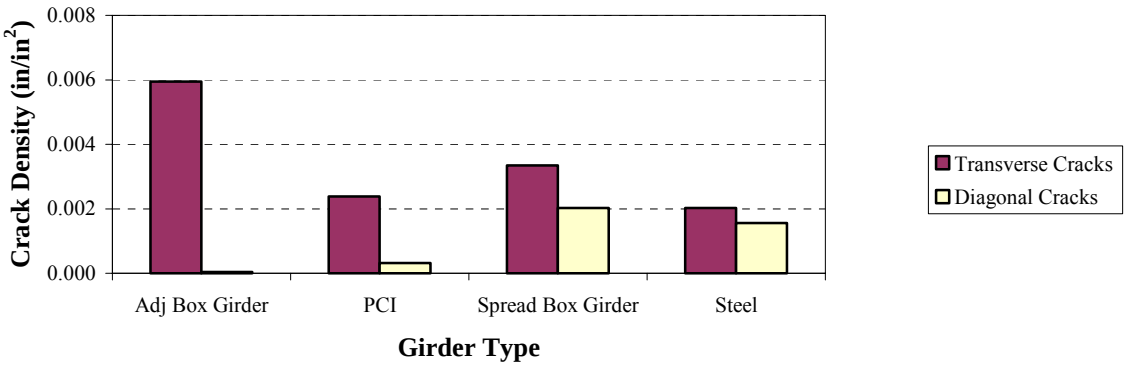

Figure 4-17. Girder type vs crack density

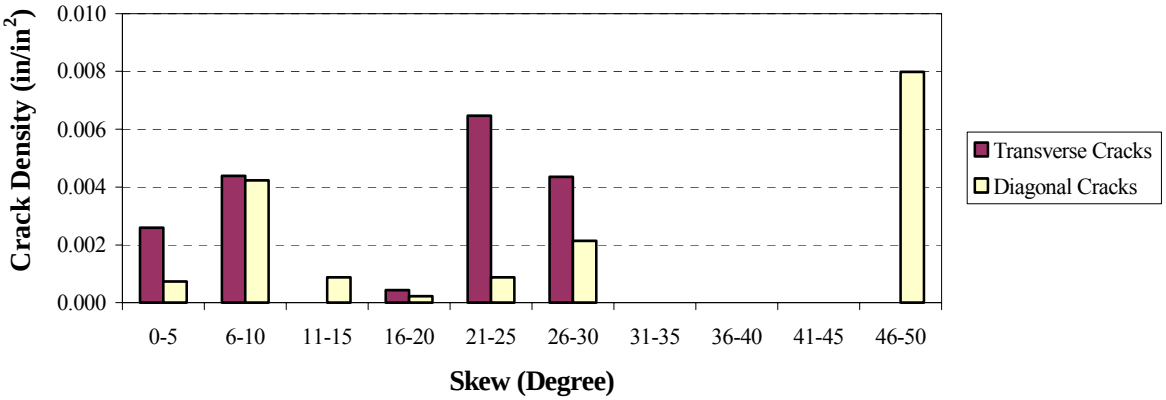

Figure 4-18. Bridge skew vs deck crack density

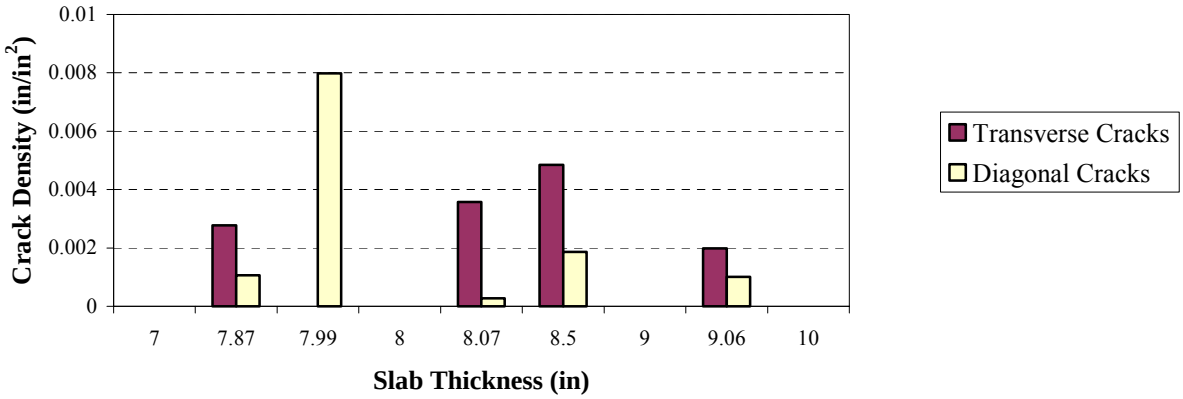

Figure 4-19. Slab thickness vs crack density

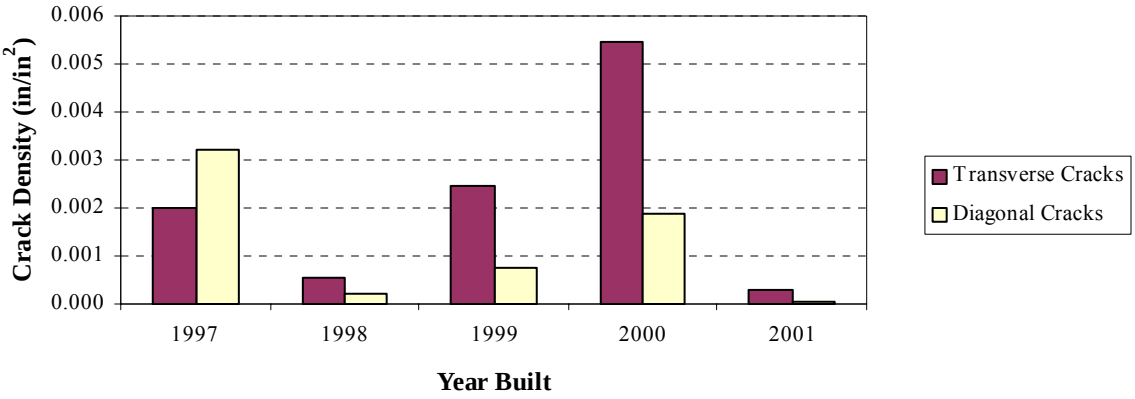

Figure 4-20. Year built vs crack density

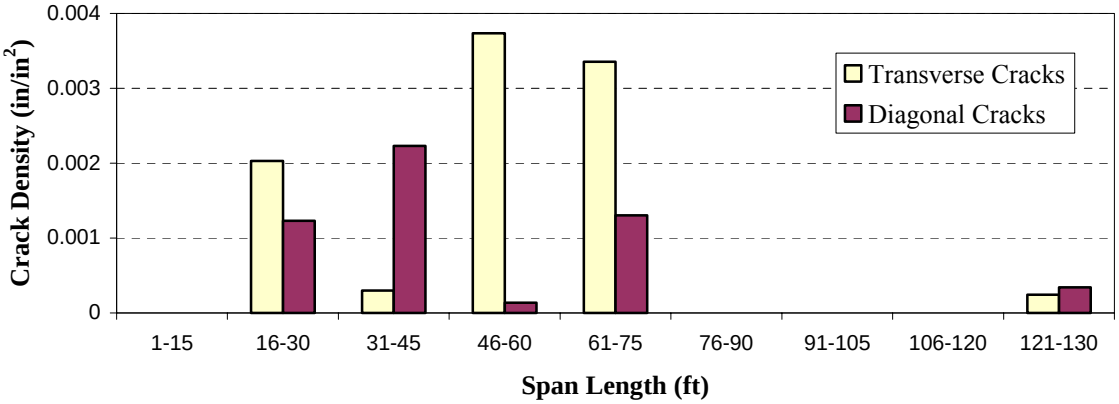

Figure 4-21. Inspected span length vs crack density

4.3.2.2 Level II

At this level, two controlling factors are considered in the analysis of the transverse and diagonal cracks. Figure 4-22 shows that multi-span continuous steel bridges crack more than simple span steel bridges. Figure 4-23 and Figure 4-24 show the relationship between the longitudinal crack density and the girder type for simple span bridges and multi span continuous bridges.

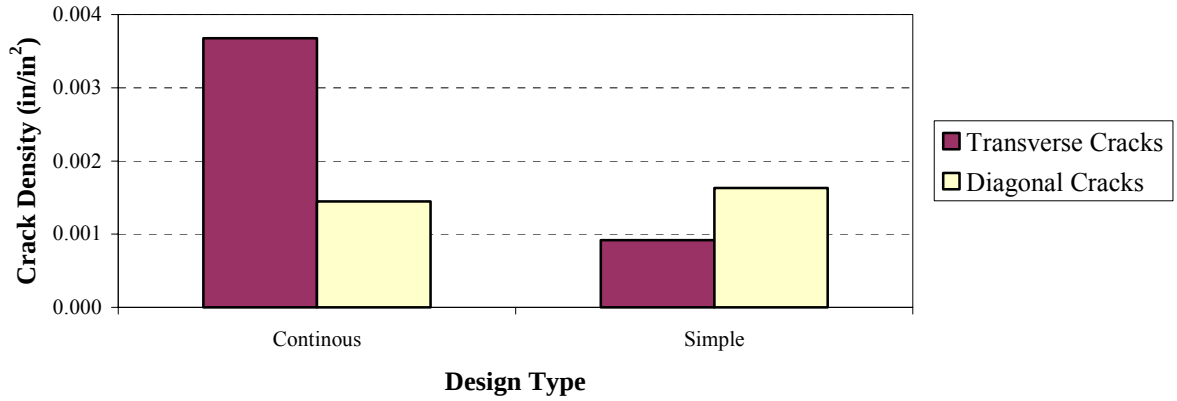

Figure 4-22. Structural type vs crack density in steel bridge

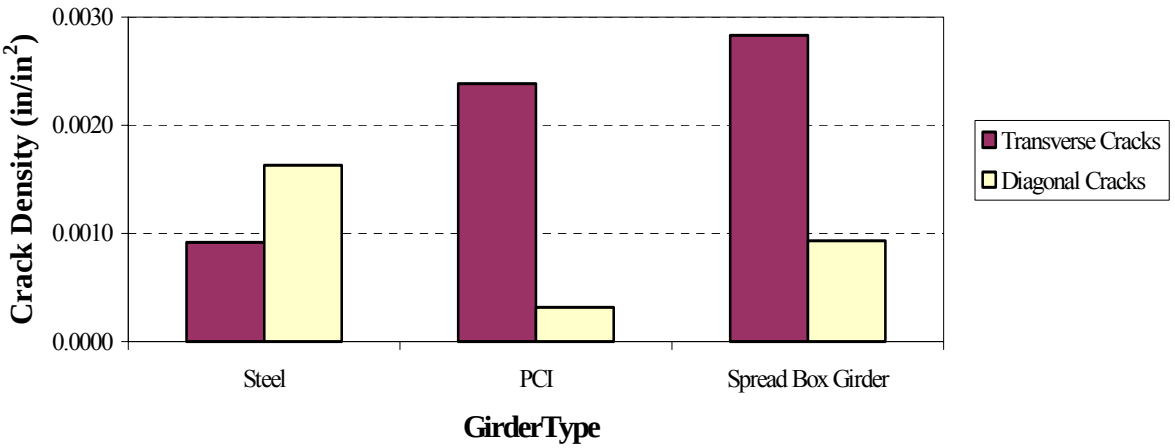

Figure 4-23. Girder type vs crack density for simple span bridges

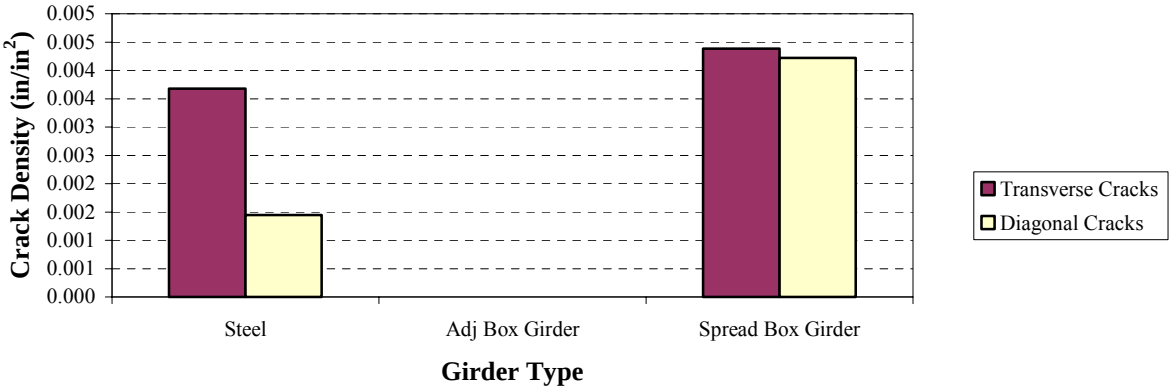

Figure 4-24. Girder type vs crack density for continuous bridges

4.3.3 Map Cracks and Controlling Factors

Figure 4-25 through Figure 4-30 shows the relationship between the map crack density and each of the following parameters: bridge design type, girder type, bridge skew, slab thickness, year built, and the inspected lane-span length.

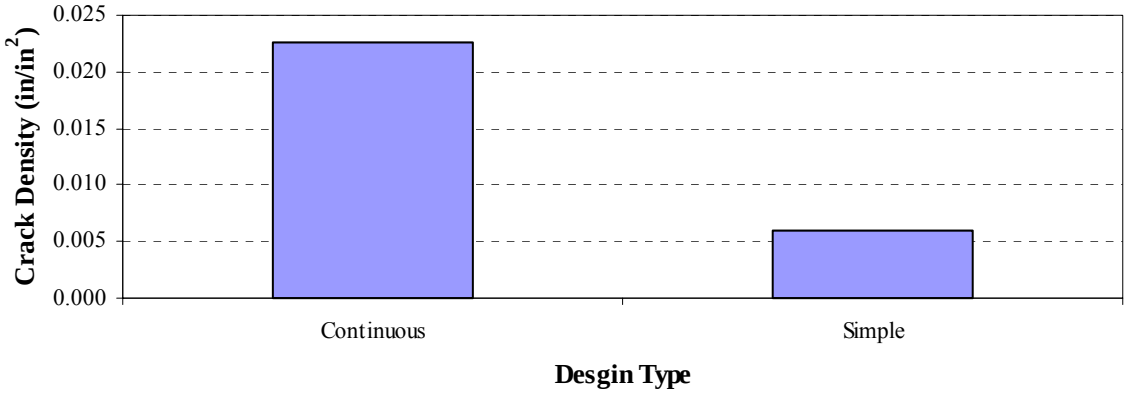

Figure 4-25. Beam structural type vs map crack density

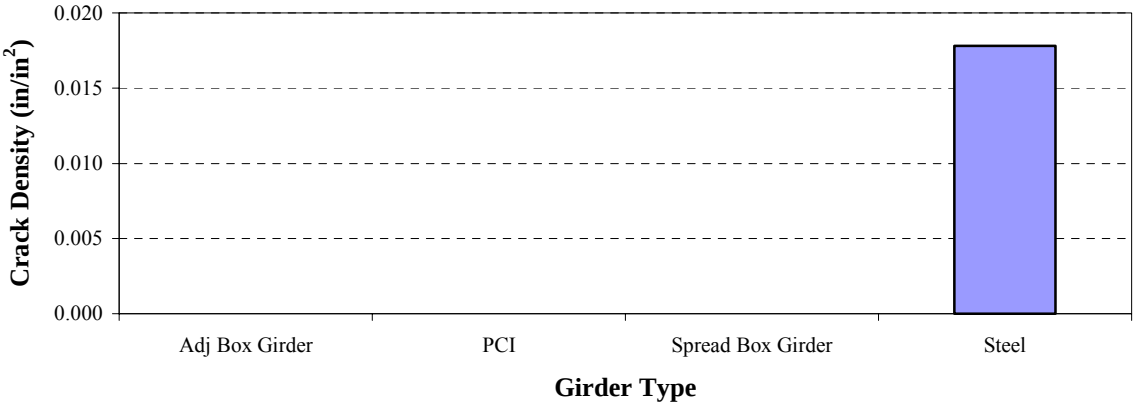

Figure 4-26. Girder type vs map crack density

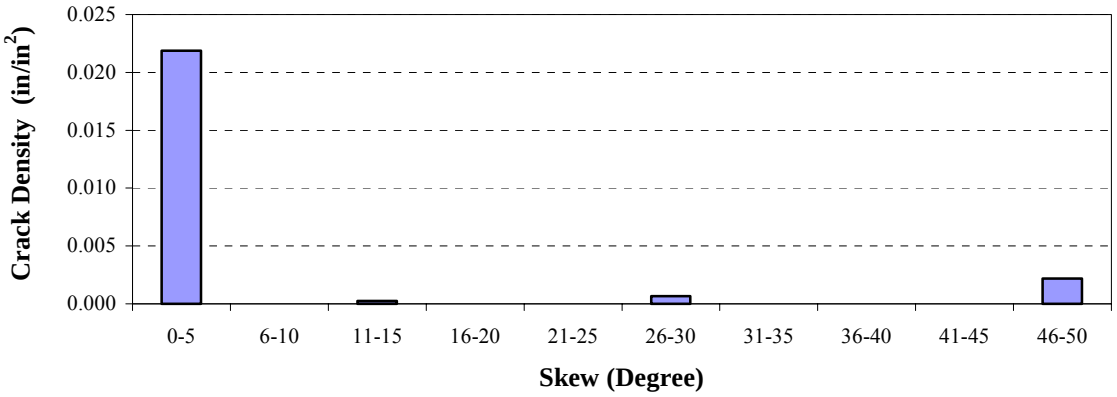

Figure 4-27. Bridge skew vs map crack density

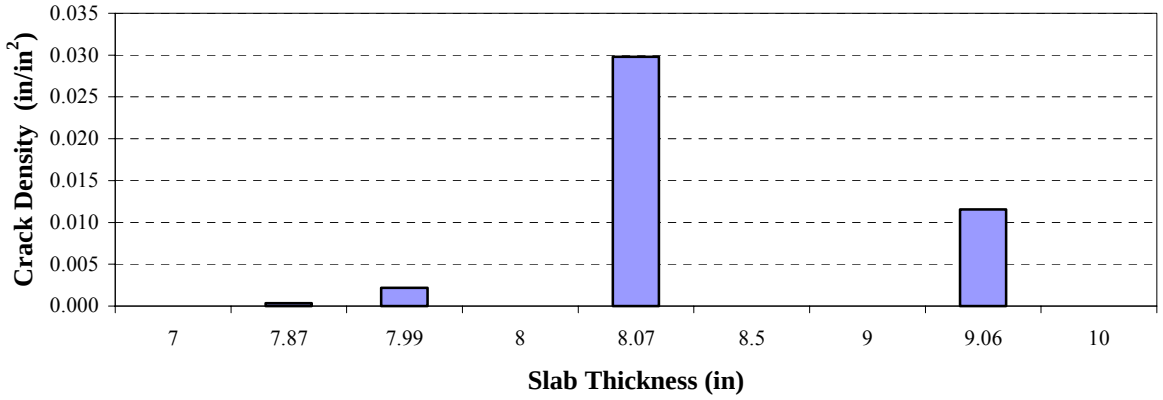

Figure 4-28. Slab thickness vs map crack density

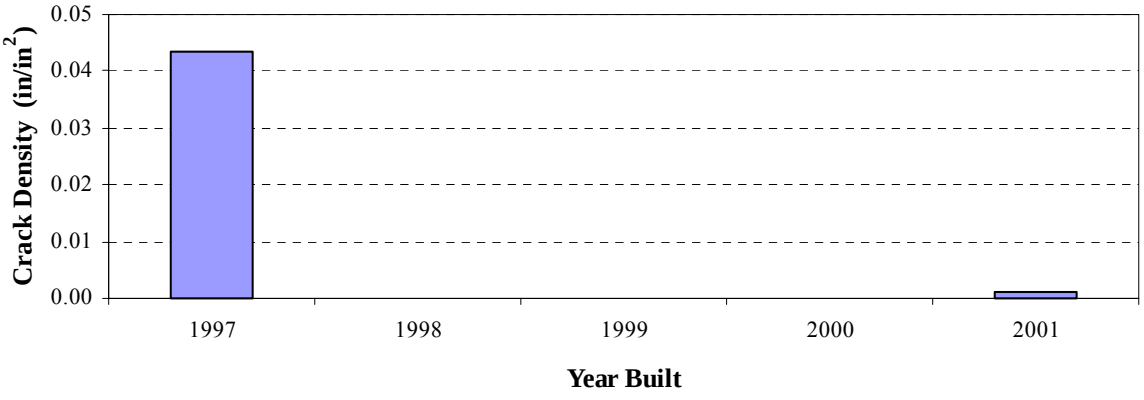

Figure 4-29. Year built vs map crack density

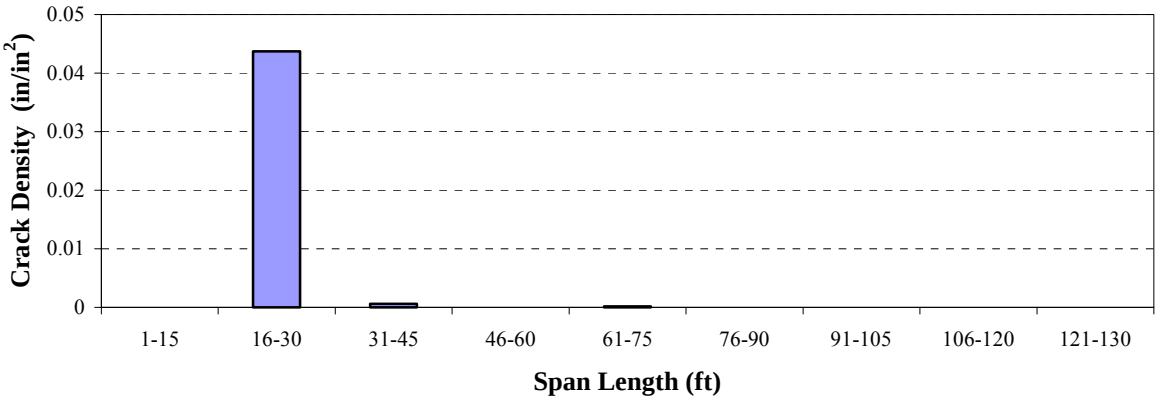

Figure 4-30. Inspected span length vs map crack density

4.3.4 ADTT Effect on Bridge Deck Cracking

Table 4-3 summarizes the ADTT and the crack density for each group. The ADTT data is collected from the MDOT 2001 annual report for the bridges located on the main trunk lines. Figure 4-31 to Figure 4-33 show the relationship between each crack density type and ADTT including the adjacent box girder bridges.

Table 4-3. ADTT and Crack Density Data for the Inspected Bridges

Bridge ID	MDOT ADTT	Longitudinal Cracks	Transverse Cracks	Diagonal Cracks	Map Cracking
B01 of 06071	417	0.01061	0.00000	0.00000	0.0
B03 of 73031	385	0.00331	0.00666	0.00027	0.0
S03 of 82024	720	Extreme Value*	0.00439	0.00422	0.0
S15 of 25032	728	Extreme Value*	Extreme Value*	0.01425	0.0
B02 of 06071	789	0.01134	0.00119	0.00000	0.0
B01 of 44012	852	0.00618	0.00492	0.00059	0.0
B03 of 64012	58	0.00082	0.00000	0.00000	0.0
B02 of 64012	119	0.00343	0.00081	0.00000	0.0

* Extreme values are determined for the histogram (Figure 4-3 and Figure 4-4) and are not included in the analysis

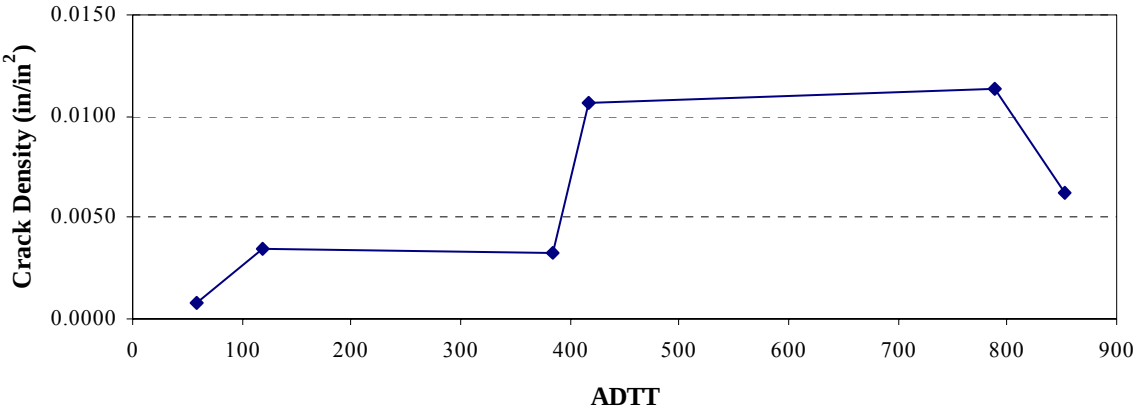

Figure 4-31. Bridge ADTT vs longitudinal crack density

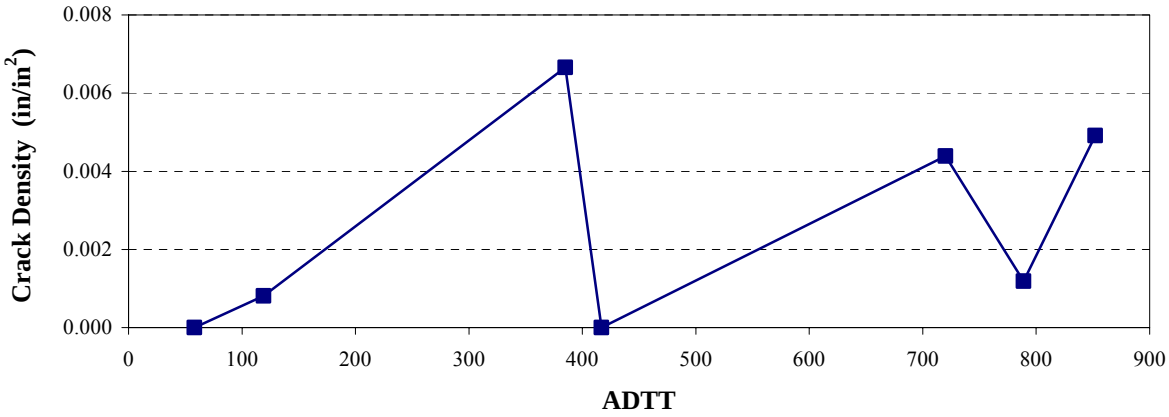

Figure 4-32. Bridge ADTT vs transverse crack density

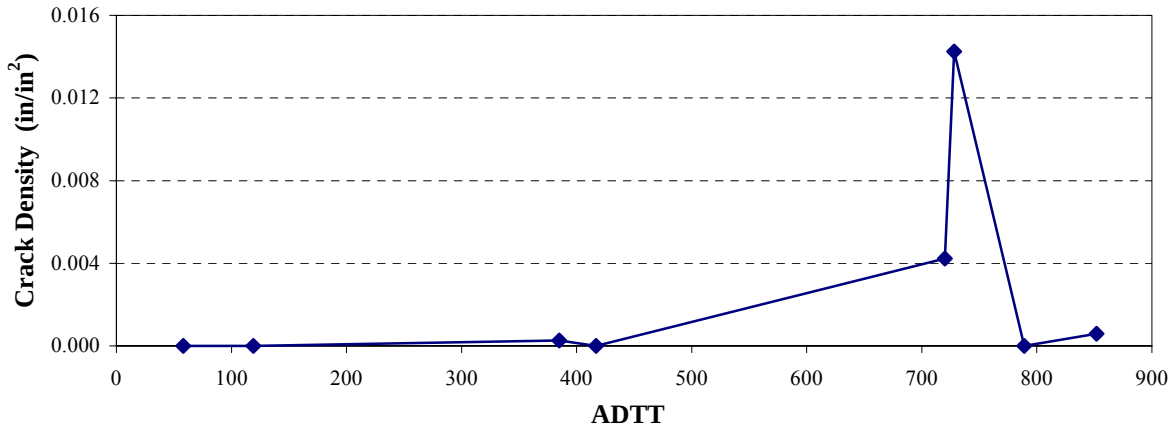

Figure 4-33. Bridge ADTT vs diagonal crack density

4.4 CONCLUSIONS

From the data analysis of the field inspection of 20 bridge decks, the following conclusions are made:

1. More cracks are observed on the continuous bridges than the simple span bridges.
2. Bridges with PCI girder show minimum longitudinal crack density compared with other bridge girder types (i.e., steel, adjacent box girder, and spread box girder).
3. No clear relationship is seen between deck crack density and bridge skew, deck thickness, span length, and ADTT.
4. More transverse and diagonal cracks are observed on bridges with adjacent box girders than other girder types.
5. Map cracking is observed only on bridges with steel girders.

5 CONSTRUCTION MONITORING

5.1 OVERVIEW

Five bridge reconstruction projects involving deck replacements were selected with consideration to the construction dates. Construction monitoring of five bridges was completed including one late season deck replacement as shown in Table 5-1.

The data collected during construction monitoring of all bridges is shown in Appendix C. Ambient temperature and ambient moisture conditions were recorded during concrete placement at 10-minute intervals using digital and analog indicators. Truck number, production time (batch time/ the time truck left the plant), truck arrival time, and unloading (start/finish) time were also recorded. In some cases, according to ticket information, the time at which the truck left the plant was earlier than the batch time. Finally, starting and finishing times for concrete placement, finishing, texturing, and curing for the areas within an approximate one-yard width were monitored and recorded. Cylinder specimens (thirty - 6-in.x12-in. and twenty four – 4-in.x 8-in.) were prepared for laboratory testing. They were tested for strength, elasticity modulus, Poisson's ratio, and permeability at different ages. Test results are given in Chapter 6.

Table 5-1. List of Bridges Monitored during Deck Placement

Bridge ID	Facility Carried	Features Intersected	Length (ft.)	Width (ft.)	Skew (Deg.)	Beam Type	Date
S05 of 82191	Vreeland Rd.	I-75	190	45	2	AASHTO B III - 36	08/14/02
S06 of 82194	I-75	Fort St.	299	123	50	Steel 39-in. plate Girder	08/21/02
S26 of 50111	I-94	Metro PKW	202	126	19	W 27 x 146	09/16/02
S20 of 50111	I-94	Little Mack	222	135	52	Steel 43-in. plate Girder	09/23/02
S05 of 82025	Conner Rd.	I-94	171	57	11	W 36x150 W27x94	11/04/02

5.2 CONCRETE MIX DESIGN, FRESH CONCRETE PROPERTIES, AND AMBIENT ENVIRONMENTAL CONDITIONS

The concrete mix designs for all the bridges monitored during deck placement are given in Table 5-2; the mix designs were obtained from the contractor. The fresh concrete properties for each bridge monitored during deck placement were measured in the field and are shown in Table 5-3. Ambient temperature and ambient relative humidity were measured periodically throughout the casting time of the deck placement. Table 5-4 shows the starting and ending temperature and humidity for each placement with the respective times of casting.

Table 5-2. Concrete Mix Designs for Bridges Monitored during Deck Placement

Bridge ID	Cement [Type 1] (lbs)	Water (lbs)	Coarse Aggregate (Dry)	Fine Aggregate (Dry)	Air Entrainer	Water Reducer	Retarder
S05 of 82191	658	270	1769	1175	AEA-92* (6.6 OZ)	WR-91** (39.48 OZ)	None
S06 of 82194	658	270	1769	1175	AEA-92* (8.54 OZ)	WR-91** (19.70 OZ)	None
S26 of 50111	658	275	1744 (SSD)	1096 (SSD)	MB MICRO AIR* (4.5 OZ)	MB 997*** (52.60 OZ)	MB 200N (26.3 OZ)
S20 of 50111	658	275	1744 (SSD)	1096 (SSD)	MB MICRO AIR* (4.5 OZ)	MB 997*** (52.60 OZ)	MB 200N (26.3 OZ)
S05 of 82025	658	272	1648	1220	AEA-92* (6.6 OZ)	WR-91** (39.48 OZ)	RET 75 (26.3 OZ)

*Micro air entrainer, ASTM C260

** Type D, ASTM C494

***Type F, ASTM C494

Table 5-3. Fresh Concrete Properties of Bridges Monitored during Deck Placement

Bridge ID	Slump (inches)	Air Content (%)	Concrete Temperature (^{o}F)
S05 of 82191	7	7	89
S06 of 82194	5	6.5	78
S26 of 50111	5	7.4	75
S20 of 50111	5	7.2	78
S05 of 82025	4	6.2	68

Table 5-4. Temperature & Relative Humidity over Time of Bridges Monitored during Deck Placement

Bridge ID	Casting Date	Casting Time		Temperature (^{o}F)		Humidity (%)	
		Start	End	Start	End	Start	End
S05 of 82191	8/14/02	21:10	23:57	77	67	65	92
S06 of 82194	8/19/02 -8/20/02	21:10	2:20	66	59	66	94
S26 of 50111	9/16/02 - 9/17/02	20:45	2:25	62	53	61	100
S20 of 50111	9/23/02 - 9/24/02	20:33	4:28	67	56	39	73
S05 of 82025	11/4/02	8:20	16:00	56	55	35	31

5.3 SPECIFICATION REQUIREMENTS AND FIELD OBSERVATIONS

The requirements for the formwork, placement of steel reinforcements, placement of concrete, finishing of plastic concrete, and curing given in MDOT Section 706 of Standard Specifications for Construction will be discussed in the following sections.

5.3.1 Formwork

Section 706.03 D of Standard Specifications for Construction describes the formwork requirements, some of which are:

1. *Strong, rigid, and motor-tight forms shall be built for placing, vibrating, and curing the concrete.*
2. *The forms are required to build following the exact dimensions and shall be in place until the concrete has sufficiently hardened to permit their removal.*
3. *Forms shall be securely braced to prevent movement while placing concrete.*
4. *The hardened concrete shall not be damaged while removing the forms.*

Field observation of the formwork showed no contradiction to the requirements set forth by the Standard Specifications.

5.3.2 Placement of Steel Reinforcements

Section 706.03 E.4 of Standard Specifications for Construction describes the requirements for the layout of steel reinforcements. The main parts of the requirements related to the research projects are:

1. *All steel reinforcement shall be accurately placed and firmly held during concrete placement.*
2. *When placed in the work, it shall be free from dirt and reasonably free from excessive rust, loose mill scale, or other foreign material.*

Field observations indicated that the top and bottom reinforcement layers were placed and firmly held in agreement with the requirements given in the Specifications. All the reinforcements were free from dirt and other foreign materials; an example is shown in Photo 5-1.

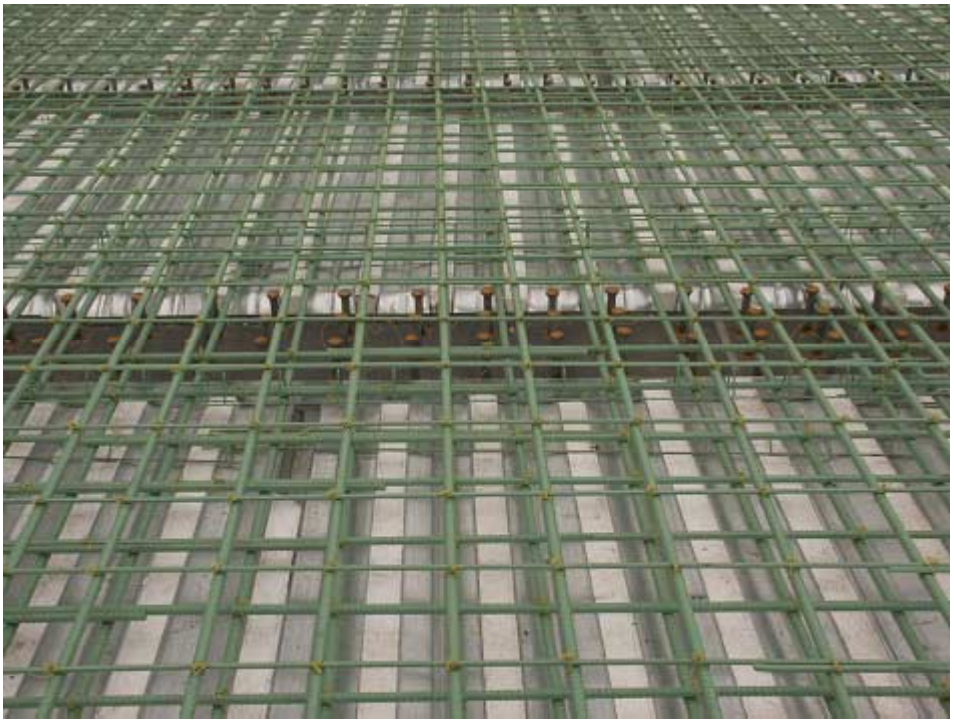

Photo 5-1. Deck reinforcement of I-75 over Fort Street

5.3.3 Concrete Placement

Section 706.03 H-1 of the Standard Specifications for Construction describes the requirements for concrete placement:

1. *At the time concrete is placed, the forms, piling, and reinforcing steel shall be clean, and all sawdust, chips and other debris shall have been removed from the interior of the forms.*
2. *Struts, stays, and braces, serving temporarily to hold the forms in correct shape and alignment, pending the placing of concrete at their location, shall be removed when the concrete placing has reached an elevation rendering their service unnecessary.*
3. *The concrete shall be promptly placed with minimum handling to avoid segregation of the materials and the displacement of the reinforcement.*
4. *The concrete shall be deposited in the forms in layers of suitable thickness and to as near final position as possible.*
5. *For concrete placed by pumping, any water-cement slurry used to lubricate the inside of the discharge pipe at the beginning of a pour shall be disposed of outside the forms.*
6. *Superstructure concrete shall not be allowed to freefall more than 6 inches to the top of reinforcing steel.*

The reinforcements as well as the interior of the formwork were cleaned before placement of concrete. The concrete crew made an effort to place the concrete uniformly and in its final position. Shovels were sometimes used to spread concrete from one location to another. Temporary supports such as struts, stays, and braces were removed after concrete was placed in its final position. These temporary supports were removed and struck off the concrete surface with a screed before finishing was carried out using a wooden float. During the five bridge deck replacement projects, concrete was placed up to the final thickness before the finishing work commenced. However, it was hard to control the free fall within the required limit of 6 inches. Most often, free fall was about one foot. In certain instances, free fall was between two and three feet as seen in Photo 5-2.

Additionally, placement was sometimes interrupted due to delays in concrete delivery to the job site. The delay sometimes exceeded 30 minutes, documented as the records taken at the job site. Consequently, the requirements in the Specifications stating that "sufficient vibrators shall be used to properly compact the incoming concrete within 15 minutes after placing" could not be satisfied. The practice of the concrete crew was to wait until concrete arrived at the job site before continuing with vibration and finishing. This left certain portions of the concrete on the deck without proper compaction and finishing. When the new concrete arrived and was placed on the deck, the old and the new portions were then compacted together.

Photo 5-2. Concrete placement of I-94 over Quinn road

Photo 5-3. Concrete placement of Vreeland over I-75

5.3.4 Vibration of Fresh Concrete

Section 706.03 H-1 of the Standard Specifications for Construction describes the requirements for vibration of fresh concrete.

1. *Mechanical, high frequency internal vibrators shall be used to consolidate the concrete during and immediately after depositing.*
2. *When epoxy coated or other coated reinforcement is used, the vibrator head shall be rubber coated to prevent damage to the coating.*
3. *The consolidation of concrete by hand methods will be permitted only where the use of vibratory equipment is not feasible.*
4. *The vibrators shall be of a type approved by the Engineer and shall be capable of visibly affecting an approved mixture for a distance of at least 18 inches from the vibrator. Sufficient vibrators shall be used to properly compact the incoming concrete within 15 minutes after placing.*
5. *Vibrators shall be manipulated so as to thoroughly work the concrete around the reinforcement, embedded fixtures, and into the corners and angles of the forms.*
6. *Vibration shall be applied at the point of deposit and in the area of freshly deposited concrete.*
7. *The vibration shall be of sufficient duration and intensity to thoroughly compact the concrete, but shall not be continued so as to cause segregation.*
8. *Vibration shall not be continued at any one point to the extent that localized areas of grout are formed.*
9. *The application of vibrators shall be at points uniformly spaced and not farther apart than twice the radius over which the vibration is visibly effective.*
10. *Vibrators shall not be held against the forms or reinforcing steel, nor shall they be used for flowing the concrete or spreading it into place.*

11. Care shall be used not to disturb partially hardened concrete.

Construction monitoring showed that vibrator applications were random rather than following a distinct pattern as required in the Specifications. In addition, vibrators seemed to be used to spread concrete into place. In Photo 5-4, the second worker from the left is vibrating the concrete.

Photo 5-4. Vibration of fresh concrete of Vreeland over I-75

5.3.5 Nighttime Casting of Superstructure Concrete

Section 706.03 I of the Standard Specifications for Construction describes the requirements for nighttime casting of superstructure concrete.

1. *Cast concrete deck slab pours at night with work starting between one hour after sunset and midnight or as designated by the Engineer.*
2. *The deck pouring sequence and curing requirements shall be strictly observed as shown on the plans and outlined in these specifications.*
3. *If approved by the Engineer, pours shown to be done simultaneously may be done consecutively that night using adequate retarder in the first pour to prevent initial set until the second pour is completed.*

According to the field observations, no discrepancy was seen between the practice and the requirements of the Specifications.

5.3.6 Finishing of Plastic Concrete.

Section 706.03 M of the Standard Specifications for Construction describes the requirements for finishing of plastic concrete as follows:

Care shall be taken to avoid over-vibration or over-finishing of the completed surface. Water may be applied to the surface of the concrete as an aid to finishing only by means of an approved fog sprayer and then only when approved by the Engineer.

Finishing of the concrete surface was in compliance with the Specifications. This observation also complied with the requirements for machine finishing (shown in Photo 5-5) and hand float surface finishing given in Section 706.03 M-1 and Section 706.03 M-2 of the Standard Specifications.

Photo 5-5. Finishing concrete of Vreeland over I-75

5.3.7 Texturing.

Section 706.03 M-3 of the Standard Specifications for Construction describes the requirements for texturing deck concrete:

1. *The final deck surface shall be grooved as soon as the deck concrete has set sufficiently to maintain a texture.*

2. *The grooves shall be constructed perpendicular to the centerline or shall be skewed, not to exceed the maximum angle of skew of the bridge.*
3. *The grooves shall be formed in the plastic concrete while the concrete is in such condition that the grooves will be formed cleanly without either slumping of the edges or tearing of the surface. The grooving shall end at a distance of 12 inches to 16 inches from the edge of the curb or barrier.*
4. *The deck shall not be grooved within 3 inches to 6 inches of the expansion or contraction joints or at the end of the slab.*
5. *The desired surface texture consists of grooves spaced on ½ inch centers, 1/8 inch wide, and 1/8 inch deep. Some randomness in spacing is allowed, provided that the spacing between grooves remains within the range of ¼ inch to 1 inch.*

Texturing work was in compliance with the Specifications. Photo 5-6 shows an example of a worker applying groves into the newly cast deck, and Photo 5-7 depicts a closer view of the newly formed grooves.

Photo 5-6. Texturing of concrete of I-75 over Fort Street

Photo 5-7. Close-up of textured concrete of I-75 over Fort Street

5.3.8 Curing of the Deck Concrete

Section 706.03 N of the Standard Specifications for Construction describes the curing procedure for concrete bridge decks. It is specified that if the air temperature is below 40 °F, structural concrete shall be cured according to subsection 706.03.J. If the air temperature is 40 °F or above, structural concrete shall be cured following certain requirements, all of which are explained below.

1. *Curing shall consist of a two-phase continuous 7-day wet cure procedure.*

The curing was applied for 7-days; however, proper precautions were not taken to ensure that it was a wet-cure operation.

2. *Prior to commencement of concreting operations, the Contractor shall demonstrate that all curing materials and equipment are on-site and in proper operating condition.*

Only the curing compound and the sprayer were available on-site. All other materials were brought to the site the day following the placement.

3. *The first phase of the curing procedure shall consist of a spray application of curing compound meeting the requirements specified in section 903.*

4. *Curing compound shall be applied in a single application beginning immediately after the sheen of bleed water has left the textured concrete surface.*

During monitoring of one bridge deck placement, curing compound was applied only after completing the placement of concrete on the full deck, rather than required by the Specifications. In another instance, curing compound had not been applied when the project team left the site, which was after the casting crew completed concrete placement, leveling, and texturing.

5. *The curing compound application rate shall not be less than 1 gallon per 150 square feet of surface.*

It was difficult to make a justifiable conclusion in this matter since it was simply assumed that the construction crew was experienced enough to meet this requirement. Photo 5-8 shows the application of the curing compound.

6. *Application of curing compound shall progress so as not to leave more than 10 feet of textured concrete surface exposed without curing compound at any time.*

This requirement was never satisfied during any of the deck replacement projects.

Photo 5-8. Application of curing compound of I-94 over Quinn road

7. *The second phase of the curing procedure shall consist of covering the concrete with clean, contaminate free wet burlap as soon as the curing compound has dried sufficiently to prevent adhesion, and the concrete surface will support it without deformation, but not more than two hours after the concrete was cast*.

The concrete surface was never covered with burlap until the next day; even then the burlap was not properly wetted.

8. *A minimum of 12 hours prior to commencement of concreting operations, the burlap shall be continuously soaked in clean water.*
9. *Prior to its use, the burlap sheeting shall be draped or suspended vertically for sufficient time to remove any excess water from its surface, which may dilute or damage the fresh concrete, however, the burlap shall not be permitted to dry. The in-place burlap shall also not be permitted to dry.*

Since the burlap could not be seen at the job site, it was not able to possible to evaluate this procedure.

10. *Burlene or other similar products with impervious surfaces are not permitted.*
11. *A network of soaker hoses shall be installed over the wet burlap as soon as the concrete surface will support it without deformation.*
12. *Soaker hoses shall be perforated throughout their lengths, within the limits of curing, and shall be capable of discharging sufficient curing water to uniformly and continuously cover the entire bridge deck surface without having to be periodically relocated. Perforations shall be sized so as to prevent excessive localized discharge of water, which may damage the concrete surface.*
13. *Non-perforated hose shall be used outside the limits of the bridge deck curing.*

The following day, observations did not show any network of soaker hoses providing a continuous discharge of curing water. Unfortunately, there is no information with regard to how the burlaps covers were kept moist, given that there was not a soaker hose system.

14. *The Contractor shall demonstrate to the Engineer that the soaker hose system provides uniform and thorough coverage of the entire deck surface. A continuous layer of 4 mils polyethylene film (transparent or white color) shall then be securely placed over the entire deck surface and the soaker hose system.*

No comments on this issue.

15. *All seams shall overlap 10 inches minimum.*

This requirement was met.

16. *The water supply shall then be activated and maintained to ensure complete and uninterrupted wet curing of the entire deck surface for the remainder of the first seven days following concrete placement.*
17. *The continue-wet cure shall be maintained until the concrete has reached an age of at least 7 days, and until the concrete has attained its minimum 7-day compressive strength.*
18. *Strength results achieved prior to seven days shall not be considered basis for removal of the continuous wet cure prior to the completion of the 7-day continuous wet curing period.*

As explained above, with the lack of soaker hose system, it was assumed that there was no continuous wet cure even though the burlap was in place for a 7-day period.

19. *Heavy equipment, such as mixers and slip form machines, will not be permitted on the deck until the deck concrete has reached an age of at least 7 days and then not until the concrete has attained at least 100 percent of its minimum 28 day flexural or compressive strength.*

Barrier casting started on some bridges when the bridge decks were seven days old. Therefore, mixers, slip-form machines, and several other vehicles traveled and parked on the newly placed bridge decks.

5.3.9 Additional Observations

Some additional observations are worth mentioning. The first two are related to concrete placement. On one deck with super elevation (S06 of 82194), fresh concrete did not have sufficient stiffness and therefore flowed to one side. The deck surface needed to be diamond ground in order to achieve appropriate leveling (Photo 5-9).

Photo 5-9. Diamond ground deck surface of bridge S06 of 82194

The second issue was common for all decks. The construction or expansion joint boundaries are quite problematic during placement. Excess concrete overflows, loses its plasticity and it is

scraped off and thrown in with the deck concrete near the joint. This creates a substandard quality concrete near the joint. Deterioration often starts at the joints. During placement, the concrete that falls off the joints should not be placed back on the deck.

In two decks (S20 of 50111 and S05 82025), the specimens prepared for the laboratory testing were not set properly at approximately 12 hours after placement. Although the concrete mix design did not indicate any excessive use of set-retarders, these observations indicate an error in the amounts used of these admixtures.

5.4 VISUAL REPRESENTATION OF THE DECK CASTING PROCESS

The data collected during construction monitoring has been analyzed with respect to time and delays and is presented below for each of the deck placements. In the case of bridge S20 of 50111, the collected data was inconsistent and difficult to interpret; therefore, it was not included in the analysis.

5.4.1 Bridge ID S06 of 82194

Figure 5-1 shows the sequence of concrete placement for the monitored sections of the deck. Each yard is color coded with respect to the amount of time required for placement of concrete in that area, and labeled with the start time. Figure 5-2 and Figure 5-3 show the information for the north and south sections in a bar chart format, allowing one to clearly see where any delays occurred. Figure 5-4 demonstrates the relationship between cumulative volume of concrete placed and elapsed time, while Figure 5-5 shows the fluctuation in placement time of concrete as it arrives on the trucks. Figure 5-6, Figure 5-7, and Figure 5-8 show data for the finishing of concrete with regard to time elapsed and observed delays. Texturing data is presented in Figure 5-9, Figure 5-10, and Figure 5-11. Information with regard to application of curing compound may be seen in Figure 5-12, Figure 5-13, and Figure 5-14. Curing was not a smooth process. It started from somewhere in the middle of north section and advanced towards the south end of the south section. Finally, the north end of the north section was completed. Figure 5-13 and Figure 5-14 illustrate this intermittent process and the delays that occurred during the process.

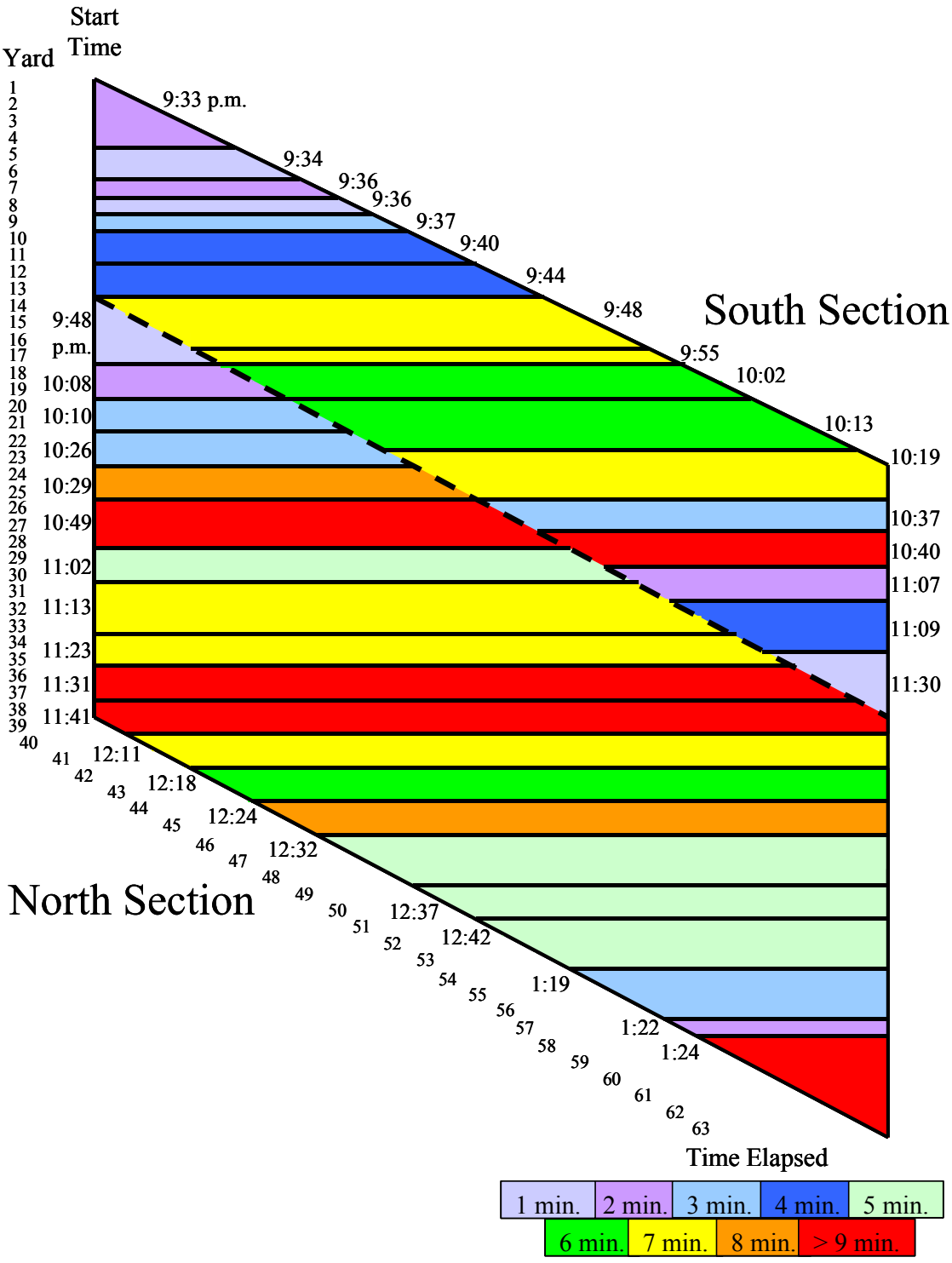

Figure 5-1. S06 of 82194 Concrete placement, time elapsed per yard

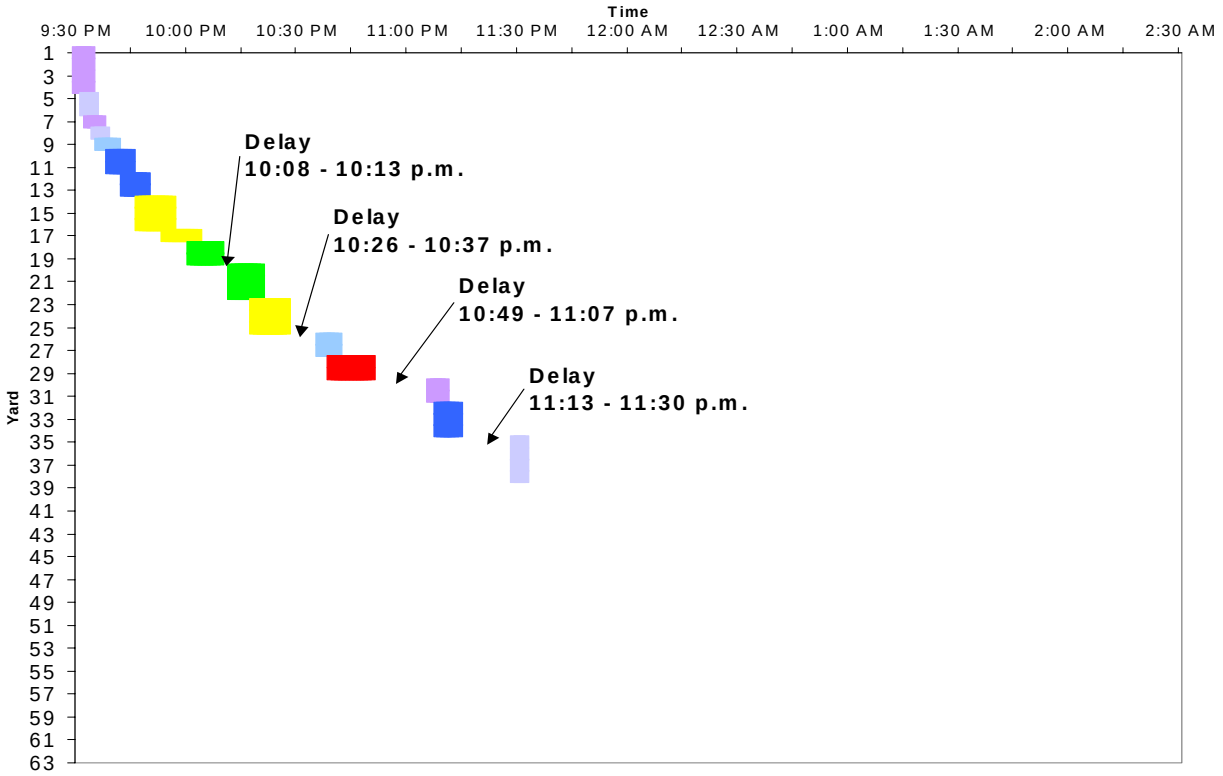

Figure 5-2. S06 of 82194, South section concrete placement time sequence

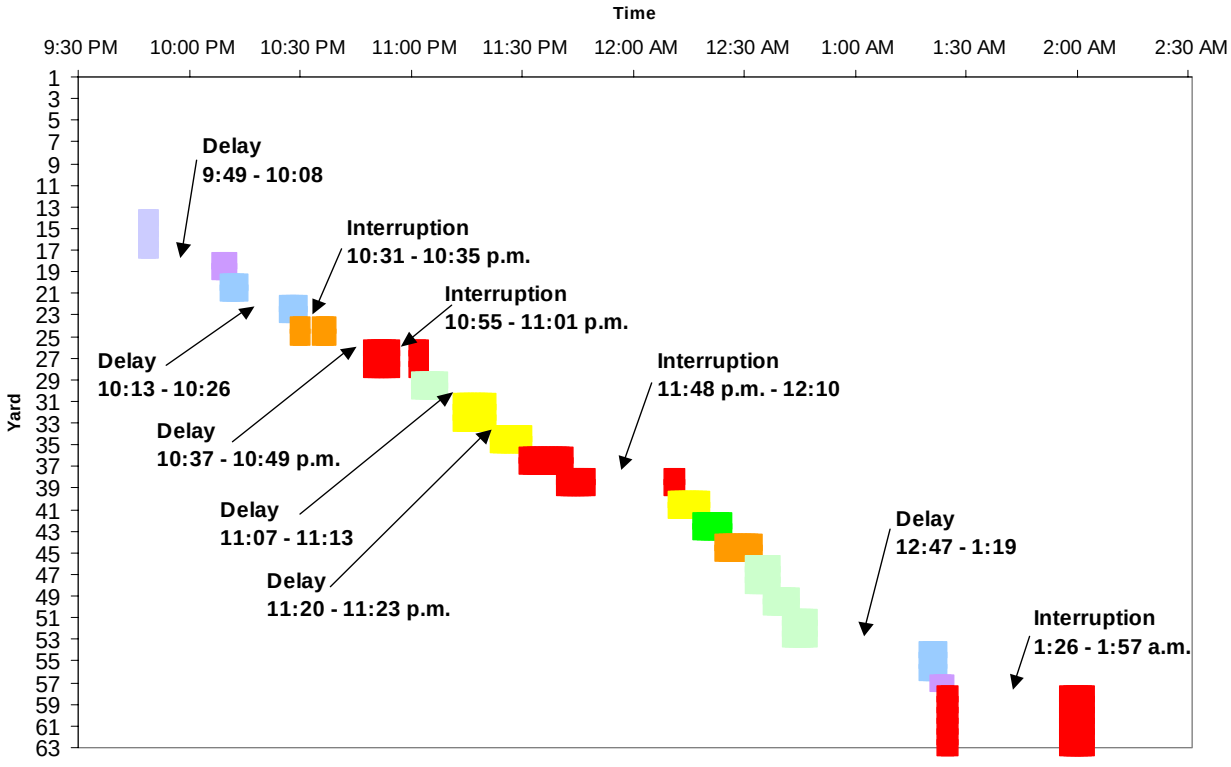

Figure 5-3. S06 of 82194, North section concrete placement time sequence

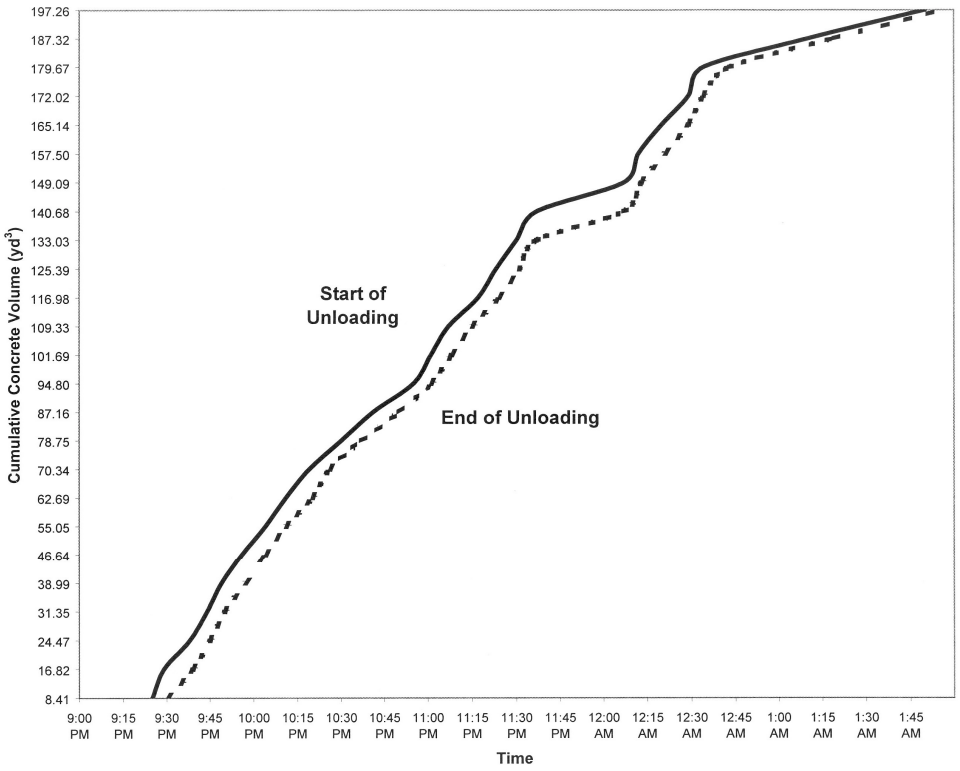

Figure 5-4. S06 of 82194, Cumulative concrete placed vs time elapsed

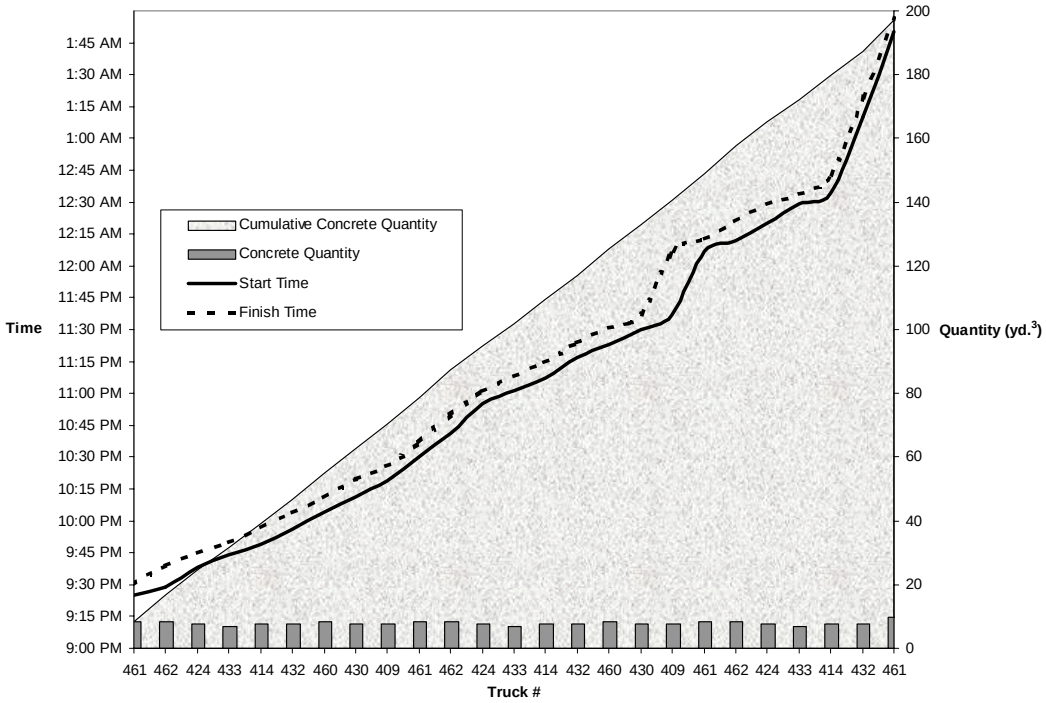

Figure 5-5. S06 of 82194, Time and volume of concrete placed vs truck arrival

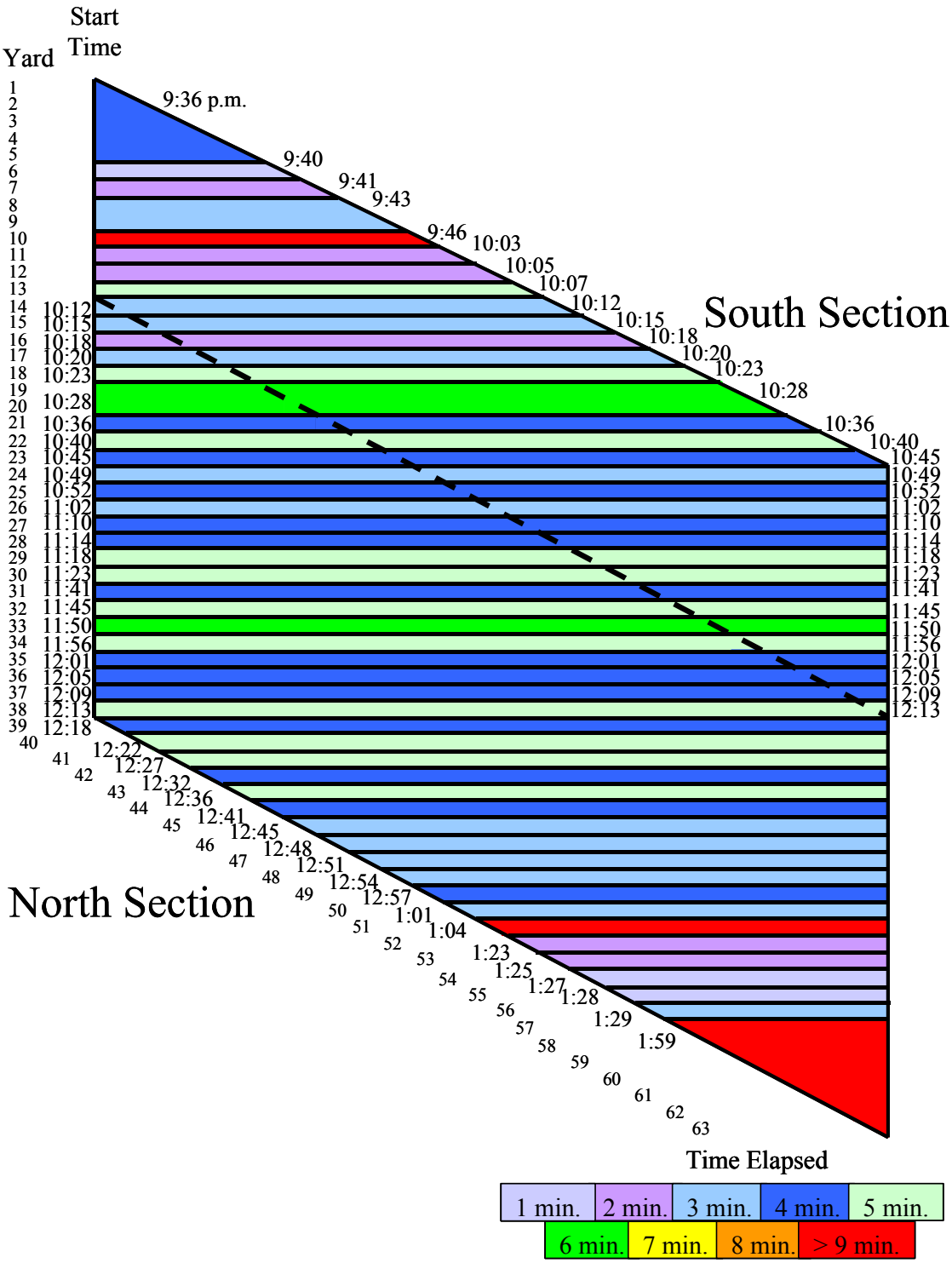

Figure 5-6. S06 of 82194, Concrete finishing, time elapsed per yard

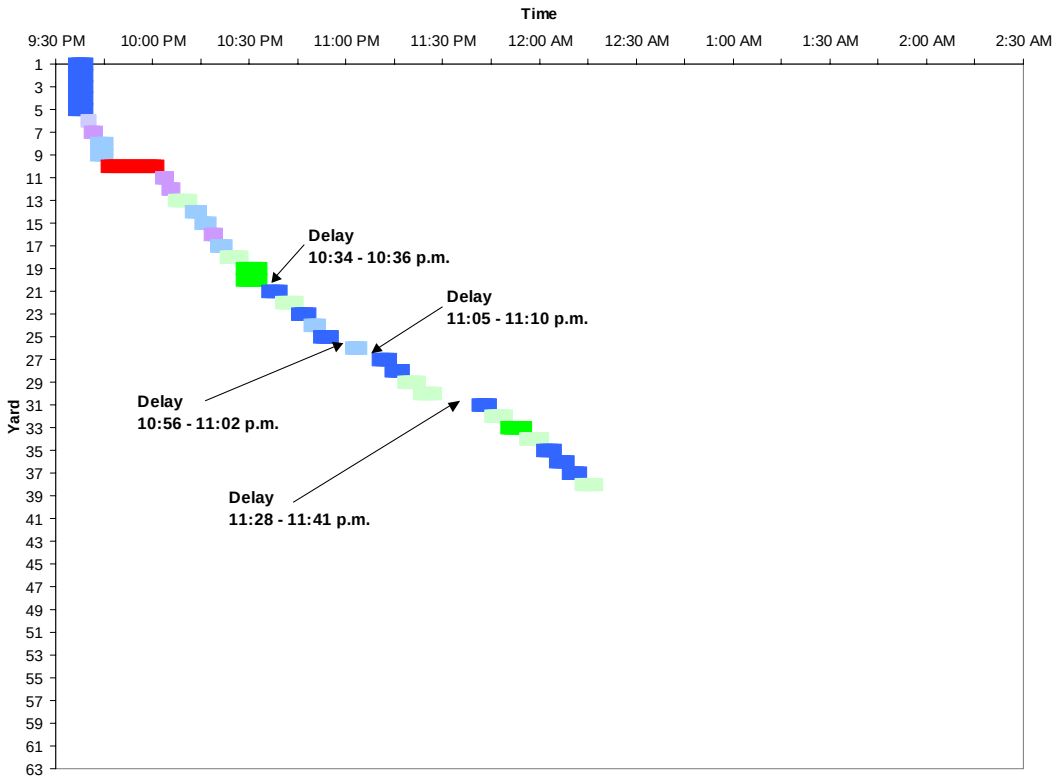

Figure 5-7. S06 of 82194, South section concrete finishing time sequence

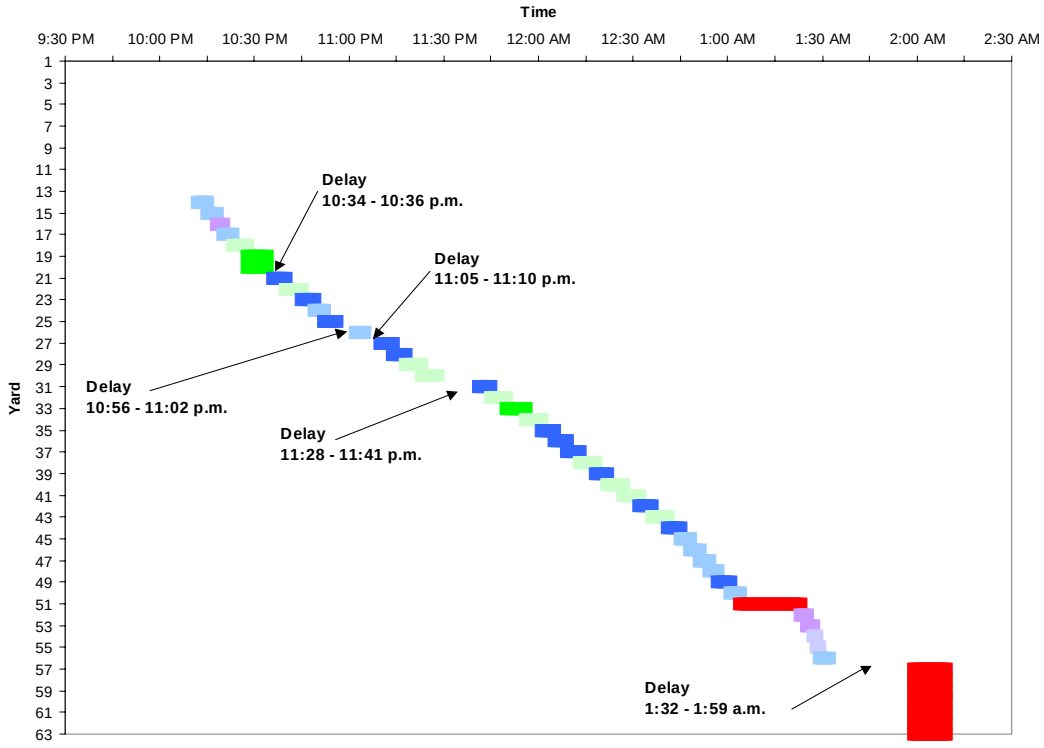

Figure 5-8. S06 of 82194, North section concrete finishing time sequence

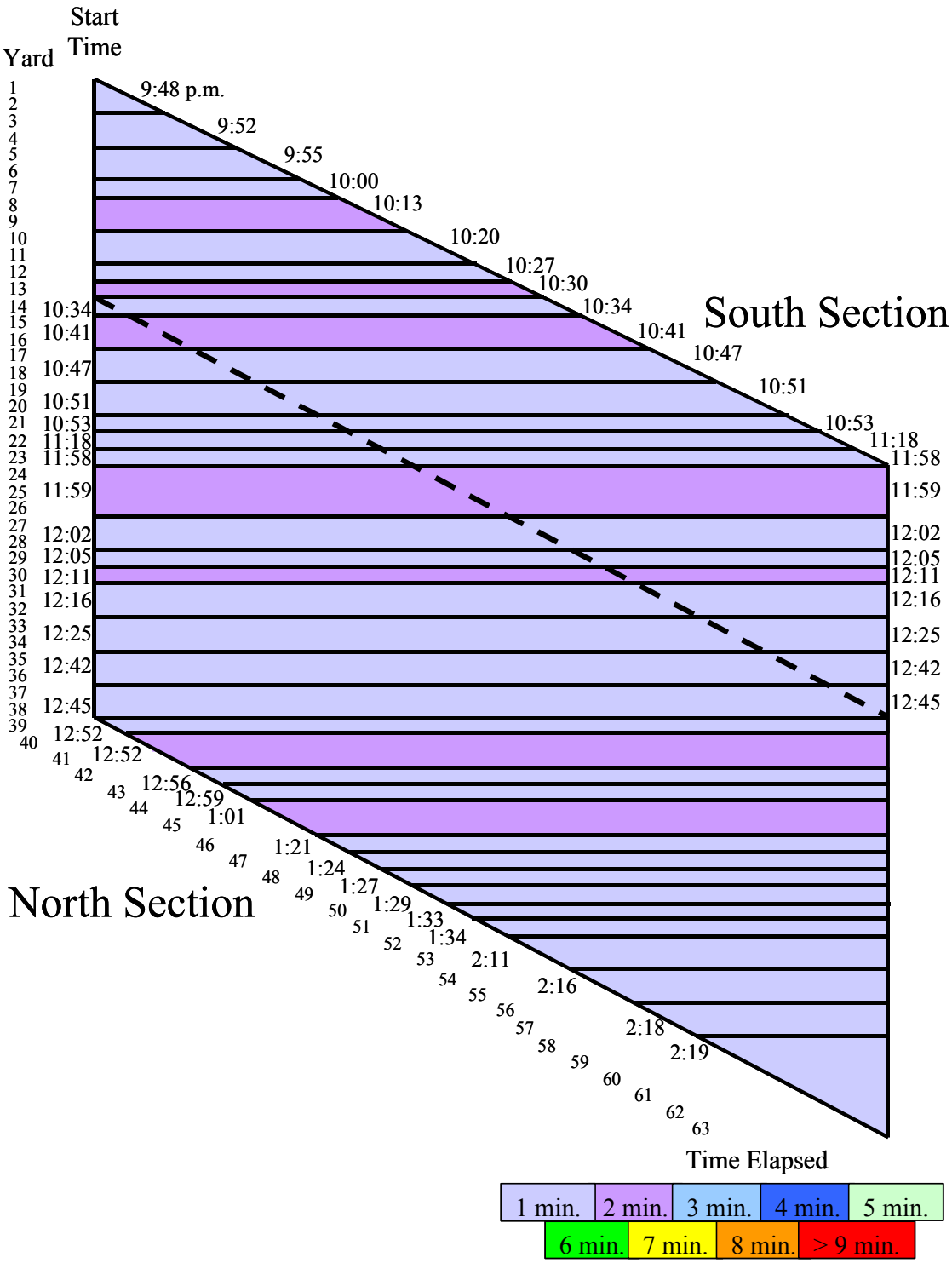

Figure 5-9. S06 of 82194, Concrete texturing, time elapsed per yard

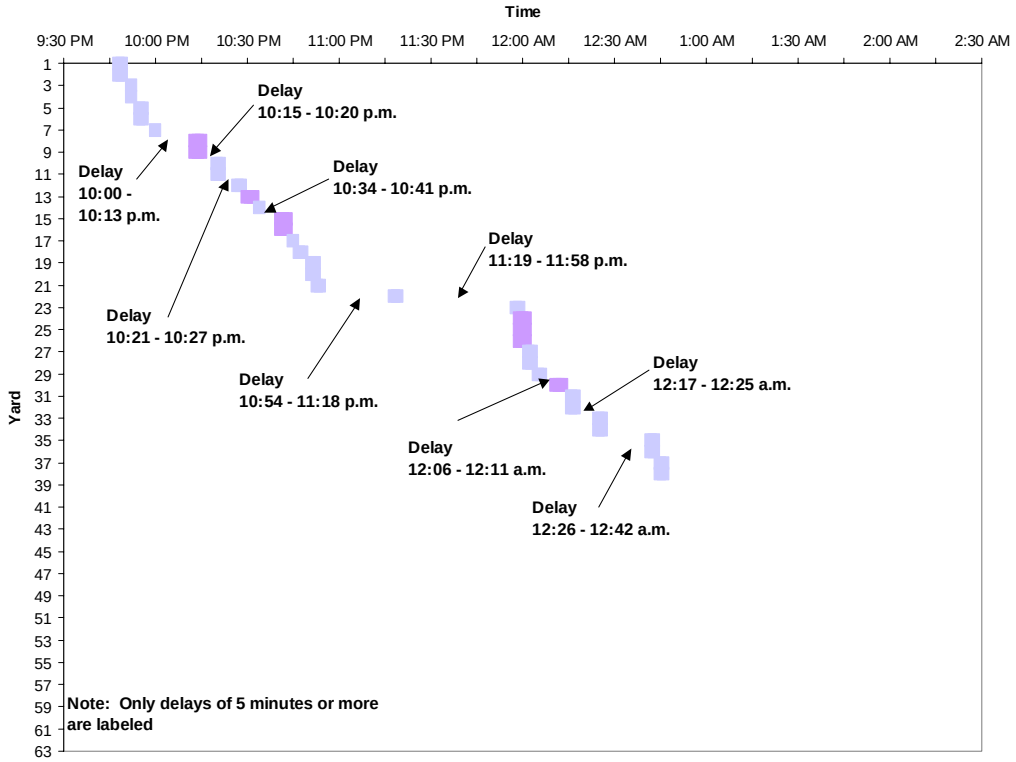

Figure 5-10. S06 of 82194, South section concrete texturing time sequence

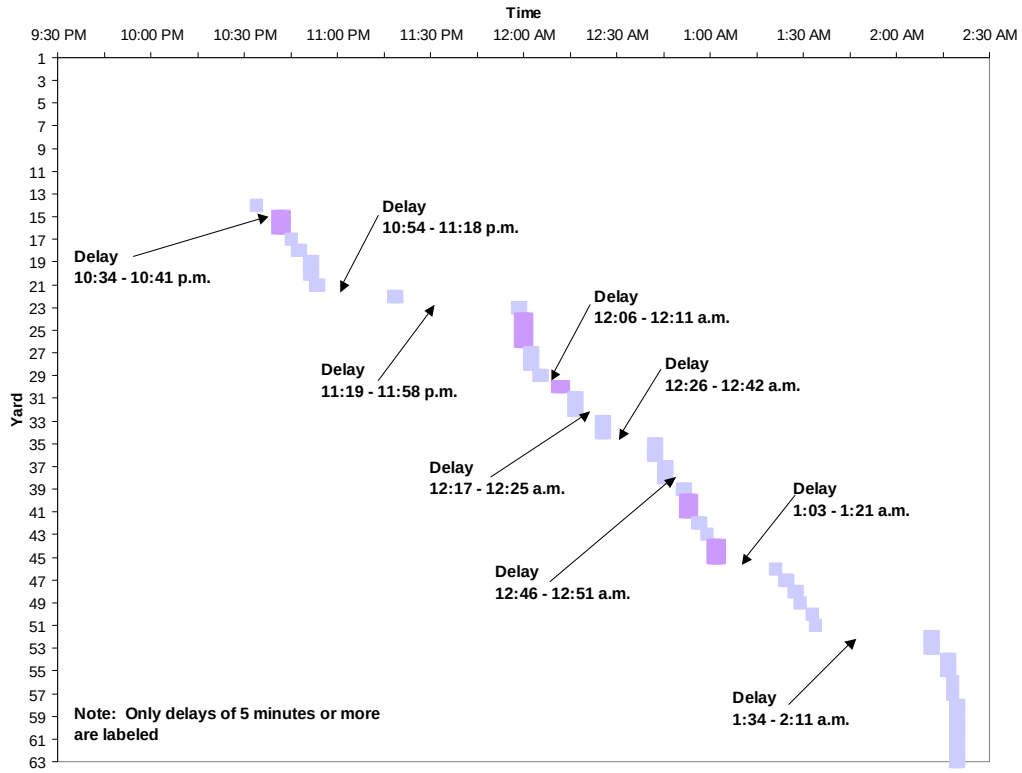

Figure 5-11. S06 of 82194, North section concrete texturing time sequence

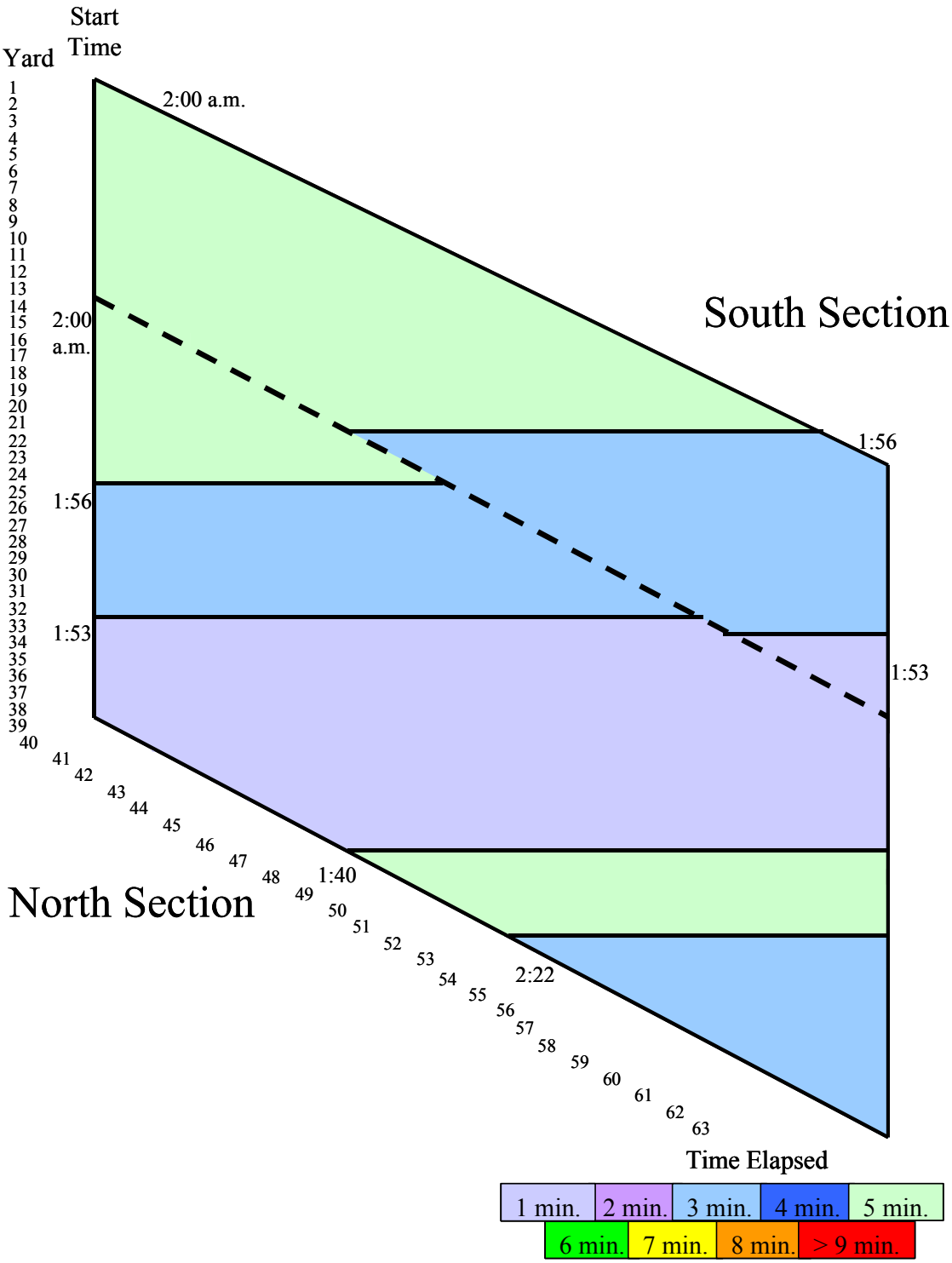

Figure 5-12. S06 of 82194, Curing compound application, time elapsed per yard

Figure 5-13. S06 of 82194, South section curing compound application time sequence

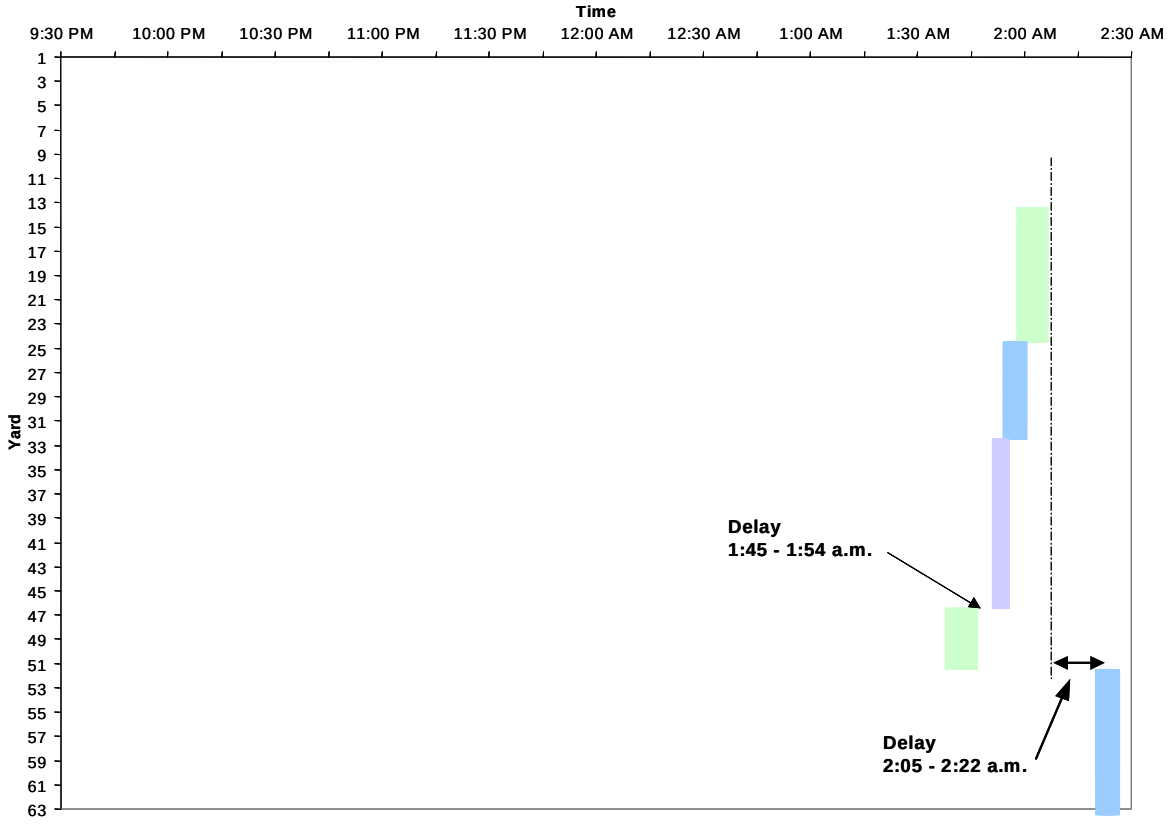

Figure 5-14. S06 of 82194, North section curing compound application time sequence

5.4.2 Bridge ID S26 of 50111

Figure 5-15 shows the sequence of concrete placement for the monitored sections of the deck. Figure 5-16 and Figure 5-17 show the information for the east and west sections in a bar chart format, allowing one to clearly see where any delays occurred. Figure 5-18 demonstrates the relationship between cumulative volume of concrete placed and elapsed time, while Figure 5-19 shows the fluctuation in placement time of concrete as it arrives on the trucks. Figure 5-20, Figure 5-21, and Figure 5-22 show data for the finishing of concrete with regard to time elapsed and observed delays. Texturing data is presented in Figure 5-23, Figure 5-24, and Figure 5-25. Information with regard to application of curing compound may be seen in Figure 5-26, Figure 5-27, and Figure 5-28.

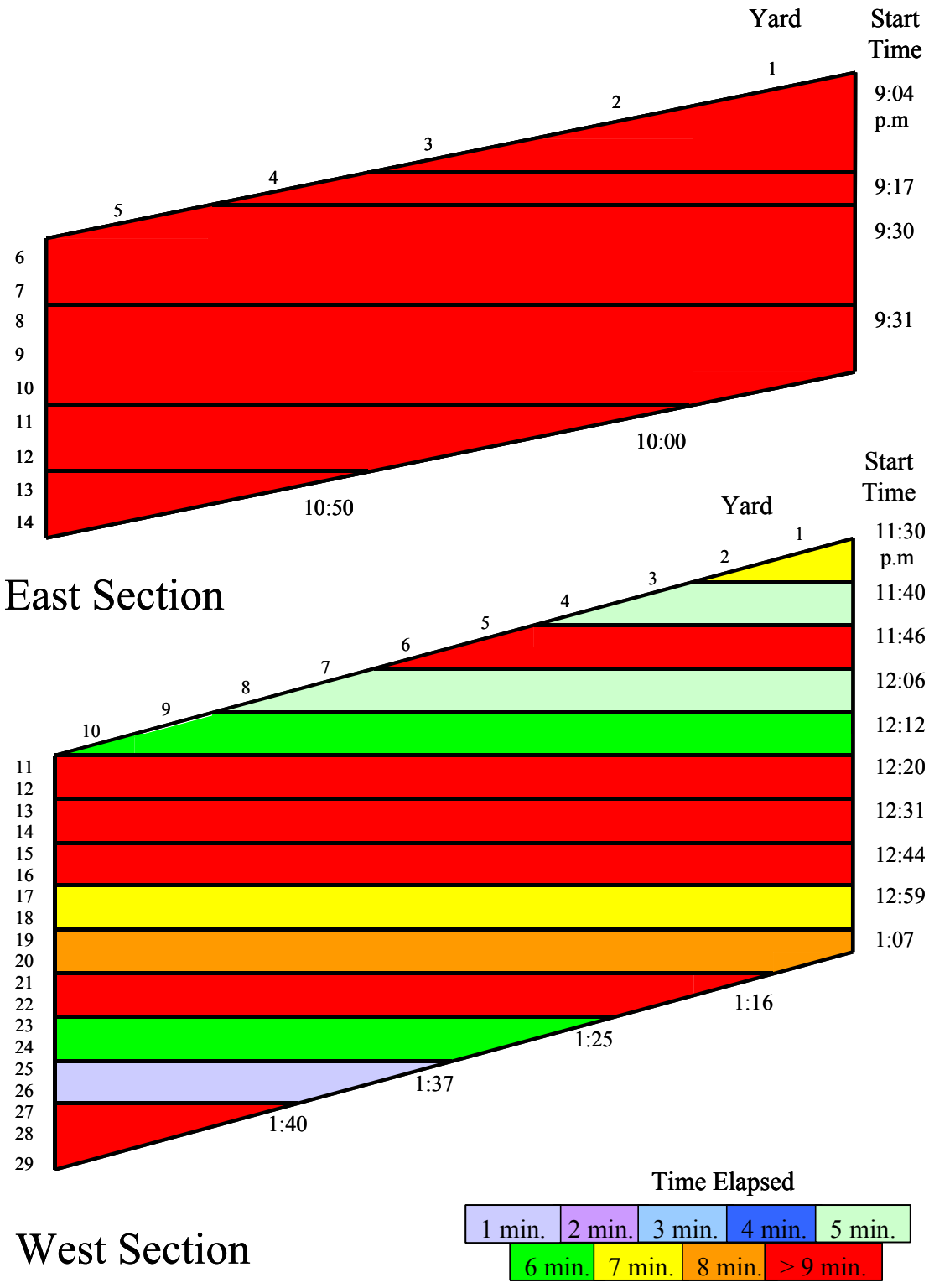

Figure 5-15. S26 of 50111, Concrete placement, time elapsed per yard

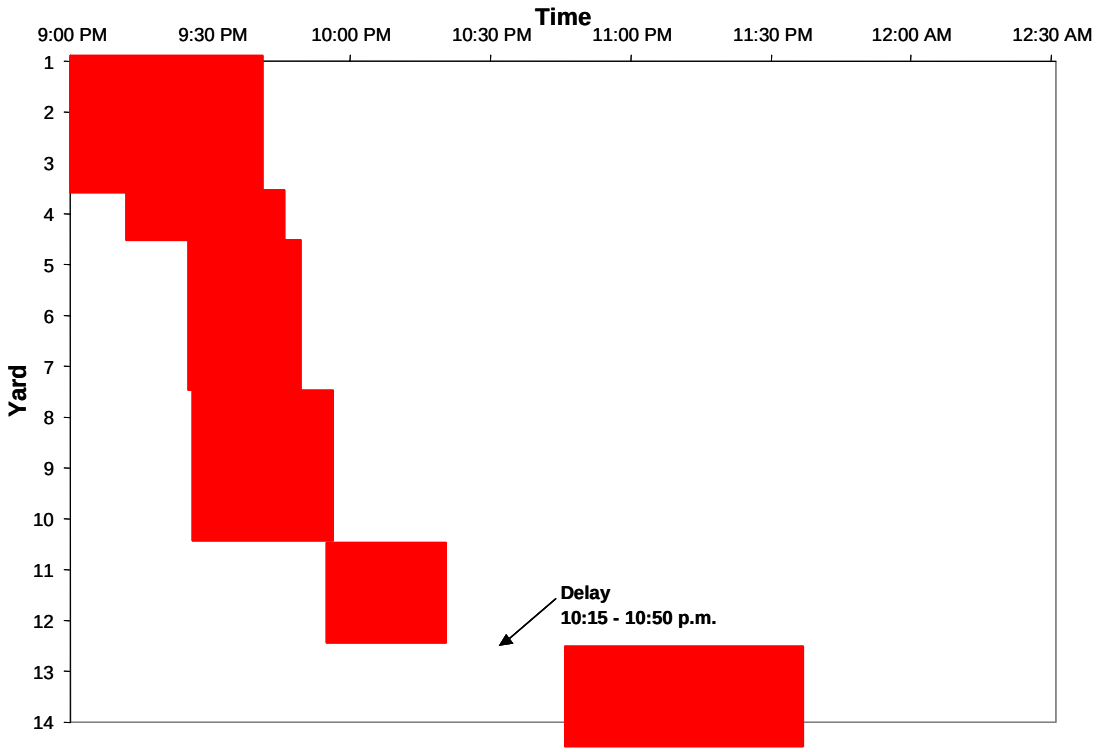

Figure 5-16. S26 of 50111, East section concrete placement time sequence

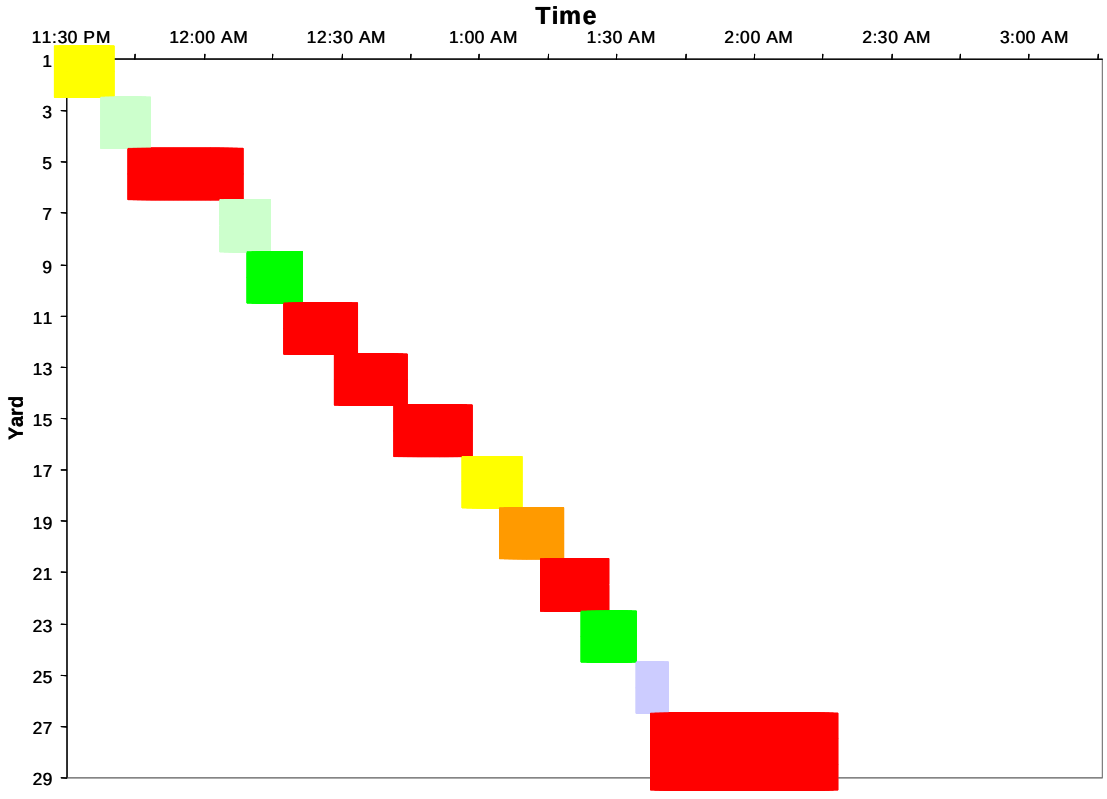

Figure 5-17. S26 of 50111, West section concrete placement time sequence

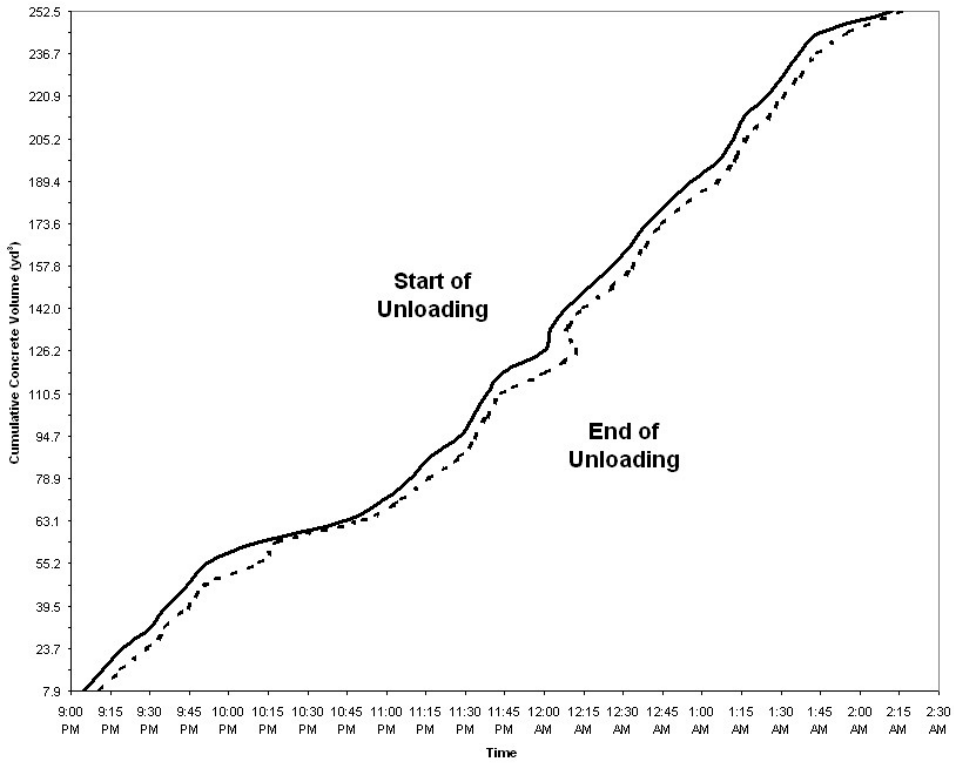

Figure 5-18. S26 of 50111, Cumulative concrete placed vs time elapsed

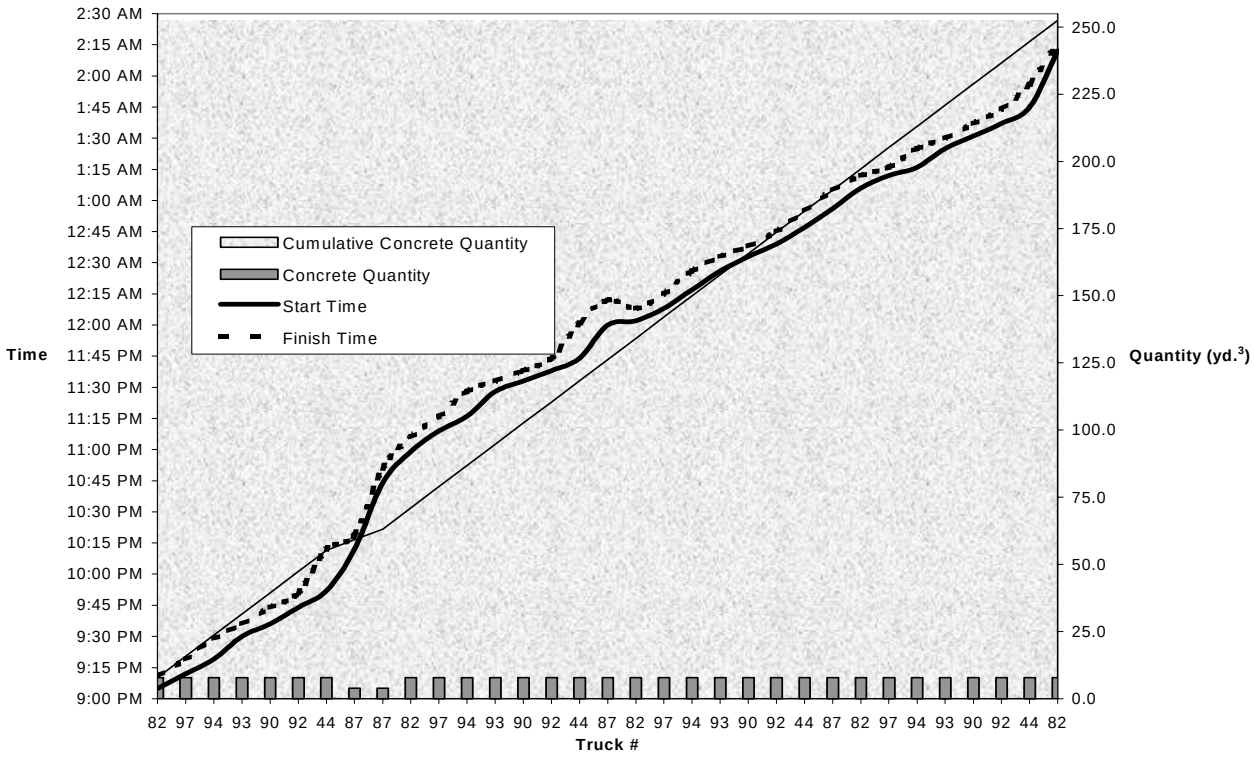

Figure 5-19. S26 of 50111, Time and volume of concrete placed vs truck arrival

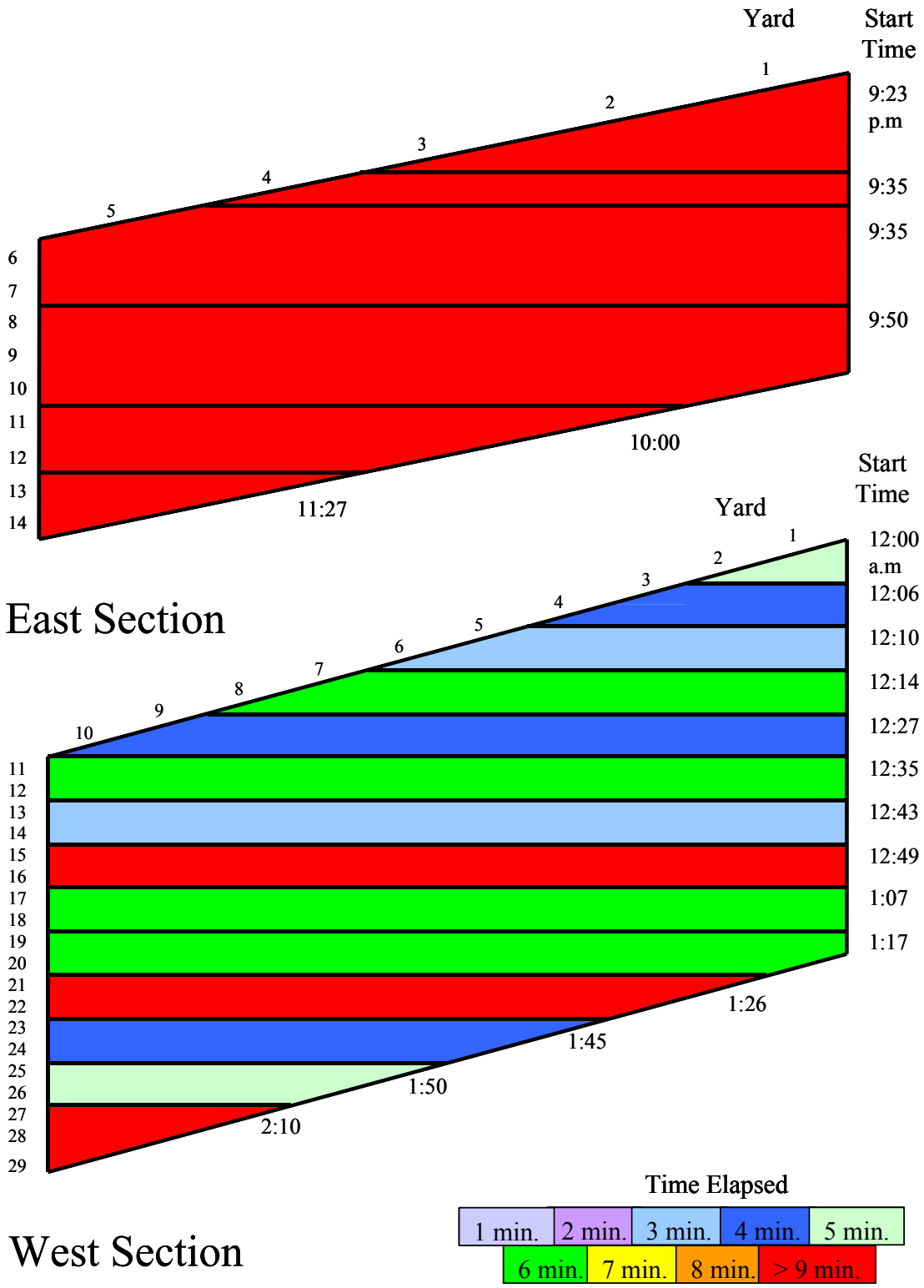

Figure 5-20. S26 of 50111, Concrete finishing, time elapsed per yard

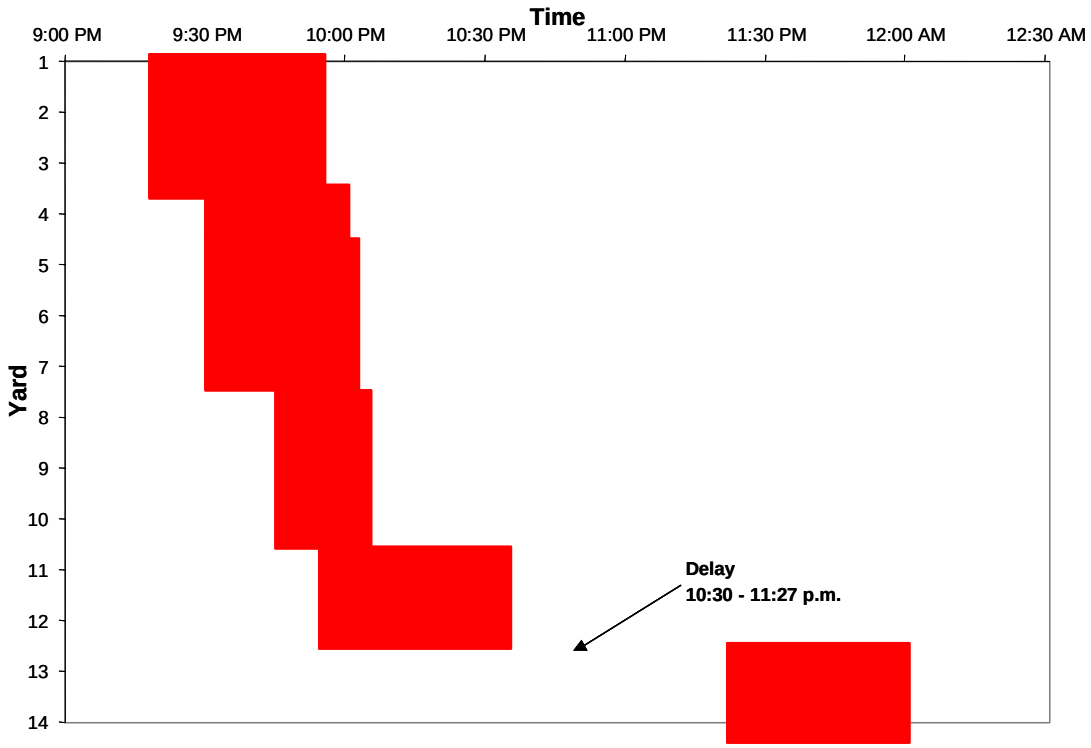

Figure 5-21. S26 of 50111, East section concrete finishing time sequence

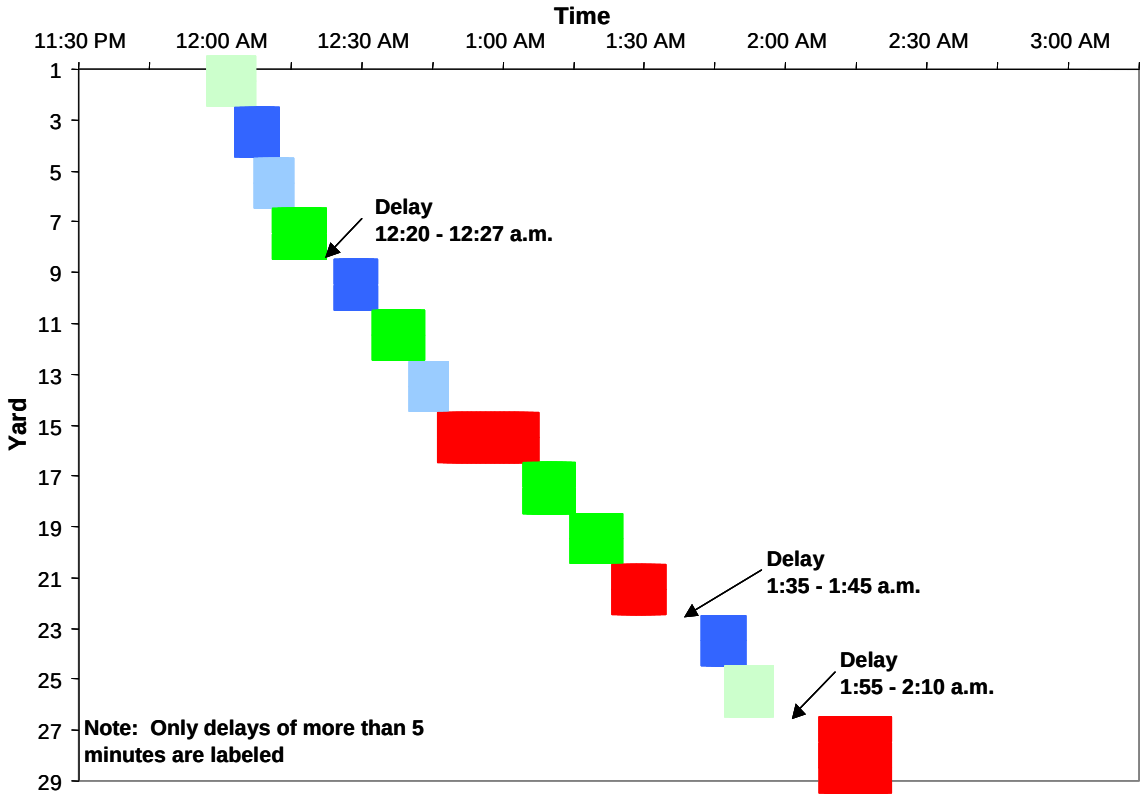

Figure 5-22. S26 of 50111, West section concrete finishing time sequence

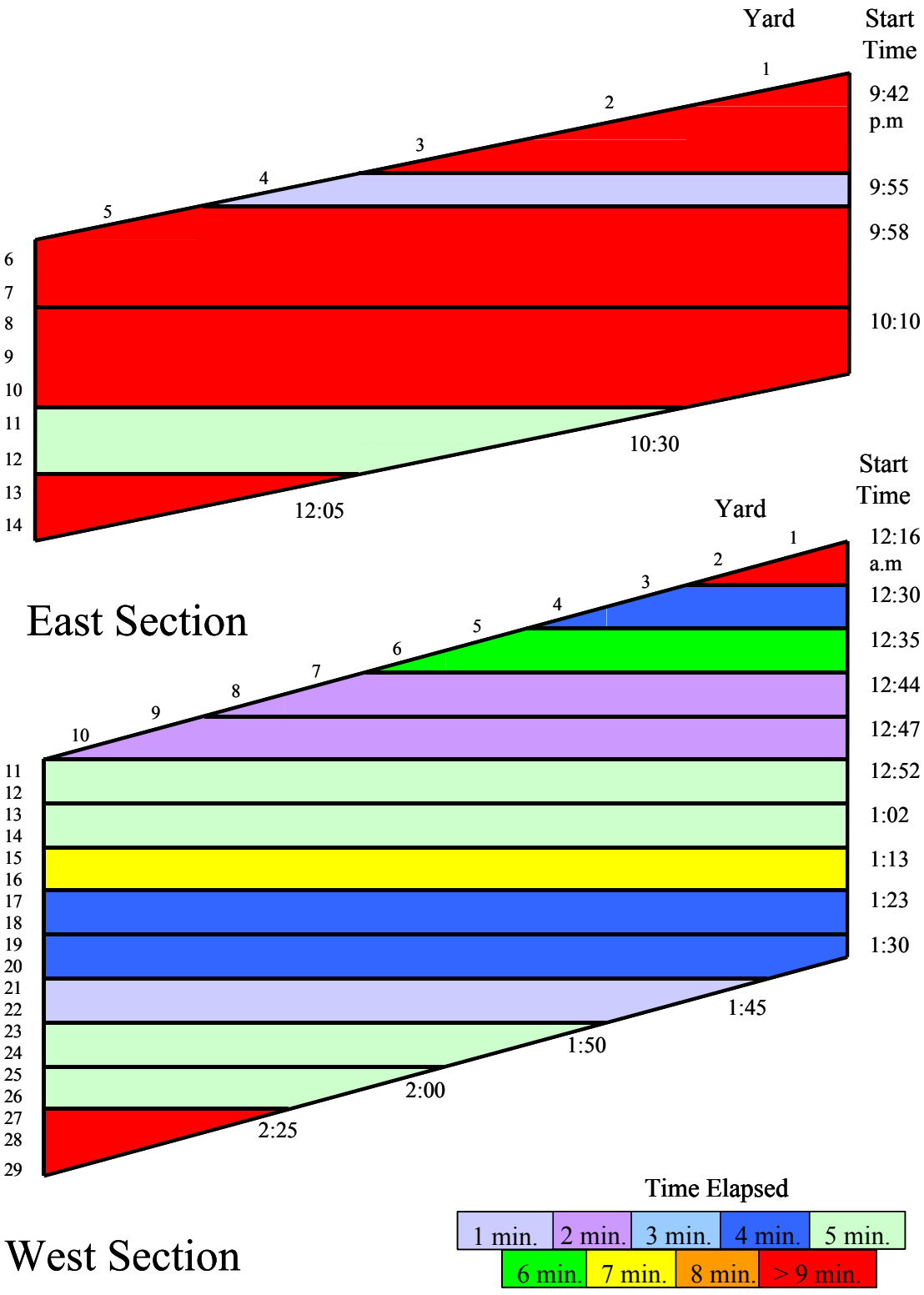

Figure 5-23. S26 of 50111, Concrete texturing, time elapsed per yard

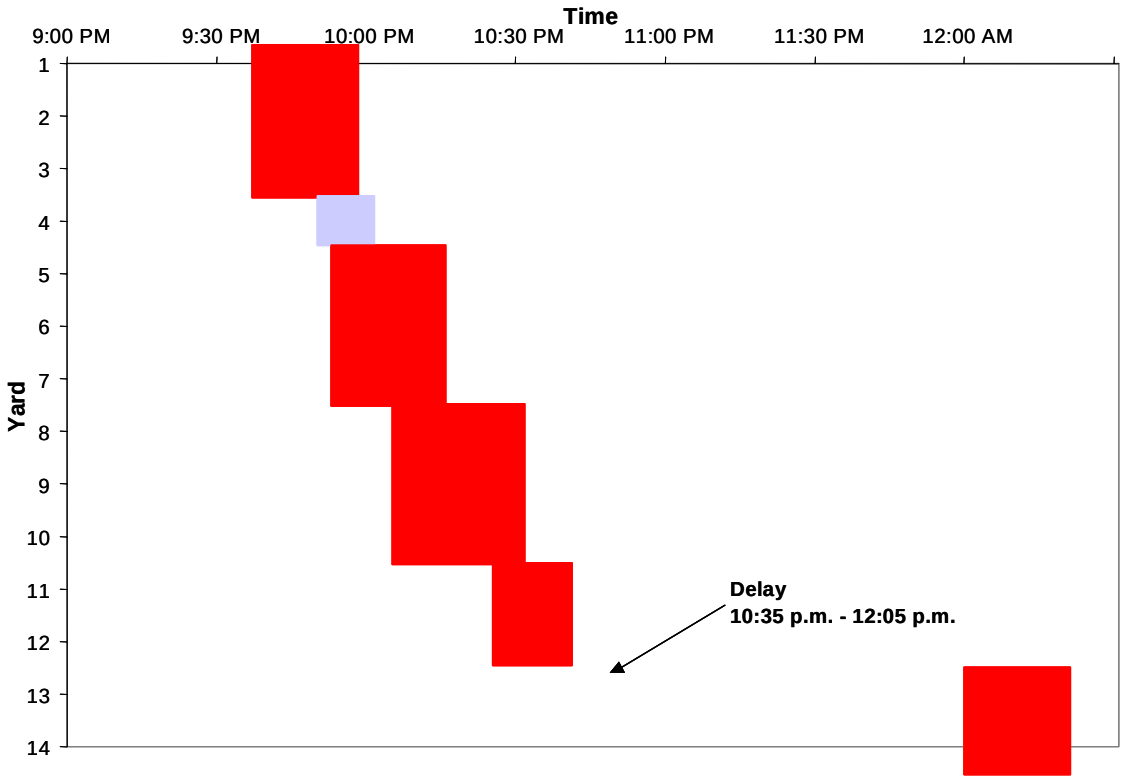

Figure 5-24. S26 of 50111, East section concrete texturing time sequence

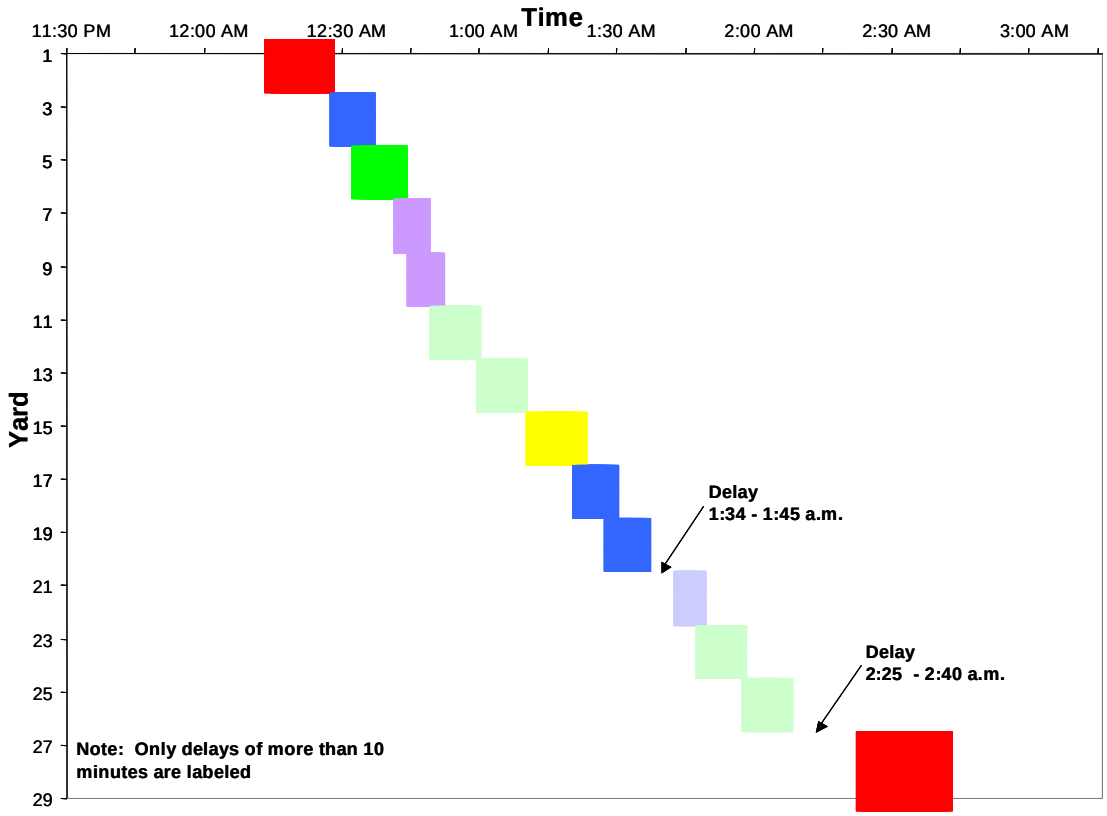

Figure 5-25. S26 of 50111, West section concrete texturing time sequence

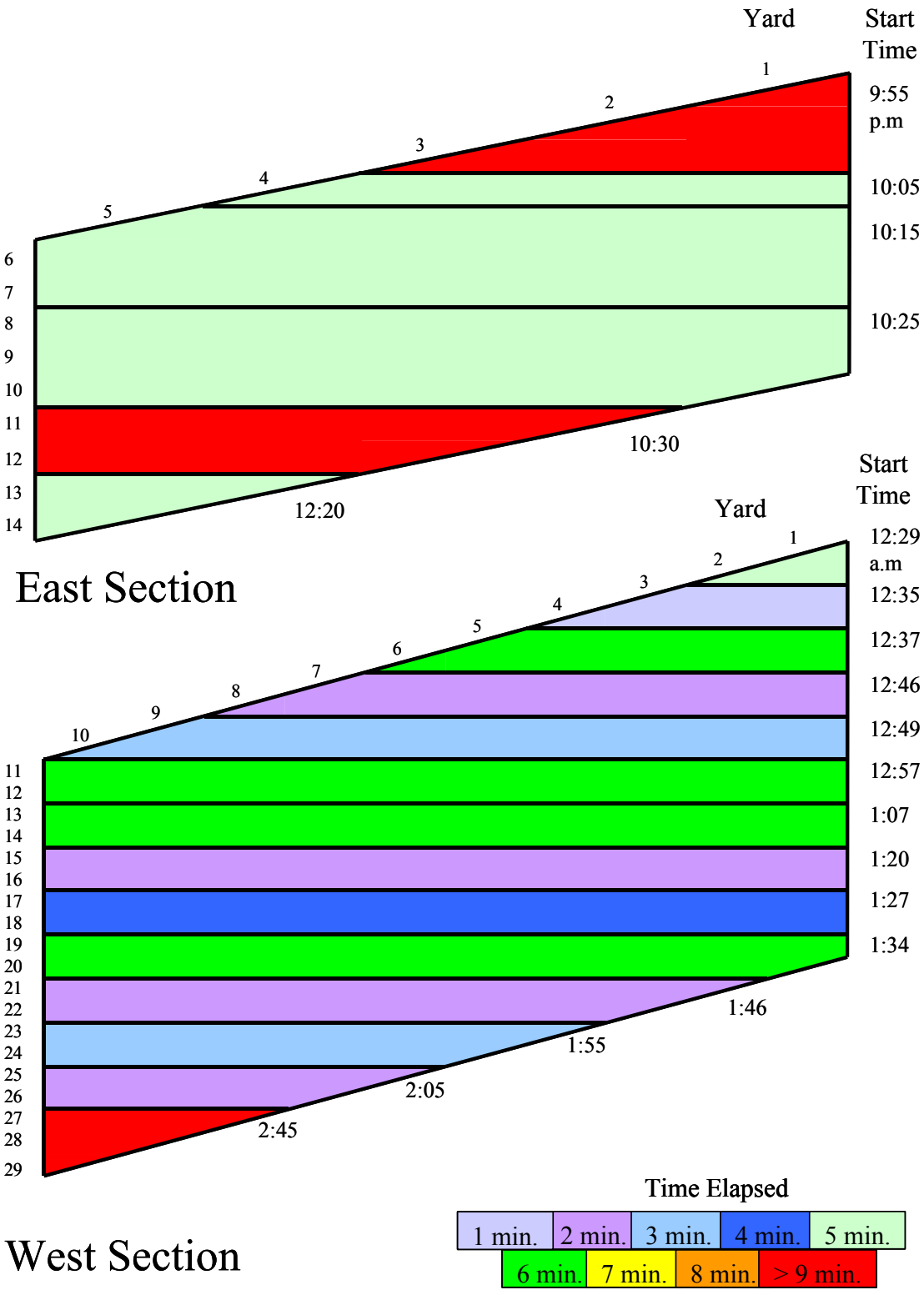

Figure 5-26. S26 of 50111, Curing compound application, time elapsed per yard

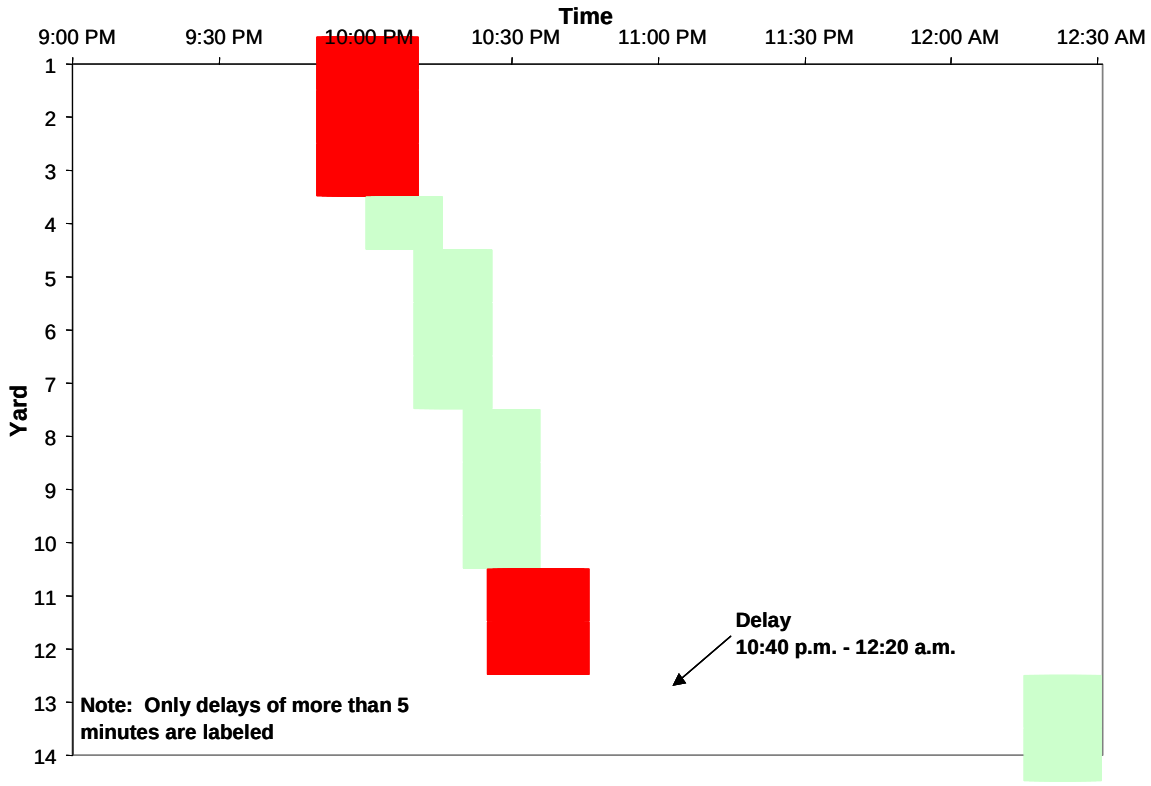

Figure 5-27. S26 of 50111, East section curing compound application time sequence

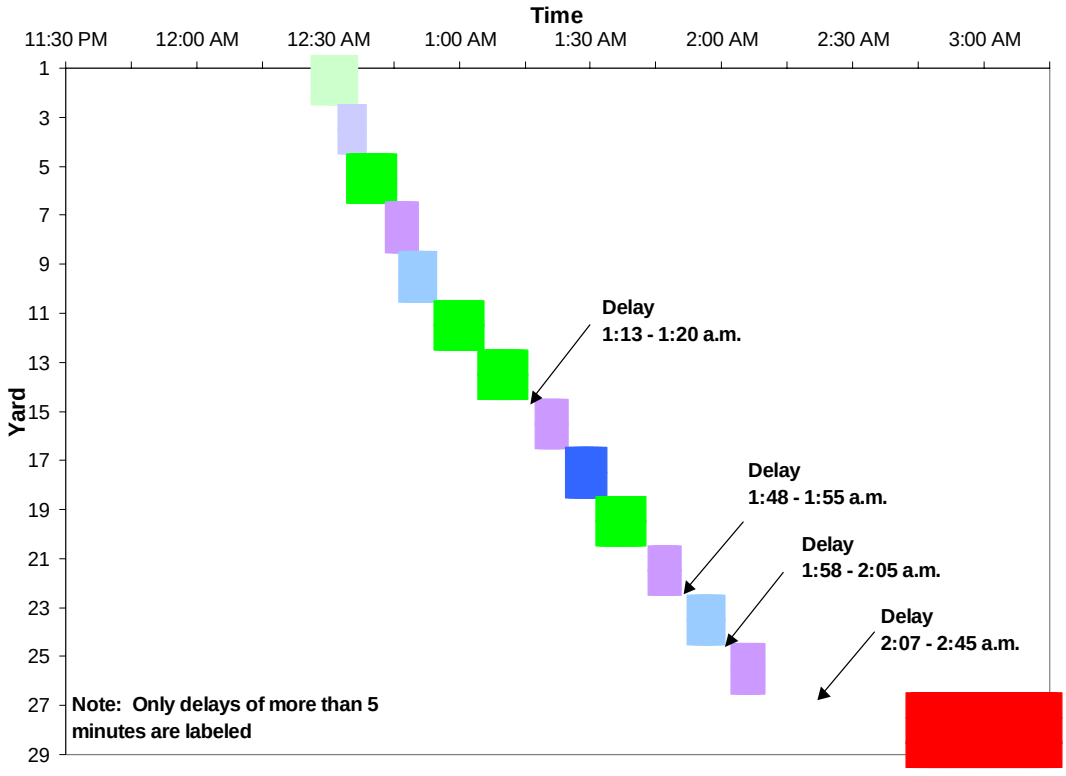

Figure 5-28. S26 of 50111, West section curing compound application time sequence

5.4.3 Bridge ID S05 of 82191

Figure 5-29 shows the sequence of concrete placement for the monitored sections of the deck. Figure 5-30 and Figure 5-31 show the information for the west and east sections in a bar chart format, allowing one to clearly see where any delays occurred. Figure 5-32 demonstrates the relationship between cumulative volume of concrete placed and elapsed time, while Figure 5-33 shows the fluctuation in placement time of concrete as it arrives on the trucks. Figure 5-34, Figure 5-35, and Figure 5-36 show data for the finishing of concrete with regard to time elapsed and observed delays. Texturing data is presented in Figure 5-37, Figure 5-38, and Figure 5-39. Since curing compound was not applied until the project team left the site, information with regard to application of curing compound was not available for this project.

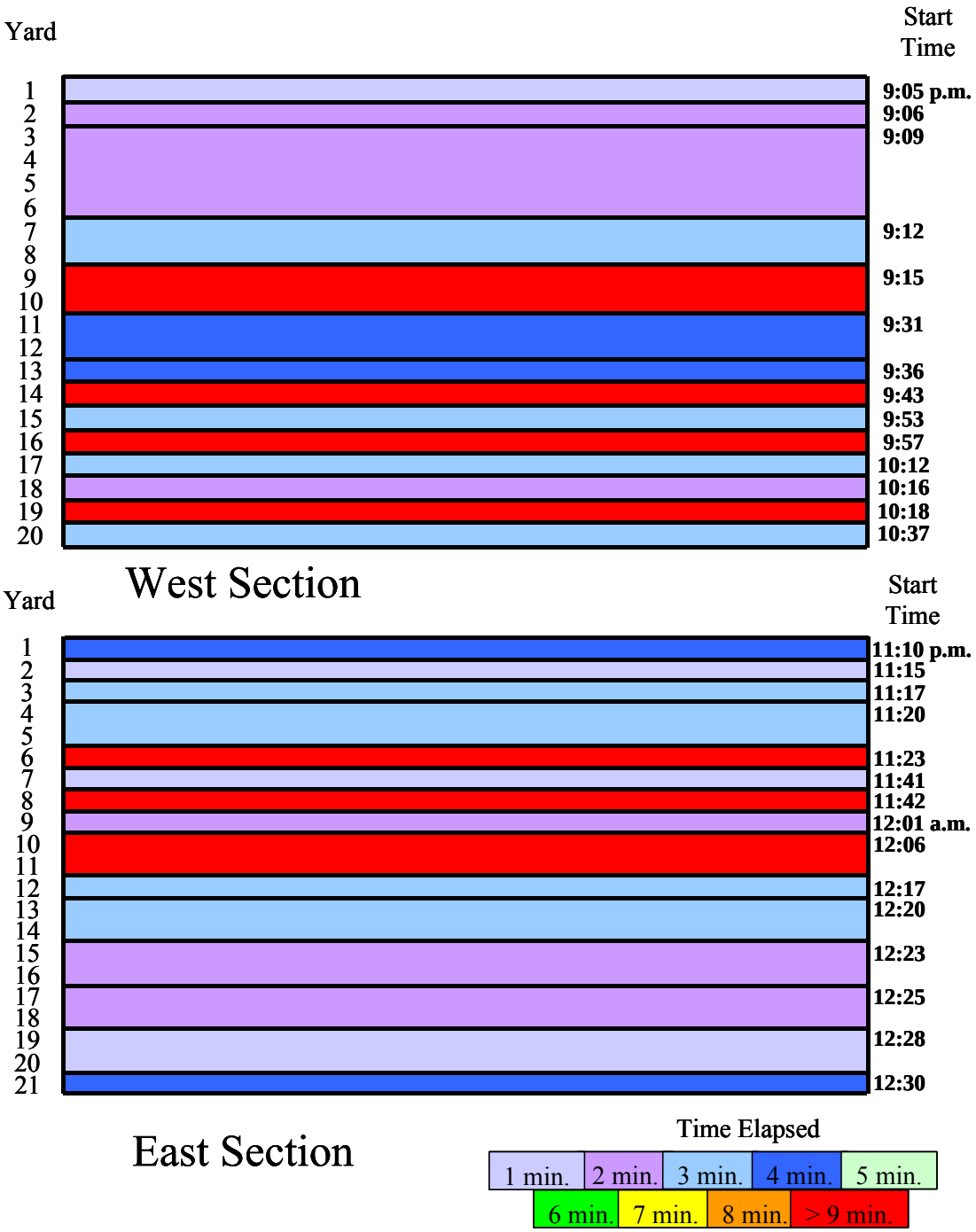

Figure 5-29. S05 of 82191, Concrete placement, time elapsed per yard

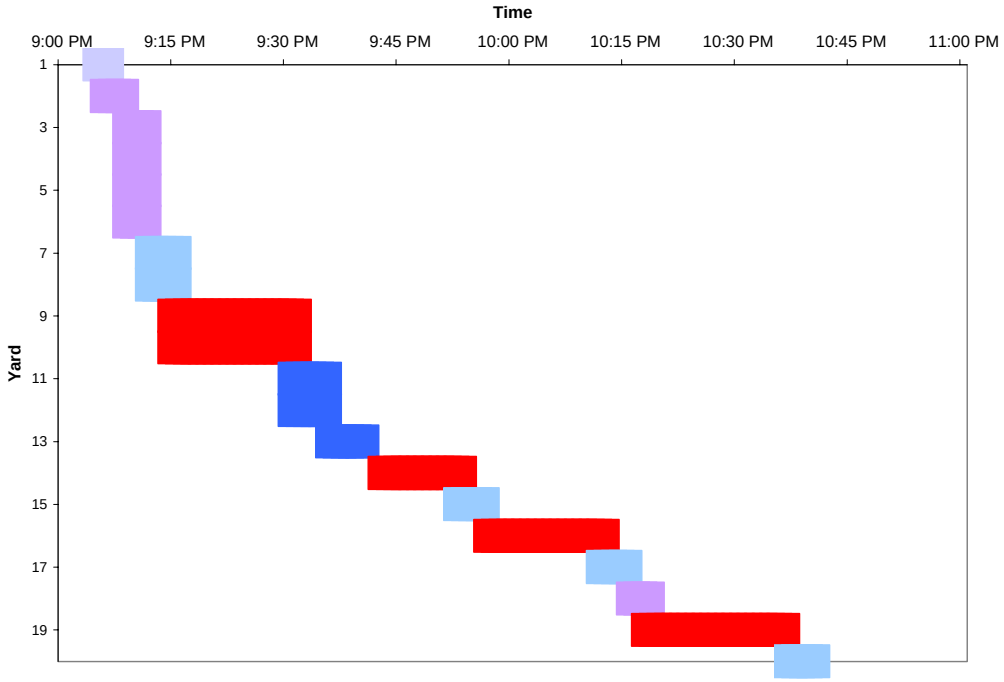

Figure 5-30. S05 of 82191, West section concrete placement time sequence

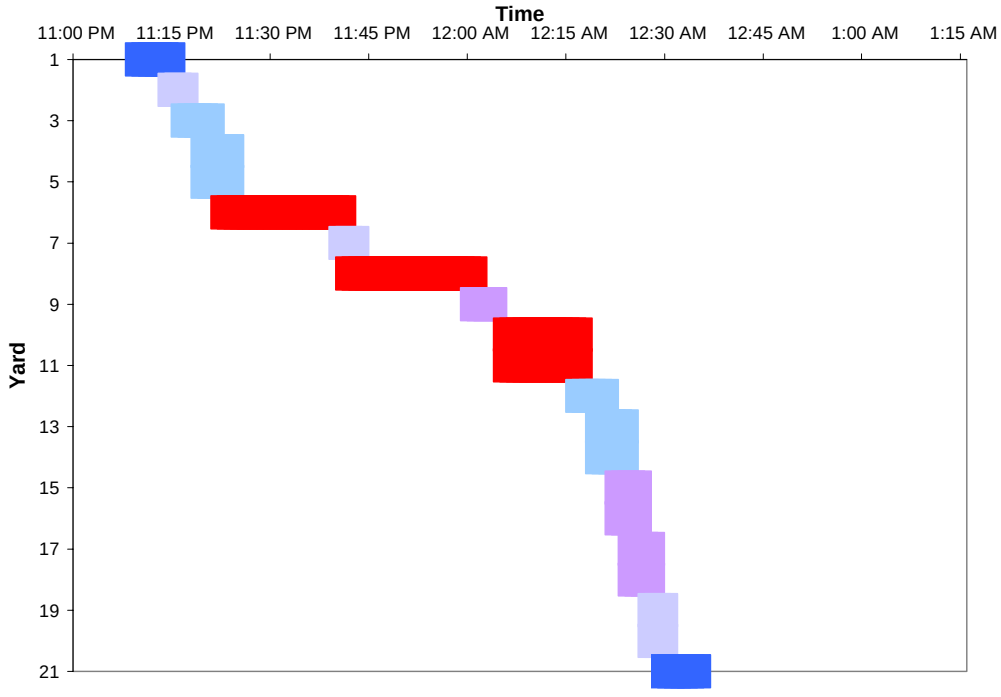

Figure 5-31. S05 of 82191, East section concrete placement time sequence

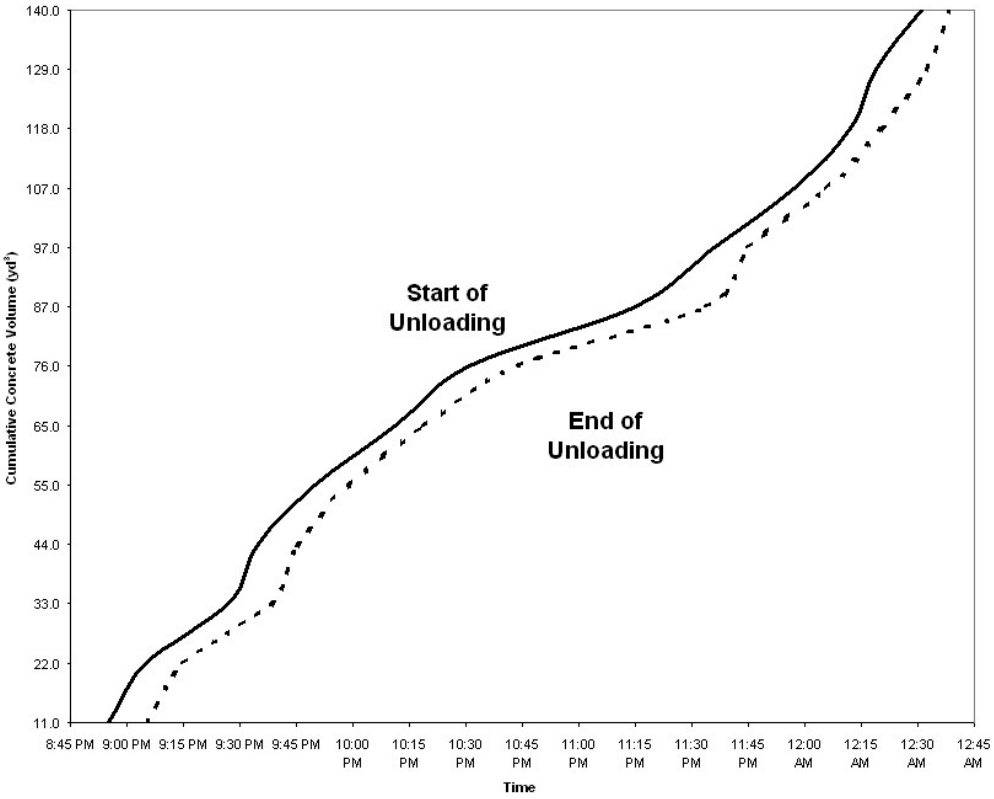

Figure 5-32. S05 of 82191, Cumulative concrete placed vs time elapsed

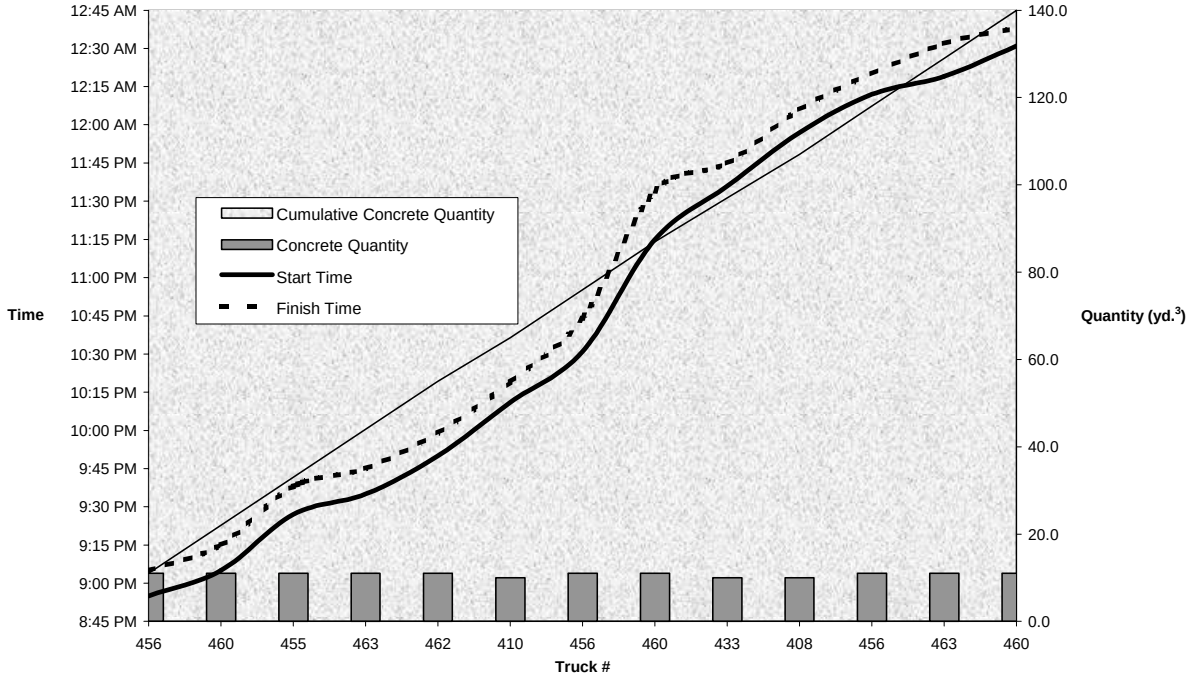

Figure 5-33. S05 of 82191, Time and volume of concrete placed vs truck arrival

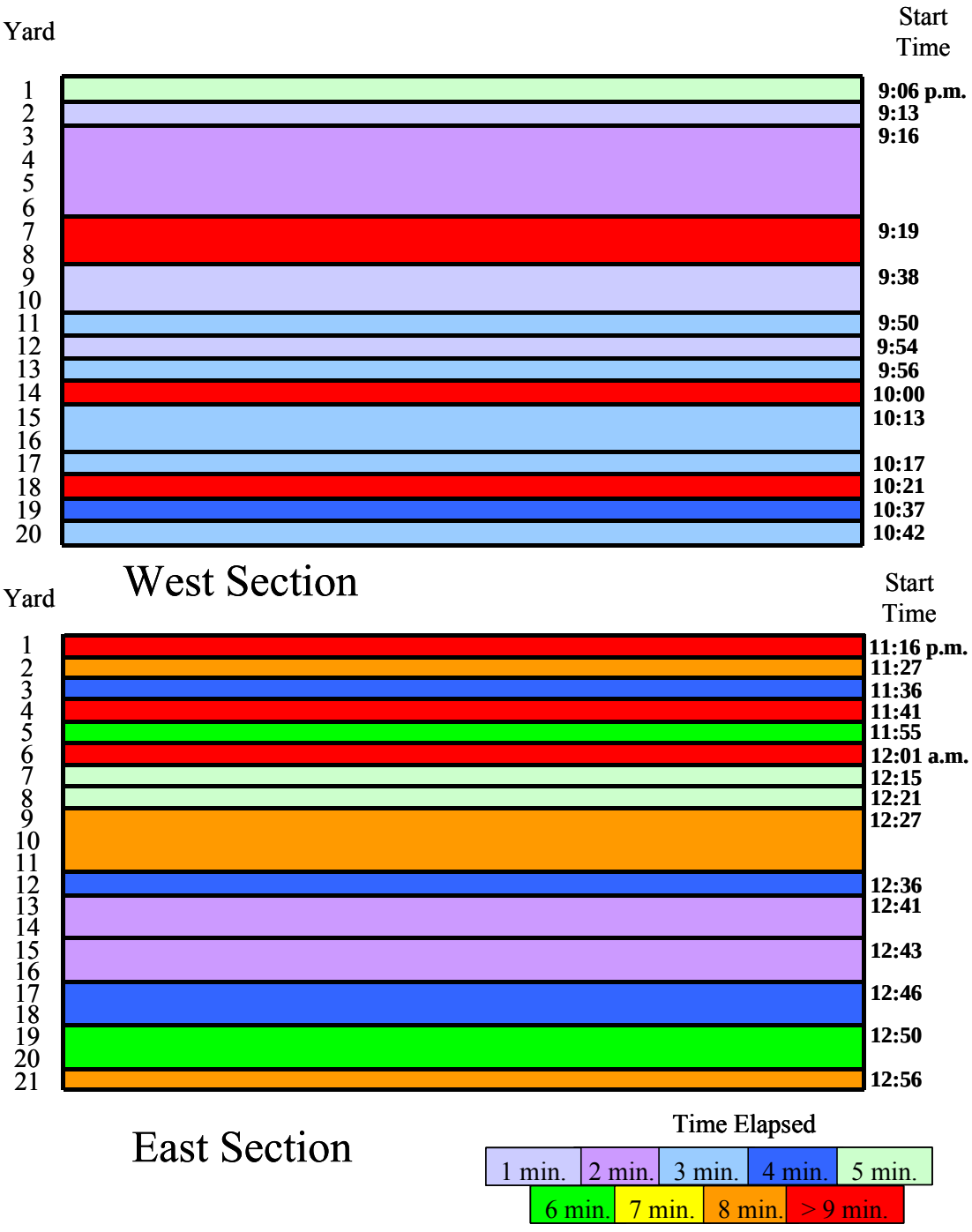

Figure 5-34. S05 of 82191, Concrete finishing, time elapsed per yard

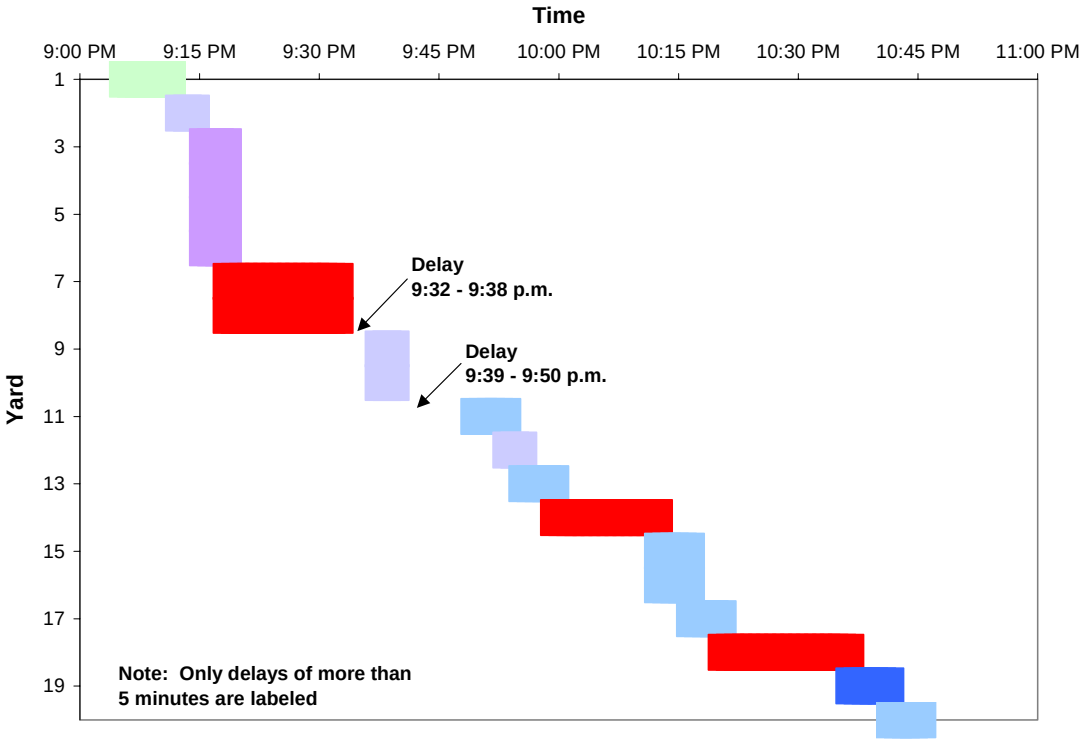

Figure 5-35. S05 of 82191, West section concrete finishing time sequence

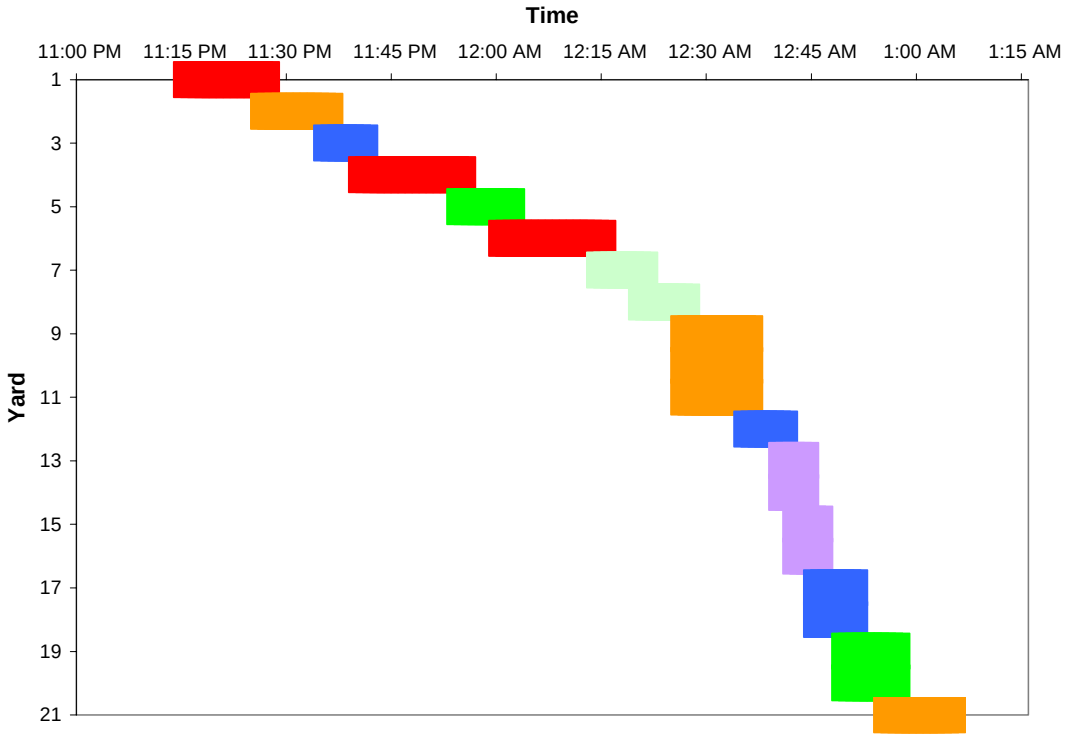

Figure 5-36. S05 of 82191, East section concrete finishing time sequence

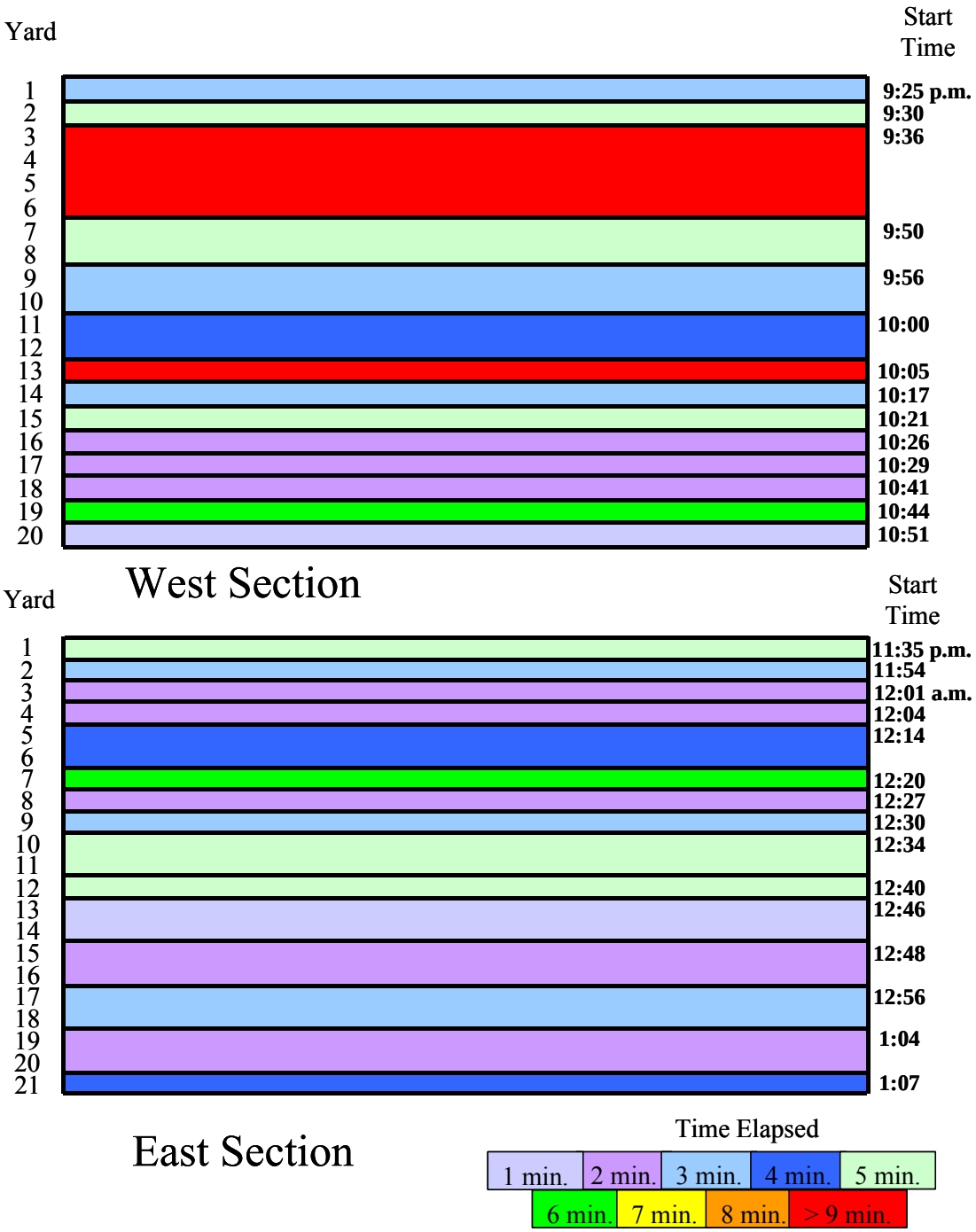

Figure 5-37. S05 of 82191, Concrete texturing, time elapsed per yard

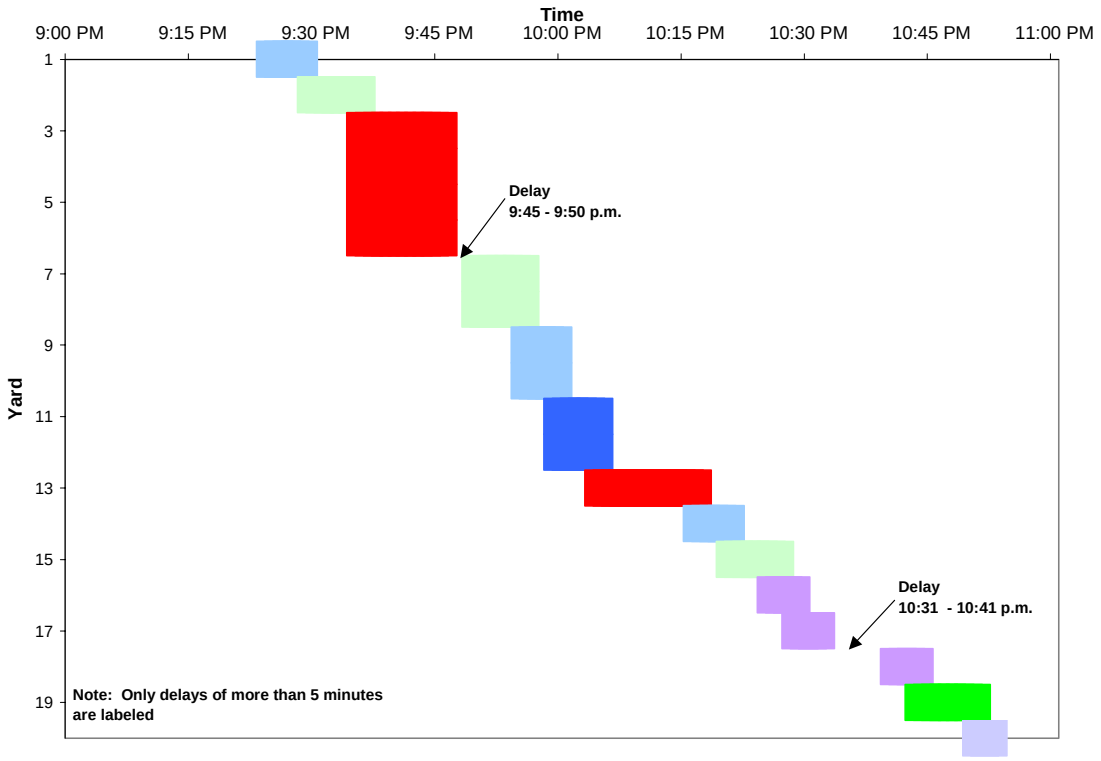

Figure 5-38. S06 of 82191, West section concrete texturing time sequence

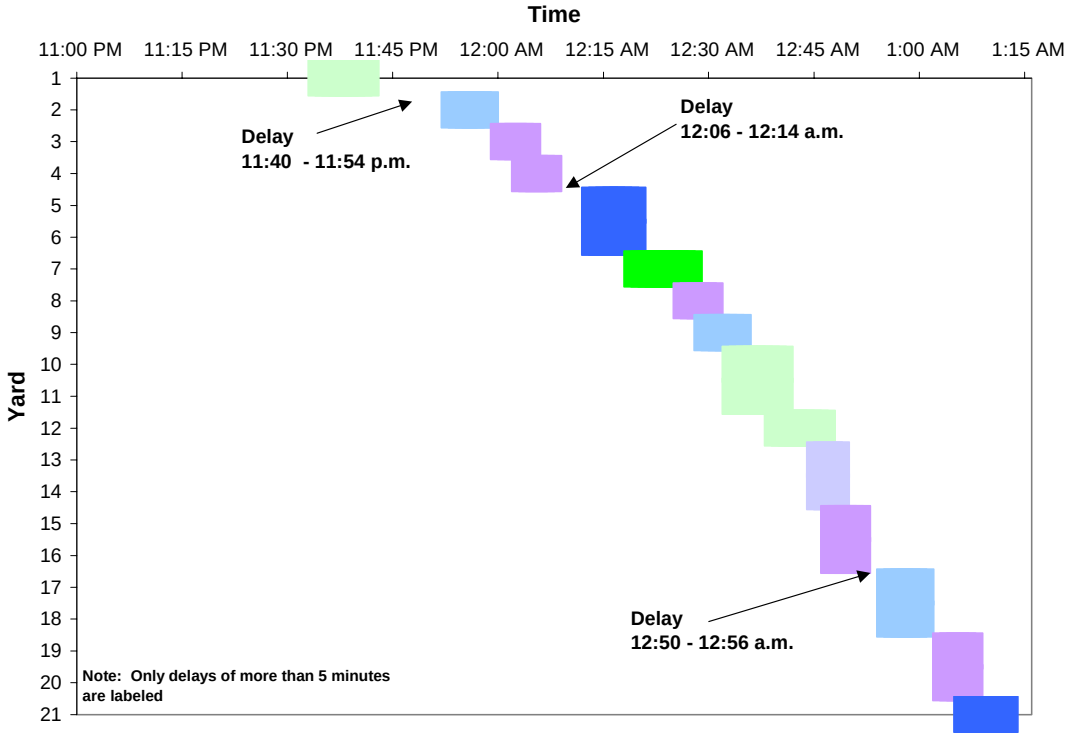

Figure 5-39. S05 of 82191, East section concrete texturing time sequence

5.4.4 Bridge ID S05 of 82025

Figure 5-40 shows the sequence of concrete placement for the monitored sections of the deck. Figure 5-41 shows the information for the section monitored in a bar chart format, allowing one to clearly see where any delays occurred. Figure 5-42 demonstrates the relationship between cumulative volume of concrete placed and elapsed time, while Figure 5-43 shows the fluctuation in placement time of concrete as it arrives on the trucks. Figure 5-44 and Figure 5-45 show data for the finishing of concrete with regard to time elapsed and observed delays. Texturing data is presented in Figure 5-46 and Figure 5-47. Information with regard to application of curing compound may be seen in Figure 5-48 and Figure 5-49.

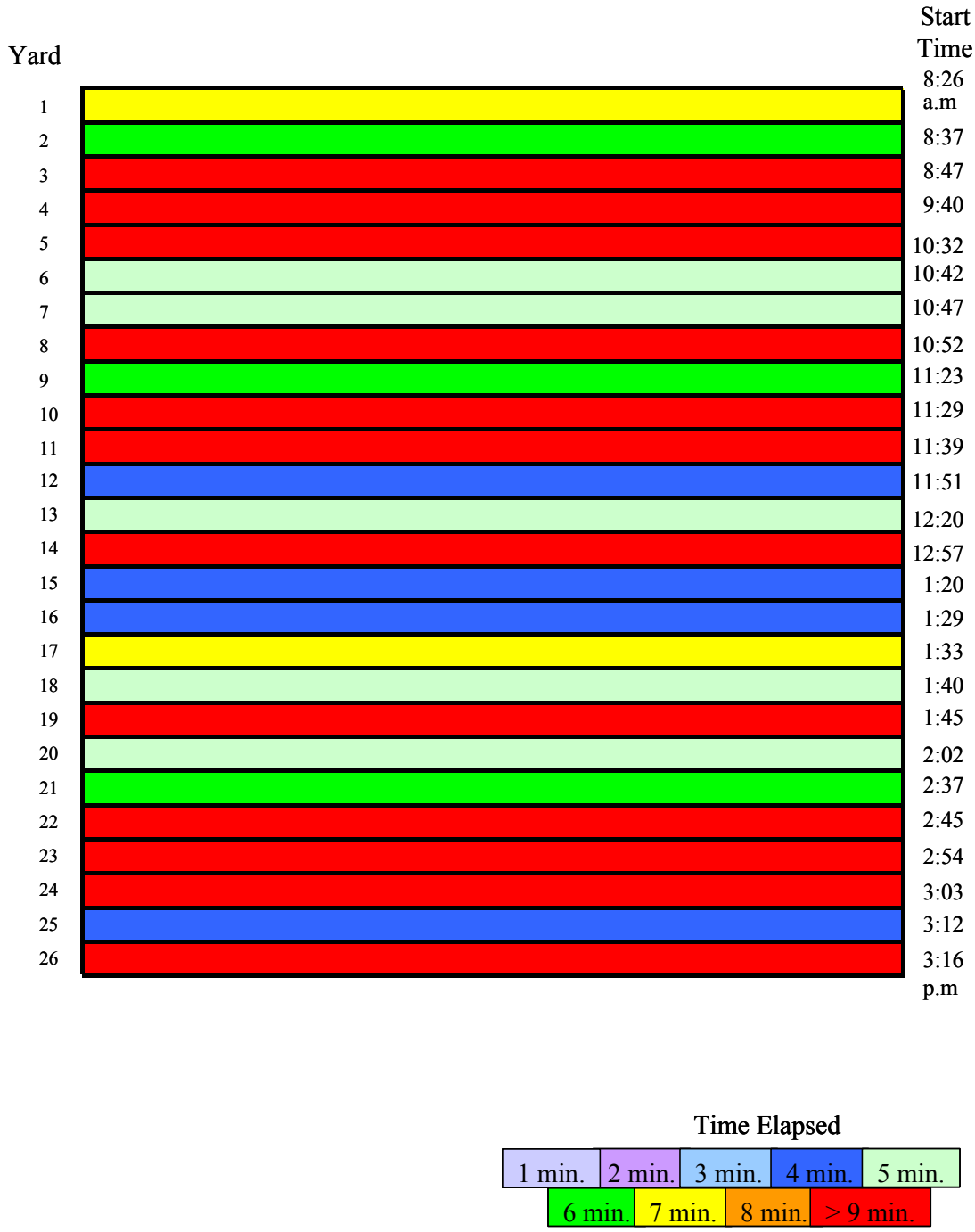

Figure 5-40. S05 of 82025, Concrete placement, time elapsed per yard

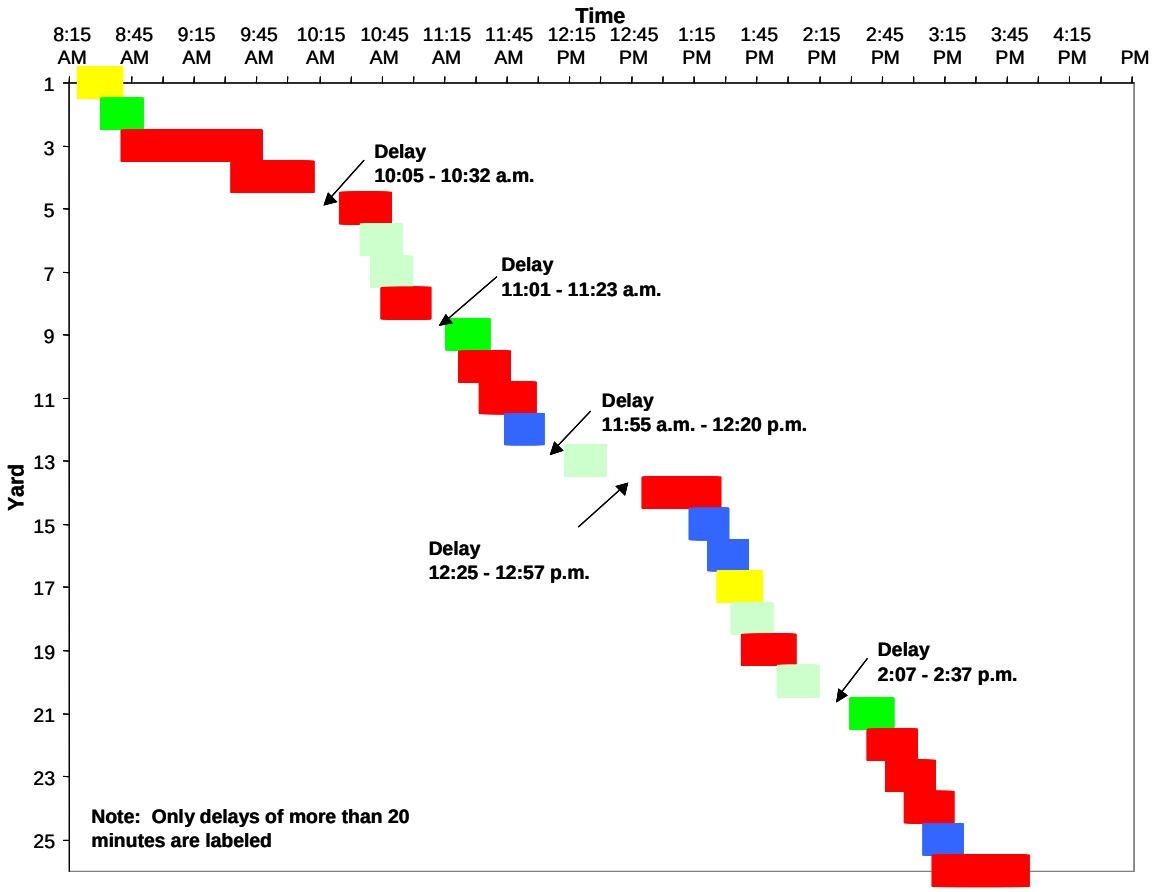

Figure 5-41. S05 of 82025, Concrete placement time sequence

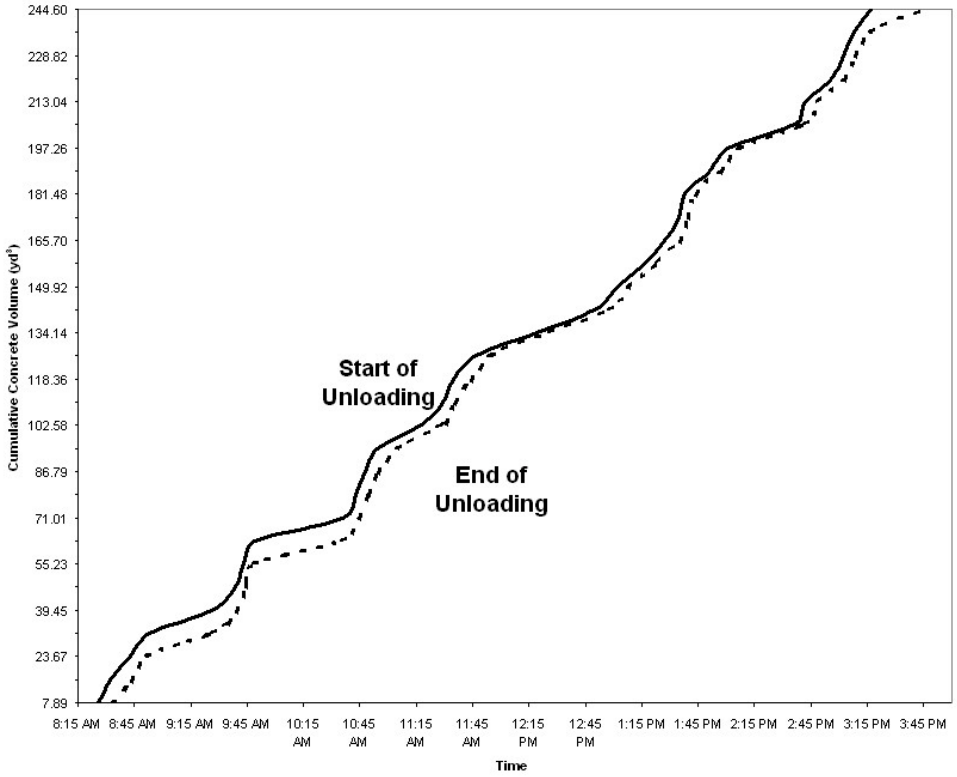

Figure 5-42. S05 of 82025, Cumulative concrete placed vs time elapsed

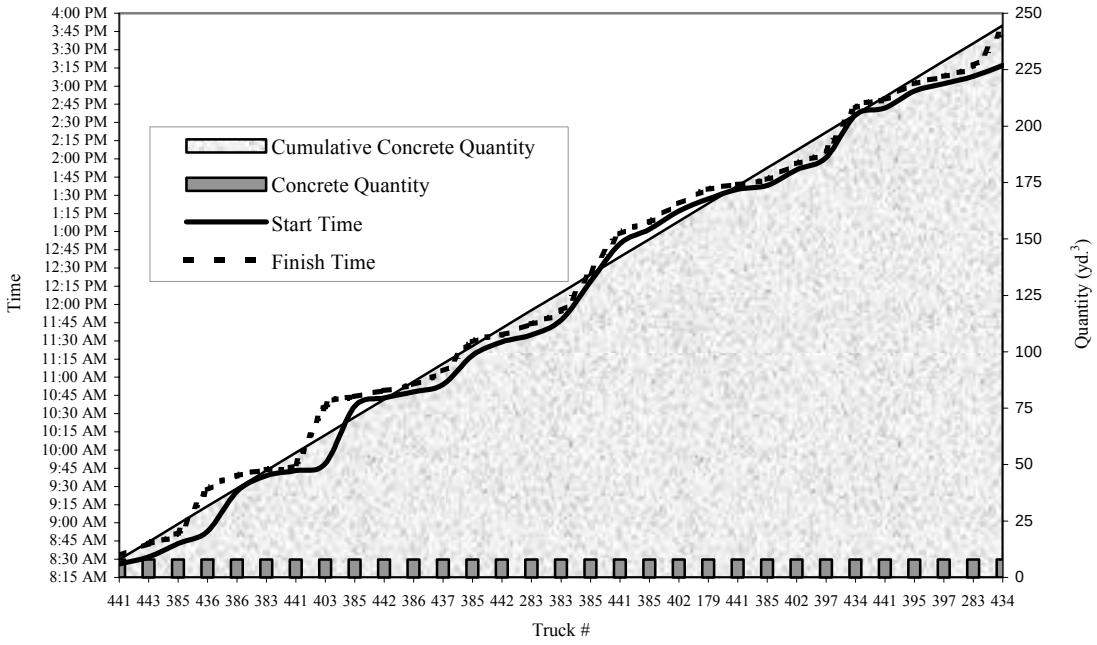

Figure 5-43. S05 of 82025, Time and volume of concrete placed vs truck arrival

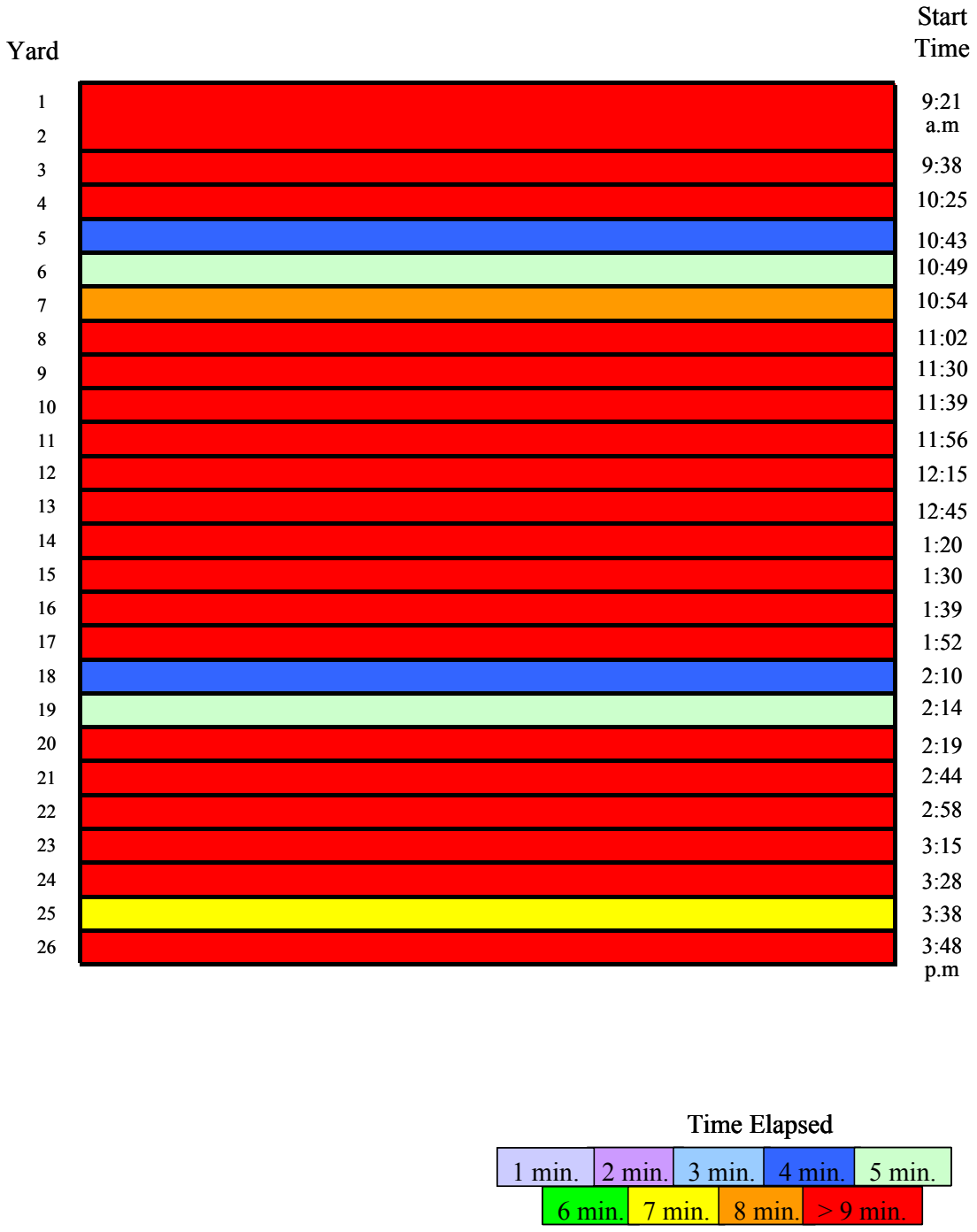

Figure 5-44. S05 of 82025, Concrete finishing, time elapsed per yard

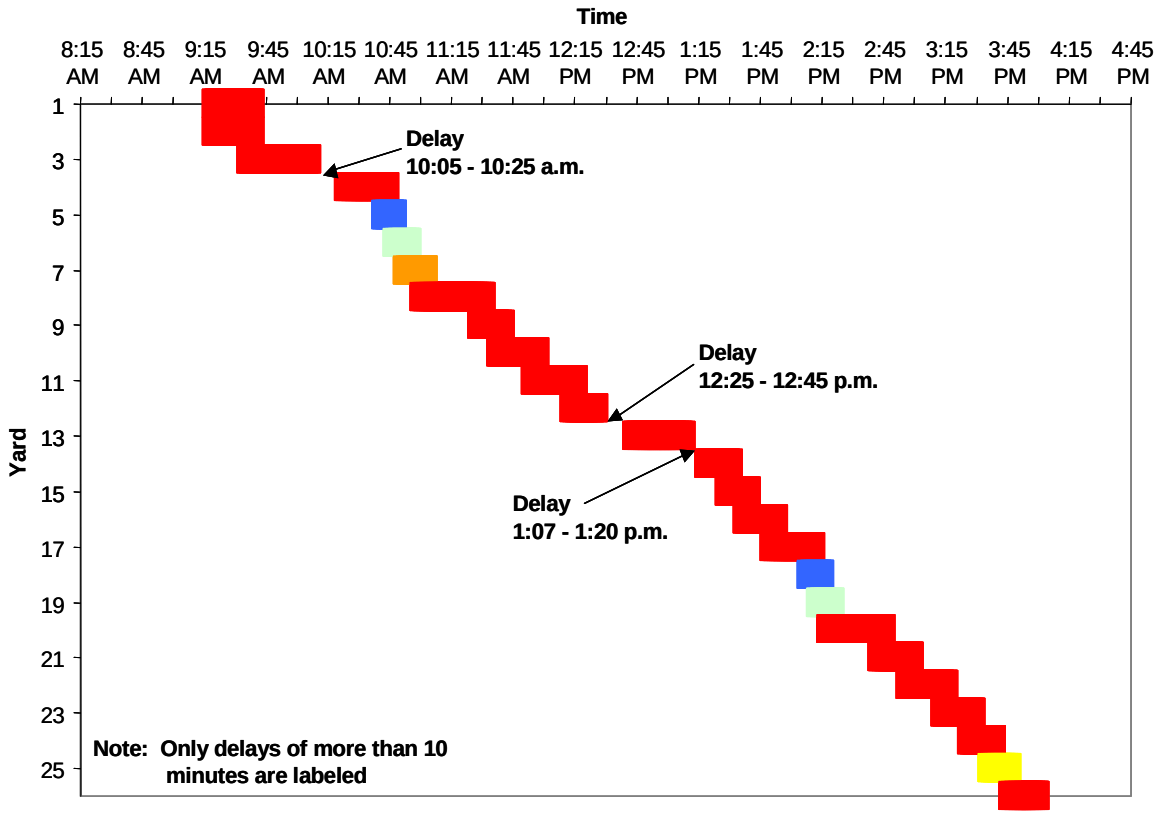

Figure 5-45. S05 of 82025, Concrete finishing time sequence

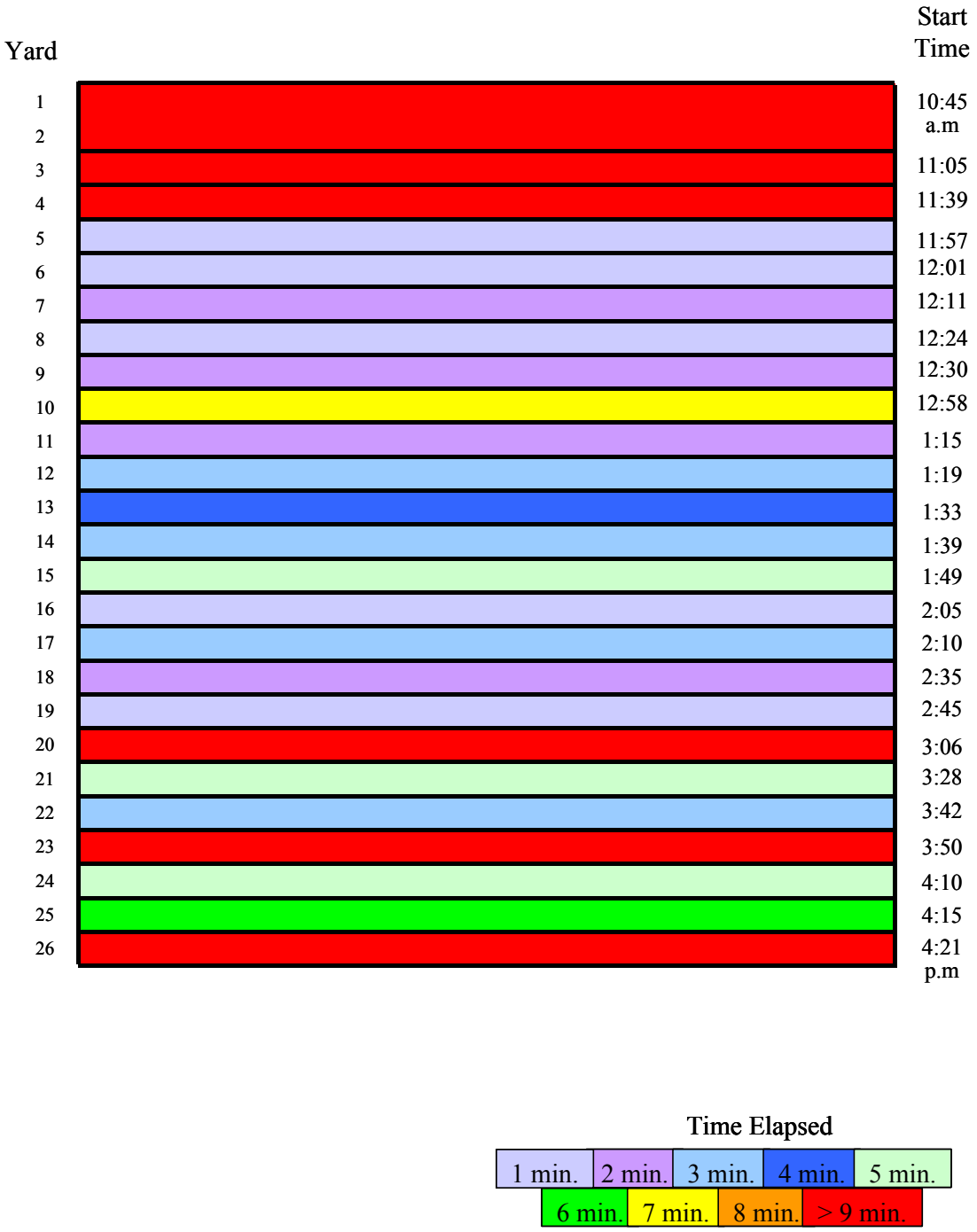

Figure 5-46. S05 of 82025, Concrete texturing, time elapsed per yard

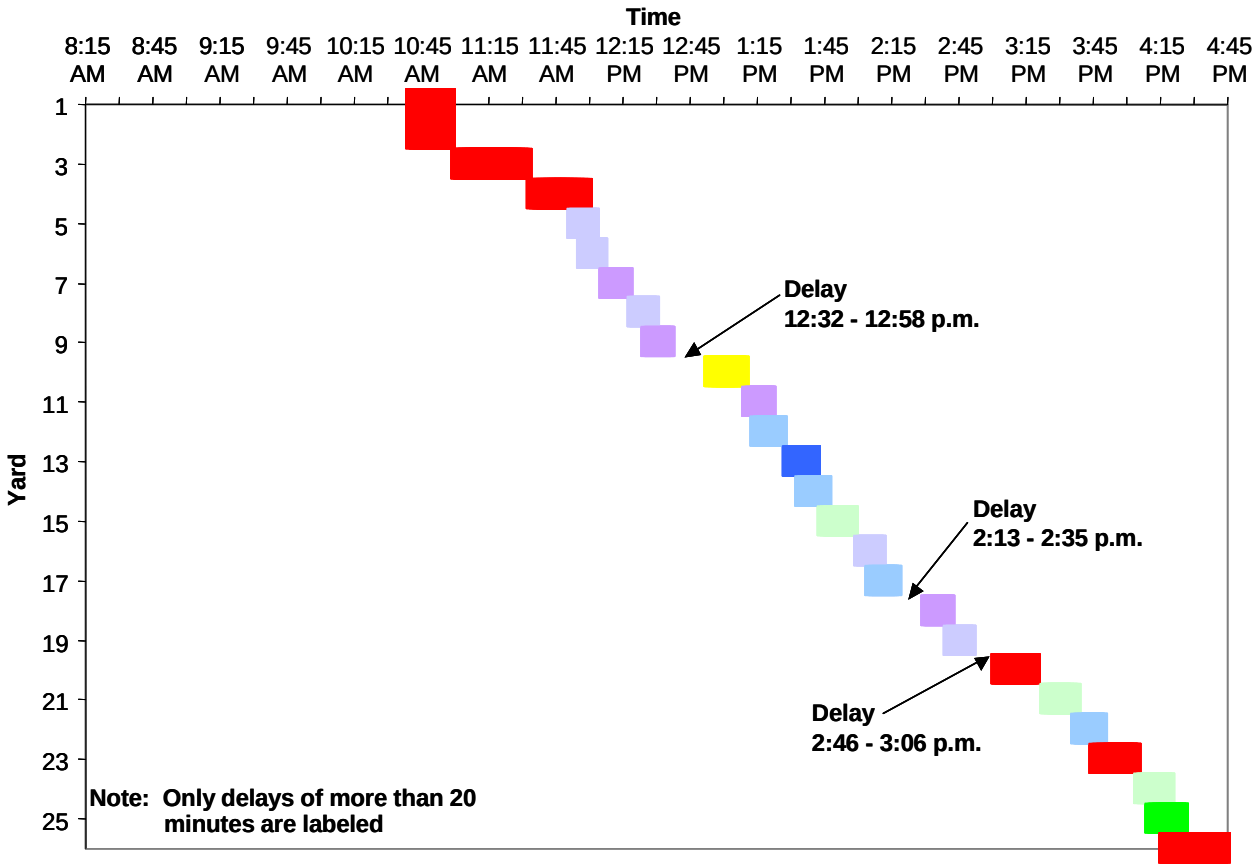

Figure 5-47. S05 of 82025, Concrete texturing time sequence

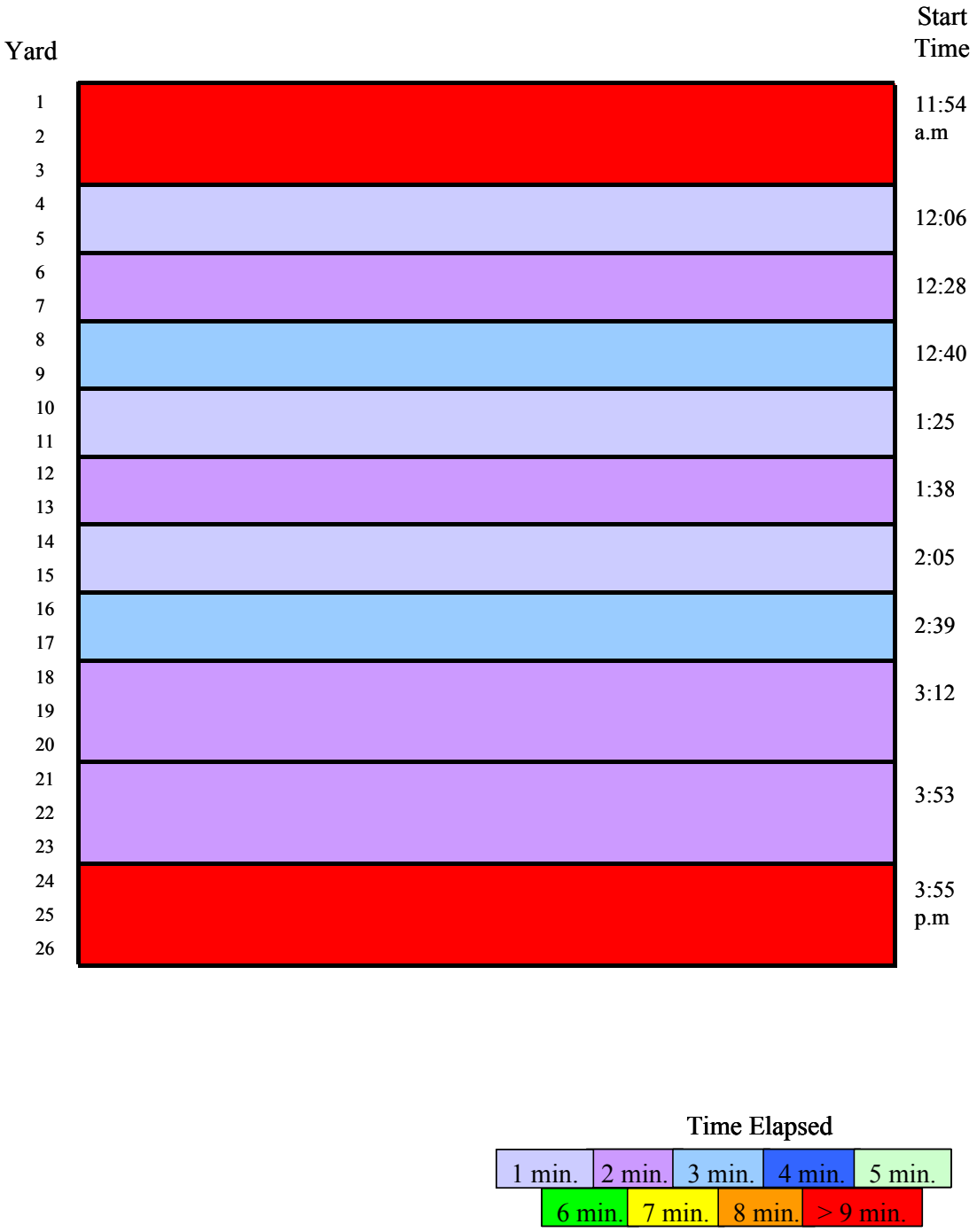

Figure 5-48. S05 of 82025, Curing compound application, time elapsed per yard

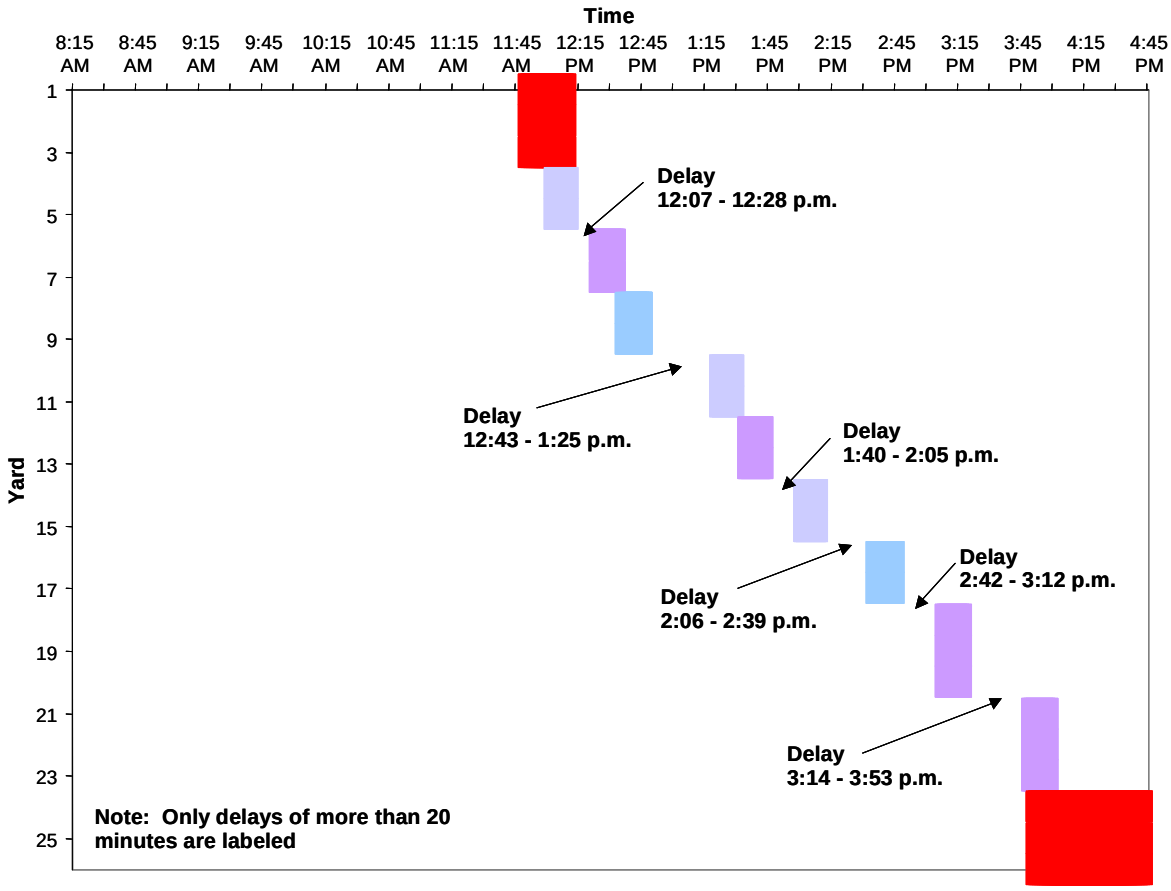

Figure 5-49. S05 of 82025, Curing compound application time sequence

5.4.5 Summary of Construction Monitoring Data

During construction monitoring, the purpose was to observe the procedures and the process timelines for concrete placement, texturing, and curing. The main focus was to identify the interruptions and delays that occurred during the process and their significance. As an example, the process timelines of concrete placement, texturing, and curing of bridge S05 of 82025 are depicted in Figure 5-50. Table 5-5, Table 5-6, Table 5-7, and Table 5-8 summarize the data gathered with regard to concrete placement, texturing, and curing compound application procedures for bridges S06 of 82194, S26 of 50111, S05 of 82191, and S05 of 82025 respectively. These tables provide data on start time and duration of each process, elapsed time between two consecutive processes, and the maximum delays that each process experienced. In the case of bridge S20 of 50111, the collected data was inconsistent and difficult to interpret; therefore, it was not included in the analysis.

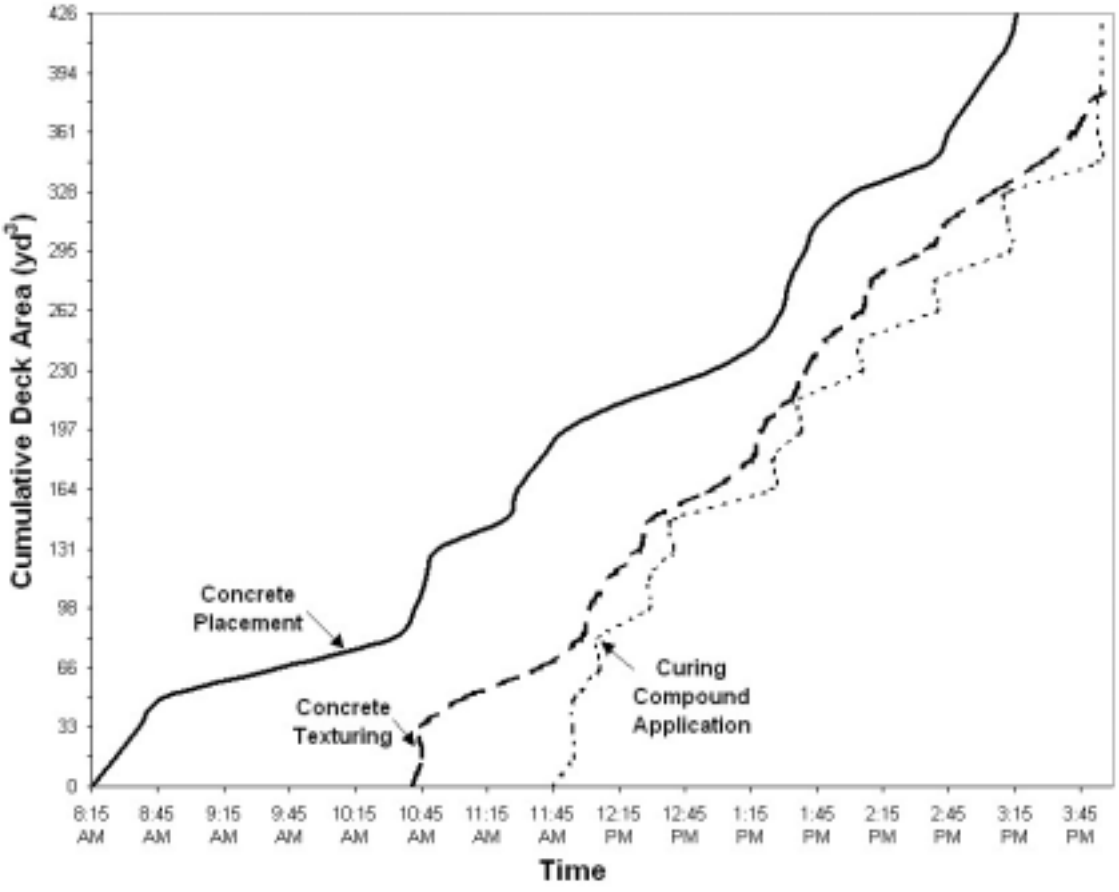

Figure 5-50. Summary of construction monitoring data of bridge S05 of 82025

Table 5-5. Summary of Construction Monitoring Data for Bridge S06 of 82194

Bridge ID		Section	Placement	Texturing	Curing
S06 of 82194	Start Time	S	9:33 p.m.	9:48 p.m.	1:40 a.m.
		N	9:48 p.m.	10:34 p.m.	
	Duration (Hours)	S	1:57	2:57	0:45
		N	3:36	3:45	
	Elapsed Time (Hours)	S	0:15		3:52
		N	0:46		
	Max: Duration Interrupted (Hours)	S	0:18	0:39	0:17
		N	0:32	0:39	

Table 5-6. Summary of Construction Monitoring Data for Bridge S26 of 50111

Bridge ID		Section	Placement	Texturing	Curing
S26 of 50111	Start Time	E	9:04 p.m.	9:42 p.m.	9:55 p.m.
		W	11:30 p.m.	12:16 a.m.	12:29 a.m.
	Duration (Hours)	E	1:56	2:33	2:30
		W	2:20	2:20	2:26
	Elapsed Time (Hours)	E	0:38		0:13
		W	0:46		
	Max: Duration Interrupted (Hours)	E	0:35	1:30	1:40
		W	0:00	0:14	0:38

Table 5-7. Summary of Construction Monitoring Data for Bridge S05 of 82191

		Section	Placement	Texturing	Curing
Bridge ID	**Start Time**	W	9:05 p.m.	9:25 p.m.	Curing compound was not applied until 1:15 a.m.
		E	11:10 p.m.	11:35 p.m.	
	Duration (Hours)	W	1:32	1:26	
		E	1:20	1:32	
S05 of 82191	**Elapsed Time (Hours)**	W	0:20		
		E	0:25		
	Max: Duration Interrupted (Hours)	W	0:00	0:10	
		E	0:00	0:14	

Table 5-8. Summary of Construction Monitoring Data for Bridge S05 of 82025

		Placement	Texturing	Curing
Bridge ID	**Start Time**	8:26 a.m.	10:45 a.m.	11:54 a.m.
	Duration (Hours)	6:50	5:36	4:01
S05 of 82025	**Elapsed Time (Hours)**	2:19		1:09
	Max: Duration Interrupted (Hours)	0:32	0:26	0:42

5.5 POST-CONSTRUCTION MONITORING OF BRIDGE DECKS

Photo 5-10 shows the replaced deck of the bridge S06 of 82194. This bridge deck replacement started on 8/19/2002, this was a two-day process. Inspection for early-age cracking was performed on 9/13/2002. The diamond ground deck surface was helpful when observing the early-age cracks. During the observations, several transverse cracks were identified (Photo 5-11). Several transverse cracks were also seen on the deck of bridge S05 of 82025 during post-construction inspection. Unfortunately, photographs are not available.

Photo 5-10. Replaced deck of bridge S06 of 82194

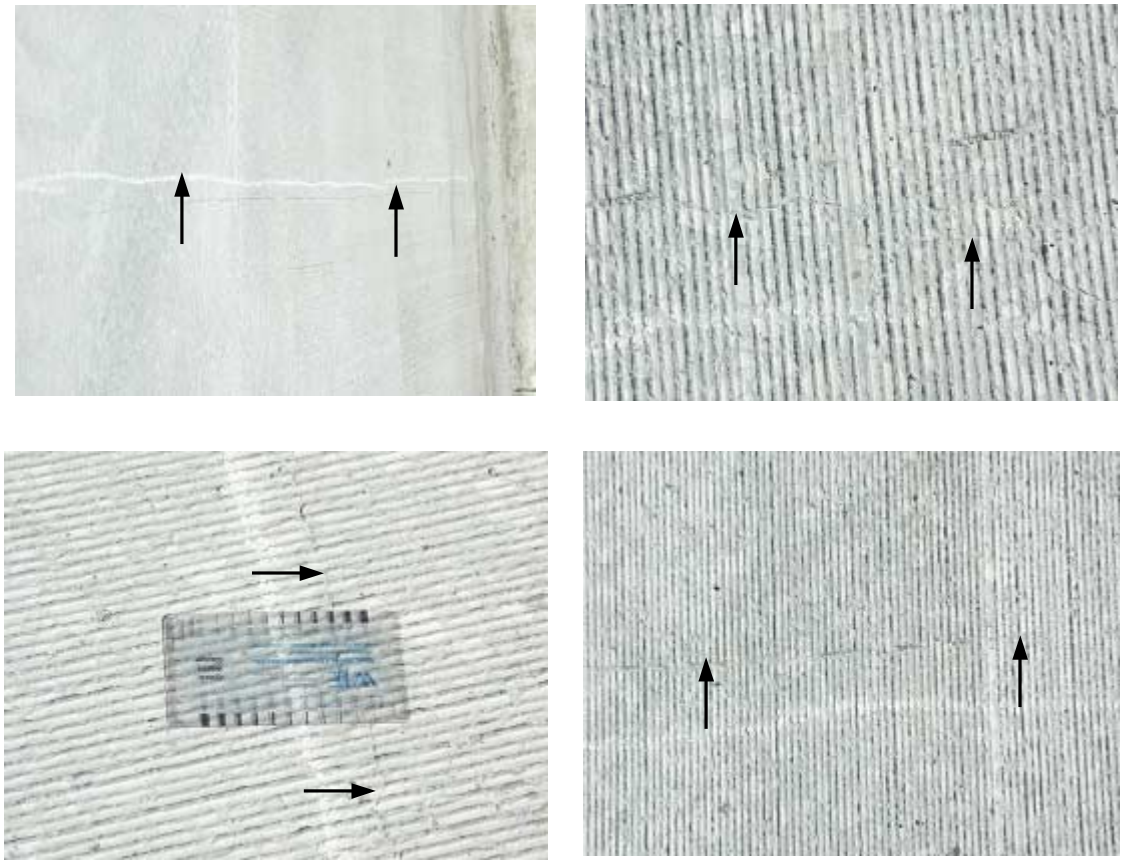

* Crack locations are shown with arrows

Photo 5-11. Observed cracking on replaced deck of bridge S06 of 82194

5.6 CONCLUSIONS

Five bridge reconstruction projects with deck replacements were selected with consideration to the construction dates. Construction monitoring of five bridges was completed including one late season deck replacement. During concrete placement, ambient temperature and ambient moisture conditions were recorded. Truck number, production time, truck arrival time, and unloading (start/finish) time were also recorded. Finally, starting and finishing time for concrete placement, finishing, texturing, and curing for the areas within an approximate one-yard width were monitored and recorded.

The requirements for the formwork, placement of steel reinforcements, placement of concrete, finishing of plastic concrete, and curing given in MDOT Section 706 of Standard Specifications for Construction were compared with the field observations.

The reinforcement as well as the interior of the formwork was cleaned before placement of concrete. The concrete crew made an effort to place the concrete uniformly and in its final position. Shovels were sometimes used to spread concrete from one location to another. It was hard to control the free-fall to within the required limit of 6 inches. Most often, free fall was about one foot. In certain instances, it was between two and three feet.

Additionally, concrete placement was sometimes interrupted due to delays in its delivery to the job site. The time data collected at the site during deck placement show that the delay sometimes exceeded 30 minutes. Consequently, the requirements in the Specifications stating that "sufficient vibrators shall be used to properly compact the incoming concrete within 15 minutes after placing" could not be satisfied. When the new concrete arrived and was placed on the deck, the old and the new portions were then consolidated together. In addition, the vibrator applications were random rather than following a distinct pattern as required in the Specifications.

Section 706.03 N of Standard Specifications for Construction describes the curing procedure for concrete bridge decks. When curing is considered, most of the Specification requirements were not met for the five projects that were monitored. One of the requirements in the Specifications is that more than 10 feet of textured concrete surface should not be left exposed without curing compound at any time. As reported earlier, this requirement was never satisfied. Out of five instances of construction monitoring, one time, a curing compound was applied after completing the placement of concrete on the full deck and in another instance, curing compound was not applied until sometime after the project team left the site, which was after the casting crew finished concrete placement, leveling, and texturing. Wet curing is another important requirement given in the Specifications. It requires covering the concrete with clean, contaminate-free wet burlap as soon as the curing compound has dried sufficiently to prevent adhesion and the concrete surface can support it without deformation. However, wet burlap should have been applied within two hours after the concrete was cast. Based on the observations, it can be concluded that the concrete surface was never covered with burlap until the next day.

Heavy equipment, such as mixers and slip form machines, are not be permitted on the deck until the deck concrete has reached an age of at least 7 days and then not until the concrete has attained at least 100 percent of its minimum 28 day flexural or compressive strength. However, barrier casting started on some bridges when the bridge decks were seven days old. Therefore, mixers, slip-form machines, and several other vehicles traveled and parked on the newly placed bridge decks.

It was observed that on one deck with super elevation (S06 of 82194), fresh concrete did not have sufficient stiffness and therefore flowed to one side. The deck surface needed to be diamond ground in order to achieve appropriate leveling. In all of the bridge decks, the construction or expansion joint boundaries were observed to be quite problematic during placement. Excess concrete overflows, loses its plasticity and it is scraped off and thrown in with the deck concrete near the joint. This creates a substandard quality concrete near the joint. Deterioration often starts at the joints. During placement, the concrete that falls off the joints should not be placed back on the deck.

In two decks (S20 of 50111 and S05 of 82025), the specimens prepared for the laboratory testing were not fully set at approximately 12 hours after placement. Although the concrete mix design did not show increased use of set-retarders, these observations show otherwise.

6 FIELD AND LABORATORY TESTING

6.1 OVERVIEW

Determination of mechanical and other important physical properties related to concrete durability may be accomplished through several standard tests. Mechanical properties of deck concrete are obtained from compressive strength and elasticity modulus tests in accordance with ASTM C39 and ASTM C 469 respectively. The compressive strength test is the most common test performed on hardened concrete. There is a strong correlation between the properties of concrete and its compressive strength. This test was used to evaluate the performance of the materials and can help establish the necessary mixture proportion to attain the required strength. An additional advantage of this test is its ability to control the quality of the concrete in the field.

Elasticity modulus and Poisson's ratio tests provide a value for stress to strain ratio and a ratio of lateral to longitudinal strain for hardened concrete at any designated curing age. The modulus of elasticity and Poisson's ratio values are applicable in stress ranges from 0 to 40% of the ultimate concrete strength. This method is helpful in sizing of reinforced and non-reinforced structural members, establishing the quantity of reinforcement, and computing the stress from intrinsic strains. In addition, by conducting compressive strength, elasticity modulus, and Poisson's ratio tests at different ages of concrete, the variation of mechanical properties with respect to time is established and may be used for further analysis of causes of distress.

The ultrasonic pulse velocity (UPV) test measures the velocity of an ultrasonic wave passing through the concrete. The pulse velocity of compressive waves in concrete is related to its elastic properties and density. This test method is used to evaluate the uniformity and relative quality of concrete, to indicate the presence of voids and cracks, to estimate the depth of cracks, and to evaluate the effectiveness of crack repairs. It may also be used to identify changes in the properties of concrete, and in the survey of structures, to estimate the severity of deterioration of cracking. From ultrasonic pulse velocity, dynamic elasticity modulus can be calculated. This test is performed in compliance with ASTM C597.

The rapid chloride permeability test (RCPT) is performed in accordance with ASTM C 1202. This test is useful in determining the electrical conductance of concrete and provides an

indication of its resistance to penetration of chloride ions. The absorption and air permeability tests are useful in developing the data required for the calculation of void ratio and to obtain the limits of absorption. Concrete with large or many pores is not desirable due to its lack of ability to protect itself from environmental attacks (i.e. chloride ion penetration); therefore, it is ideal to obtain a low pore-volume ratio for quality concrete. The absorption test is performed in compliance with ASTM C642. The air-permeability test is performed using a special apparatus not yet specified by ASTM.

6.1.1 Samples Obtained During Construction Monitoring

A comprehensive list, which enumerates the tests performed on the cylinder specimens and the required number of samples for the tests, is given in Table 6-1. Compressive strength, elasticity modulus, Poisson's ratio, rapid chloride permeability test (RCPT), ultrasonic pulse velocity (UPV), air-permeability, and absorption tests were conducted and the test results are shown in Table 6-3, 6-4, 6-5, 6-6, 6-7, 6-8, and 6-9 respectively.

Table 6-1. Tests to be Conducted and the Required Number of Samples

Tests	Type of Specimen	Number of Specimens	Test Days					Total Number of Specimens
			3	7	28	56	90	
Compressive Strength (ASTM – C 39)	6 x 12 in	4	x	x	x	x	x	20
Modulus of Elasticity (ASTM – C 469)	6 x 12 in	2	x	x	x	x	x	10
UPV (ASTM – C 597)	4 x 8 in	12	x	x	x	x	x	12
Permeability	4 x 2 in	4			x	x	x	12
RCPT (ASTM – C 1202)	4 x 2 in	4			x	x	x	
Absorption (ASTM – C 642)	4 x 2 in	4			x	x	x	

6.1.2 Test Procedures for Samples Obtained During Construction Monitoring

During the placement of concrete bridge decks, a number of cylindrical test specimens (minimum thirty-two 6-in.x12-in. and twenty four 4-in.x 8-in.) were prepared for laboratory testing according to Table 6-1. The specimens were kept in the field for one day. After twenty-four hours, specimens were taken to the laboratory. Specimens were cataloged according to their size and wet cured for 28 days. After the 28 days of initial curing, the specimens were kept under ambient laboratory air. Compressive strength, modulus of elasticity, Poisson's ratio, and ultrasonic pulse velocity tests were conducted at the ages of 3, 7, 28, 56, and 90 days. Rapid chloride permeability (RCPT), absorption, and air-permeability tests were conducted at the ages of 28, 56, and 90 days. The test schedule and the laboratory data sheets are presented in Appendix D and Appendix E respectively.

6.1.3 Test Procedure for Fresh Concrete Properties

Standard field tests are conducted on freshly mixed concrete to ensure that the material is properly constituted to meet the requirements of a particular construction task. For most construction projects involving the use of concrete, these field tests are the quickest and most cost effective way to make certain that the composition of the concrete used is right for the job. The tests conducted are the C143-Slump of Portland Cement Concrete, C231-Air Content of Freshly Mixed Concrete (Pressure Method), and C1064-Temperature of Freshly Mixed Portland Cement Concrete.

6.2 TEST RESULTS

6.2.1 Fresh Concrete Properties

Table 6-2. Field Tests for Quality Control of Fresh Concrete

Bridge ID	Slump (inches)	Air Content (%)	Concrete Temperature (^{o}F)
S05 of 82191	7	7	89
S06 of 82194	5	6.5	78
S26 of 50111	5	7.4	75
S20 of 50111	5	7.2	78
S05 of 82025	4	6.2	60

6.2.2 Construction Monitoring Samples

Tables 6-3, 6-4, and 6-5 show mean values and coefficient of variance for compressive strength, elasticity modulus, and Poisson's ratio respectively. Rapid Chloride Permeability Test (RCPT), Ultrasonic Pulse Velocity (UPV), air permeability, and absorption test results are given in Tables 6-6, 6-7, 6-8, and 6-9 respectively.

All the tests were conducted according to ASTM Standards and the respective Standards are given in Table 6-1. Air permeability tests were performed at University of Windsor.

Table 6-3. Compressive Strength Test Results

Bridge ID	Compressive Strength (psi)									
	$f'_{c,3}$	COV (%)	$f'_{c,7}$	COV (%)	$f'_{c,28}$	COV (%)	$f'_{c,56}$	COV (%)	$f'_{c,90}$	COV (%)
S05 of 82191	3580	5.2	4248	5.0	5098	6.4	5913	2.4	6090	3.2
S06 of 82194	3748	3.2	4455	2.2	5067	4.9	-	-	6245	4.0
S26 of 50111	4710	3.4	5353	4.0	-	-	7098	2.0	7283	3.3
S20 of 50111	4708	1.9	5550	4.0	-	-	7490	1.4	7417	1.4
S05 of 82025	5090	0.7	5650	2.3	6770	2.8	7628	1.9	7848	2.2

- Missing data

Table 6-4. Modulus of Elasticity Test Results

Bridge ID	Modulus of Elasticity (ksi)									
	$E_{,3}$	COV (%)	$E_{,7}$	COV (%)	$E_{,28}$	COV (%)	$E_{,56}$	COV (%)	$E_{,90}$	COV (%)
S05 of 82191	4519	-*	4818	-*	5216	-**	5392	2.9	5050	2.4
S06 of 82194	4761	-*	4654	-*	5402	1.7	-	-	4986	4.0
S26 of 50111	4195	-*	4515	-*	-	-	4225	2.0	3953	1.4
S20 of 50111	4412	-*	4627	-*	-	-	4432	0.6	4081	2.4
S05 of 82025	5424	-*	5386	-*	5877	2.9	5665	0.8	5630	0.9

- Missing data

-* - Only two readings are available

-** - Only three readings are available

Table 6-5. Poisson's Ratio Test Results

Bridge ID	Poisson's Ratio									
	$\nu_{,3}$	COV (%)	$\nu_{,7}$	COV (%)	$\nu_{,28}$	COV (%)	$\nu_{,56}$	COV (%)	$\nu_{,90}$	COV (%)
S05 of 82191	0.23	-*	0.24	-*	0.26	-**	0.24	2.4	0.25	5.4
S06 of 82194	0.25	-*	0.22	-*	0.25	2.5	-	-	0.25	3.8
S26 of 50111	0.25	-*	0.24	-*	-	-	0.24	4.7	0.21	0.2
S20 of 50111	0.25	-*	0.25	-*	-	-	0.23	1.2	0.23	4.9
S05 of 82025	0.25	-*	0.26	-*	0.25	2.0	0.26	3.2	0.25	2.5

- Missing data

-* - Only two readings are available

-** - Only three readings are available

Table 6-6. RCPT Test Results

Bridge ID	Test Age (days)	RCPT (Coulombs)					COV (%)
		#1	#2	#3	#4	Mean	
S05 of 82191	**28**	4830	4670	5700	4765	**4994**	10
	56	4770	4370	4940	3700	**4445**	12
	90	5380	9720	8470	6340	**7478**	26
S06 of 82194	**28**	3880	3290	3350	3460	**3495**	8
	56	-	7520	7020	-	-	-
	90	-	-	-	-	-	-
S26 of 50111	**28**	-	9220	-	-	-	-
	56	-	-	-	-	-	-
	90	8130	5850	6410	6780	**6790**	14
S20 of 50111	**28**	-	10660	-	-	-	-
	56	5485	5955	6210	5740	**5850**	5
	90	7700	7020	7800	6380	**7230**	9
S05 of 82025	**28**	-	-	-	-	-	-
	56	5390	9080	7700	7630	**7440**	21
	90	6500	6730	9930	7190	**7590**	21

- Missing data

Table 6-7. UPV Test Results

Bridge ID	UPV Speed (in/sec)				
	3 Day	7 Day	28 Day	56 Day	90 Day
S06 of 82194	-	-	199,000	200,000	201,000
S26 of 50111	182,000	183,000	186,000	184,000	179,000
S20 of 50111	178,000	183,000	186,000	186,000	181,000
S05 of 82191	-	-	194,000	196,000	196,000
S05 of 82025	195,000	193,000	203,000	206,000	206,000

- Missing data

Table 6-8. Air Permeability Test Results

Bridge ID	Test Age (Day)	Intrinsic Gas Permeability (in^2) 10^{-13}					COV (%)
		#1	#2	#3	#4	Mean	
S05 of 82191	28	3.4	2.7	2.8	4.4	**3.3**	23.1
	56	3.1	3.1	4.9	4.4	**3.9**	24.0
	90	-	-	-	-	-	-
S06 of 82194	28	3.2	3.0	3.6	4.9	**3.7**	23.9
	56	5.0	4.1	4.3	5.8	**4.8**	15.5
	90	13.9	6.9	10.2	8.3	**9.8**	30.8
S26 of 50111	28	8.7	8.1	11.1	9.6	**9.4**	14.0
	56	16.3	20.8	20.5	-	-	-
	90	-	-	-	-	-	-
S20 of 50111	28	5.4	5.9	6.0	5.3	**5.7**	6.0
	56	13.4	10.4	13.2	9.4	**11.6**	17.1
	90	-	-	-	-	-	-
S05 of 82025	28	-	-	-	-	-	-
	56	2.3	3.2	3.4	3.4	**3.1**	18.1
	90	-	-	-	-	-	-

- Missing data

Table 6-9. Absorption Test Results

Bridge ID	Volume of Permeable Pore Space (Voids), %					
	28 day	COV (%)	56 day	COV (%)	90 day	COV (%)
S05 of 82191	10.7	1.7	13.5	6.4	12.4	5.1
S06 of 82194	10.5	3.3	11.6	14.9	12.7	8.7
S26 of 50111	13.4	5.0	13.2	4.5	14.0	5.7
S20 of 50111	12.6	5.4	12.0	4.5	12.7	2.4
S05 of 82025	12.4	4.9	13.1	3.2	12.3	4.0

6.3 CONCLUSIONS

Determination of mechanical and permeability properties of concrete is accomplished through several standard tests. Mechanical properties of deck concrete are obtained from compressive strength and elasticity modulus tests in accordance with ASTM C39 and ASTM C469 respectively. In addition, the ultrasonic pulse velocity (UPV) test is performed in compliance with ASTM C597 to evaluate relative quality of concrete and to obtain elastic properties of deck concrete. The rapid chloride permeability test (RCPT) is performed in accordance with ASTM C1202 for evaluating the concrete resistance to chloride ion penetration. Permeability properties of deck concrete are obtained from the absorption and the air-permeability tests. The absorption test is performed in compliance with ASTM C642. The air-permeability test is performed using a special apparatus not yet specified by ASTM.

The conclusions that are drawn from the test results are as follows. Grade D concrete is used for concrete bridge decks in Michigan and the design compressive strength is 4000 psi, with a 28-day strength of 4500 psi. Test results indicate that out of the five bridges monitored, in possibly three of the bridges, deck concrete gained 28-day compressive strength in excess of 6000 psi. Concrete with a 28-day compressive strength greater than 6000 psi is classified as high strength concrete and requires special construction procedures. In addition, rapid increases in compressive strength and elasticity modulus are observed. Test results show that the strength and elasticity modulus of concrete increases with the age but the concrete resistance to permeability does not improve as expected. Therefore, there is no clear correlation between mechanical and permeability properties of concrete samples obtained from field samples. Though the strength requirements are satisfied as per design codes, durability of deck concrete is uncertain.

7 PARAMETERS INFLUENCING DECK CRACKING

7.1 OVERVIEW

The findings described in the chapters of this report – Literature Review, Multi-State Survey, and Construction Monitoring, indicate that there are a limited number of factors that influence early-age cracking of reinforced concrete bridge decks. The major parameter influencing early-age deck cracking is established to be the volume change due to shrinkage and thermal effects combined with the restraints caused by the girders and boundary conditions. It is also established that early-age cracking is the leading type of distress and its reduction or prevention will improve bridge deck service life.

Shrinkage and thermal effects are inherent to concrete construction. Cement hydration is an exothermic process that generates heat and consequently a temperature difference between the concrete mass and the ambient air. As discussed in Chapter 2, several factors affect the heat magnitude that develops within the concrete mass. At a specific duration after placement, during the hydration process, the concrete mass reaches its peak temperature. Consequently, a temperature gradient is formed between the interior and the exterior surface of the deck. As a result of the cooling process, tensile stresses develop at the bottom of the deck where the restraint is the highest.

There are computational tools to estimate the level of tensile stresses that will develop at the deck-girder interface due to volume change. Krauss and Rogalla (1996) derived a group of equations for calculating the restraint in a composite reinforced concrete bridge deck subjected to uniform and linear temperature distributions. These equations first calculate the girder and reinforcement restraints. The stresses due to the restraints at the top and bottom fibers of the deck are calculated next. The formulation considers multiple layers of reinforcement in the deck to account for the restraint effects of longitudinal deck reinforcement as well as stay-in-place (metal) forms. The evaluations of these equations for a Michigan deck are described in a subsequent section.

Using the equations derived by Krauss and Rogalla (1996), tensile stress developed at the deck-girder interface of a standard 9-inch concrete deck supported on Michigan 1800 girders (Figure

7-1) is calculated. A uniform temperature distribution within the concrete deck is assumed Figure 7-2). The peak thermal load is assumed to be reached at 12 hours after placement.

Thermal loads alone can generate significant stresses within the deck; for example, an 18 ^{0}F of differential thermal loading in conjunction with a typical girder restraint generates a tensile stress of 150 psi at the bottom of the deck. The tensile strength of concrete at early-age (12 hours after placement) can equal to the level of tensile stress developed at the bottom of the deck.

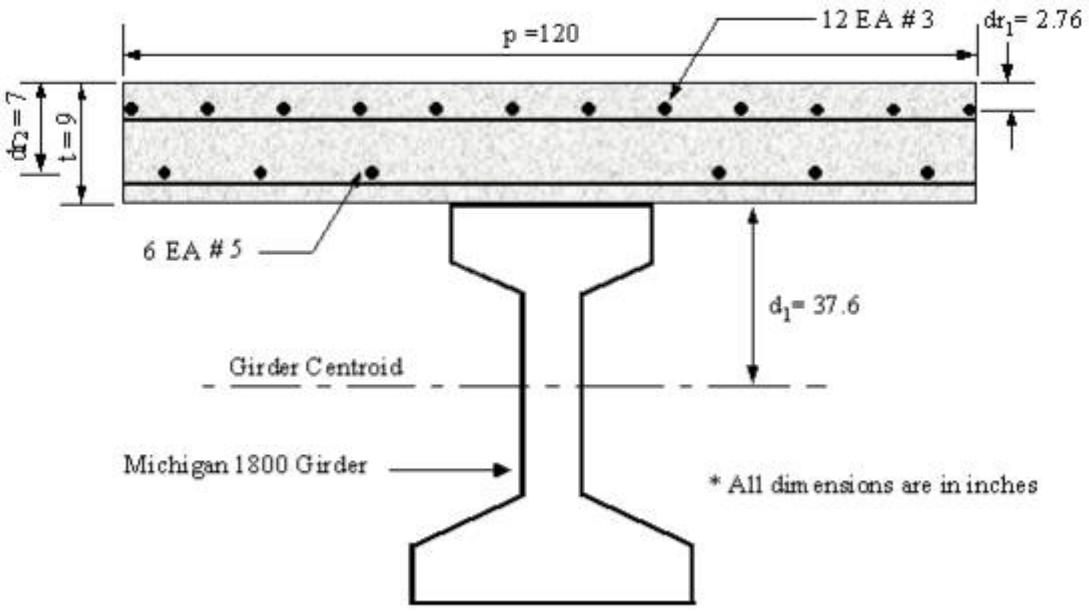

Figure 7-1. Geometry and reinforcement arrangement of the deck section supported on PCI girders

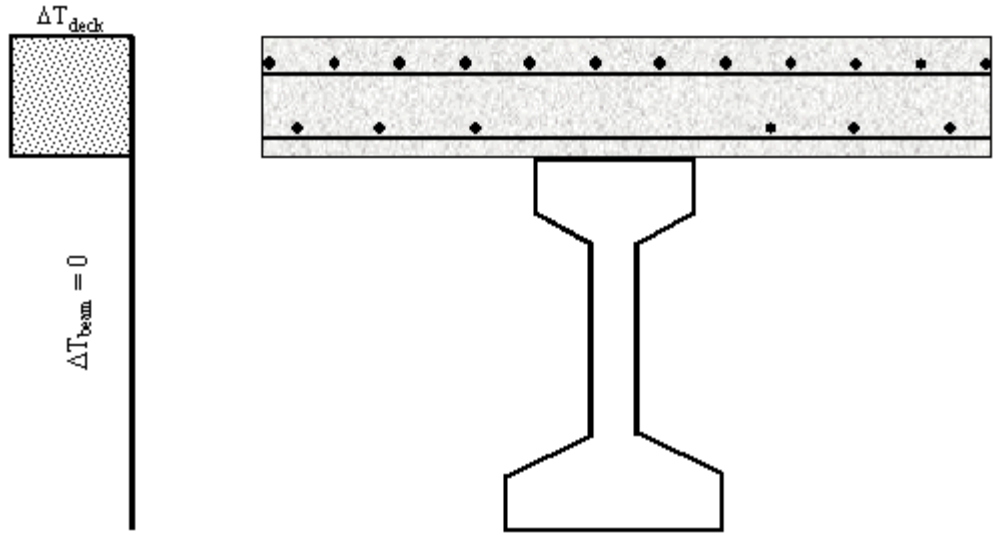

Figure 7-2. Uniform temperature distribution within the deck

Drying shrinkage begins as soon as concrete is placed. As discussed in Chapter 2, several factors affect drying shrinkage. Until concrete starts hardening, stresses do not develop due to lack of available restraint. When wet curing is not promptly initiated, though curing compound is applied, drying shrinkage stresses can develop. There are several shrinkage prediction models that estimate drying shrinkage following wet or moist curing. In this study, the interest is to calculate the drying shrinkage strain that forms before wet curing begins. Although, specific models for predicting the amount of very early-age drying shrinkage are not available, the formulation discussed in Chapter 2 for determination of rate of water evaporation from fresh concrete gives an indication of the importance of implementing appropriate curing procedure immediately upon concrete placement.

If drying shrinkage alone can be the cause of deck cracking at very early-age (12 hours after placement), a tensile stress of 150 psi at the bottom of the deck, which is about the same level as the tensile strength of concrete at that age, is required. Given the deck restraints from the girders and reinforcements, in order to generate a 150 psi tensile stress at the bottom of the 9-inch deck supported on Michigan 1800 girders, a drying shrinkage strain of 150 microstrain is required. According to ACI 209 (2001) the ultimate shrinkage strain of concrete is about 780 microstrain. Thus, attainment of a strain of 150 microstrain, which is 20% of ultimate shrinkage, within a day only due to drying shrinkage, is not realistic. For this reason, drying shrinkage cannot be the primary cause of deck cracking. The thermal loads must be the governing factor for early-age

deck cracking. However, the volume change due to shrinkage and thermal loading occurs simultaneously. Though the shrinkage contribution alone cannot induce cracking, the combined effects of shrinkage and thermal loading increase the cracking potential.

In order to provide a quantifiable detailed assessment of the volume change and restraint effects on early-age cracking, the knowledge of the change in the mechanical properties of concrete during early-age is important. The testing program conducted in this research obtained the compressive strength and elasticity modulus of concrete at 3, 7, 28, 56, and 90 days. The models for thermal and shrinkage effects require mechanical properties of concrete between 12 to 48 hours be known. For this reason, the estimation of compressive strength, elasticity modulus, and tensile strength of concrete at very early ages are discussed in the next section.

Shrinkage models can predict the shrinkage starting from the end of the wet or moist curing process. Although it is established that stresses due to thermal load alone can initiate deck cracking, volume change due to drying shrinkage will expose the cracks by increasing the width. Though the objective is to determine the causes of early-age deck cracking, the mitigation is not feasible unless all factors are investigated. For this purpose, the shrinkage prediction models are discussed for the quantification of shrinkage within the concrete deck upon the completion of wet curing.

7.2 PREDICTION MODELS FOR MECHANICAL PROPERTIES OF CONCRETE

The purpose of using the mechanical property prediction models is to have a continuous relationship describing concrete strength and elasticity modulus (stiffness) with respect to time. The following sections explain the process for selection of the prediction models to express the variation of compressive strength and modulus of elasticity of concrete with respect to time. To understand the initiation of concrete cracking, knowledge of direct tensile strength of concrete is required. A prediction model for direct tensile strength of concrete is also presented in a following section.

7.2.1 Compressive Strength

The two concrete compressive strength prediction models compared here are given by ACI and CEB-FIP.

ACI Committee 209 recommended model for moist-cured concrete made with normal Portland cement (ASTM Type I):

$$(f'_c)_t = \frac{t}{4 + 0.85t}(f'_c)_{28} \qquad (7\text{-}1)$$

The relationship suggested by CEB-FIP Models Code (1990) for concrete specimens cured at 20 ^{0}C (Mehta 1993):

$$(f'_c)_t = exp\left[s\left(1 - \left(\frac{28}{t/t_1}\right)^{1/2}\right)\right](f'_c)_{28} \qquad (7\text{-}2)$$

where $(f'_c)_t$ = mean compressive strength at age t days

$(f'_c)_{28}$ = 28-day compressive strength

s = coefficient depending on the cement type, such as s = 0.2 for high early strength cements; s = 0.25 for normal hardening cements; s = 0.38 for slow hardening cements

t = time in days

t_1 = 1-day

Both CEB-FIP and ACI 209 models require 28-day concrete strength for calculating compressive strength variation against time. A complete set of compressive strength test data is available only for three out of five bridge deck replacement projects (see Chapter 6). Therefore, CEB-FIP and ACI 209 predictions are compared with the test results obtained from deck concrete of bridges S05 of 82191, S05 of 82025, and S06 of 82194. Experimental data generated in this study shows high early-age strength. In that case, CEB-FIP Models Code (1990) requires using s = 0.2 for Eq. 7-2. When s = 0.2 is used, Eq. 7-2 represents a higher early-age compressive strength than Eq. 7-1. Consequently Eq. 7-2 provides more accurate predictions for 3 and 7 days than Eq. 7-1 (Figure 7-3, Figure 7-4, and Figure 7-5). Within the total time spectrum of interest, CEB-FIP model provided the best fit with the experimental results obtained in this study.

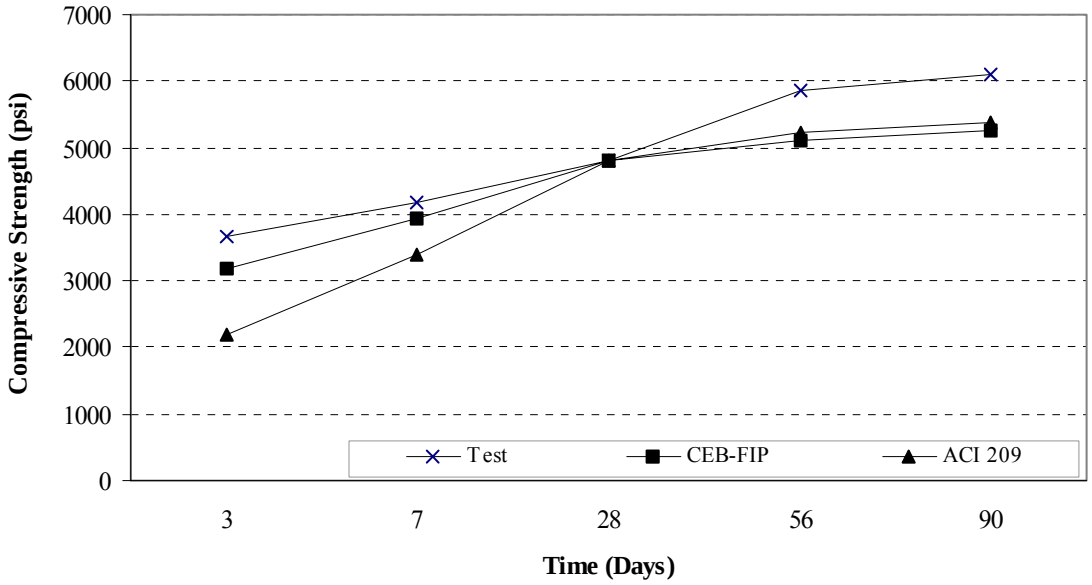

Figure 7-3. Compressive strength variation against time (S05 of 82191)

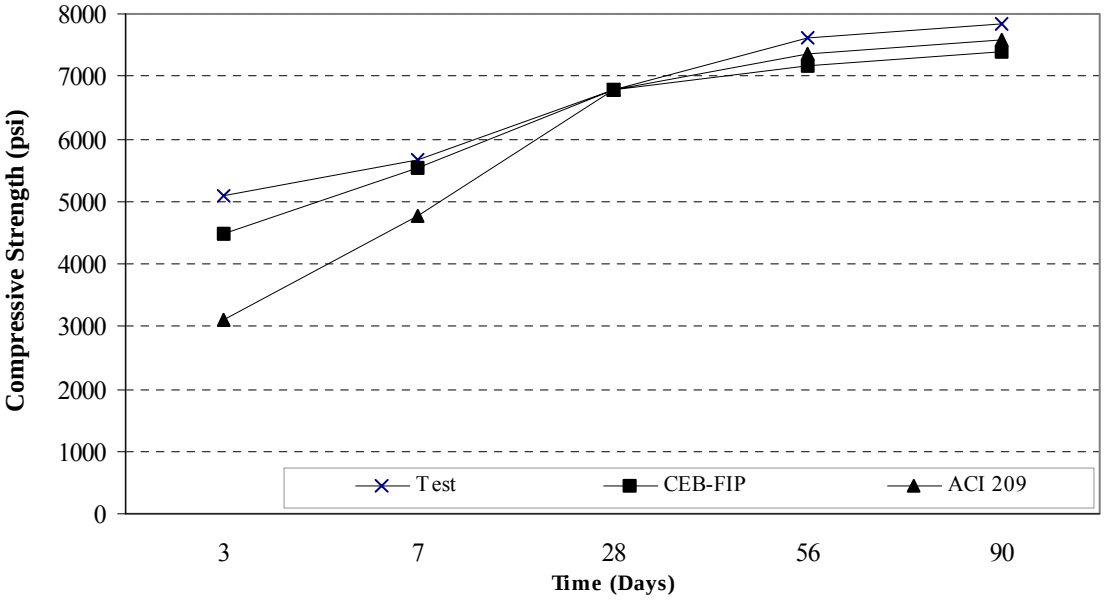

Figure 7-4. Compressive strength variation against time (S05 of 82025)

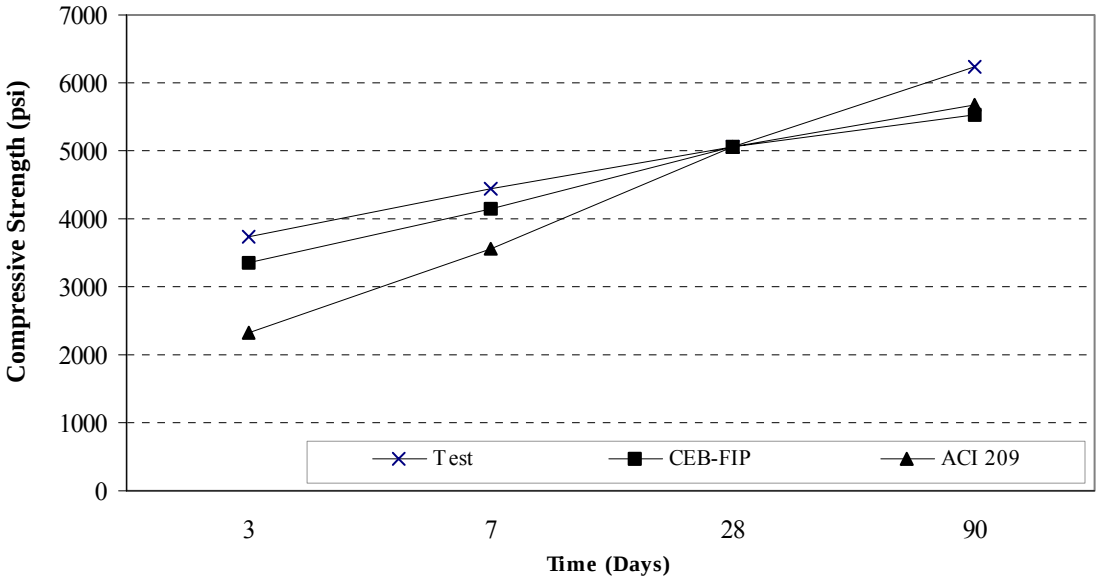

Figure 7-5. Compressive strength variation against time (S06 of 82194)

7.2.2 Elasticity Modulus

ACI Committee 209, ACI 318, and CEB-FIP are the most commonly used models for the prediction of static modulus of elasticity.

The model recommended by ACI Committee 209 is given as:

$$E_{ct} = g_{ct}\left[w^3 (f'_c)_t\right]^{1/2} \tag{7-3}$$

where w is the unit weight of concrete in *pcf* and $g_{ct} = 33$ is a constant.

The model most commonly used in the literature and in ACI 318 is:

$$E_{ct} = 57000\sqrt{(f'_c)_t} \tag{7-4}$$

The relationship suggested by CEB-FIP Models Code (1990) (Vincent 2003):

$$E_{ct} = E_c e^{[s/2(1-\sqrt{28/t})]} \tag{7-5}$$

where E_c is the mean modulus of elasticity of concrete at 28-days (*psi*).

ACI 209 and ACI 318 models require concrete compressive strength for calculating variation of elasticity modulus against time. Similarly, CEB-FIP model requires 28-day mean modulus of

elasticity of concrete. A complete set of compressive strength and elasticity modulus test data is available only for two out of five bridge deck replacement projects (see Chapter 6). Therefore, CEB-FIP, ACI 318 and ACI 209 predictions are compared with the test results obtained from deck concrete of bridges S05 of 82191 and S05 of 82025.

Figure 7-6 and Figure 7-7 show the comparison of the three models with their experimental counterparts.

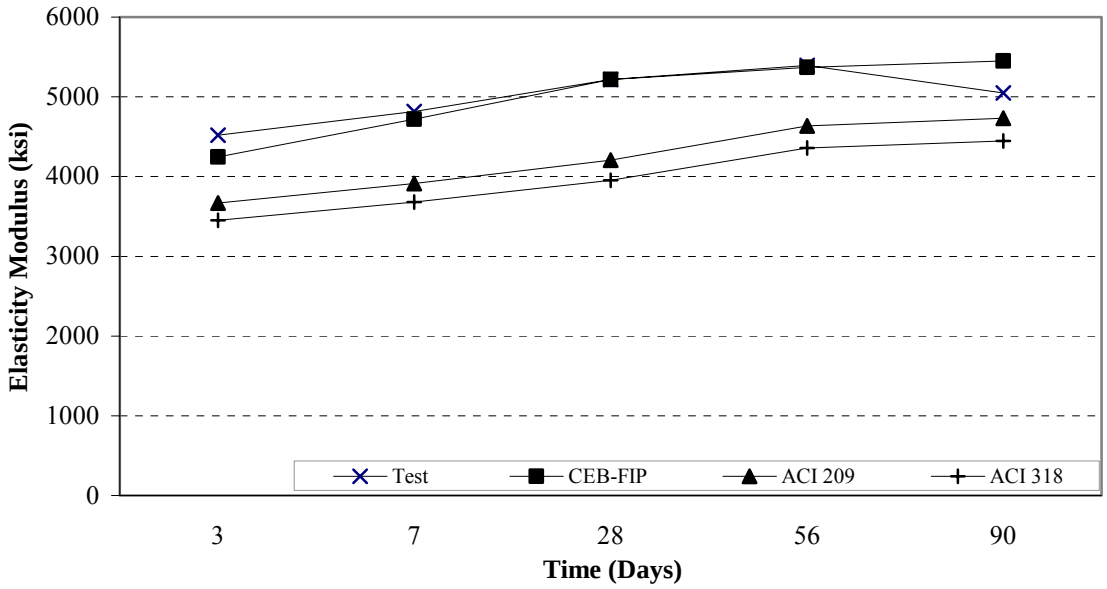

Figure 7-6. Variation of elasticity modulus against time (S05 of 82191)

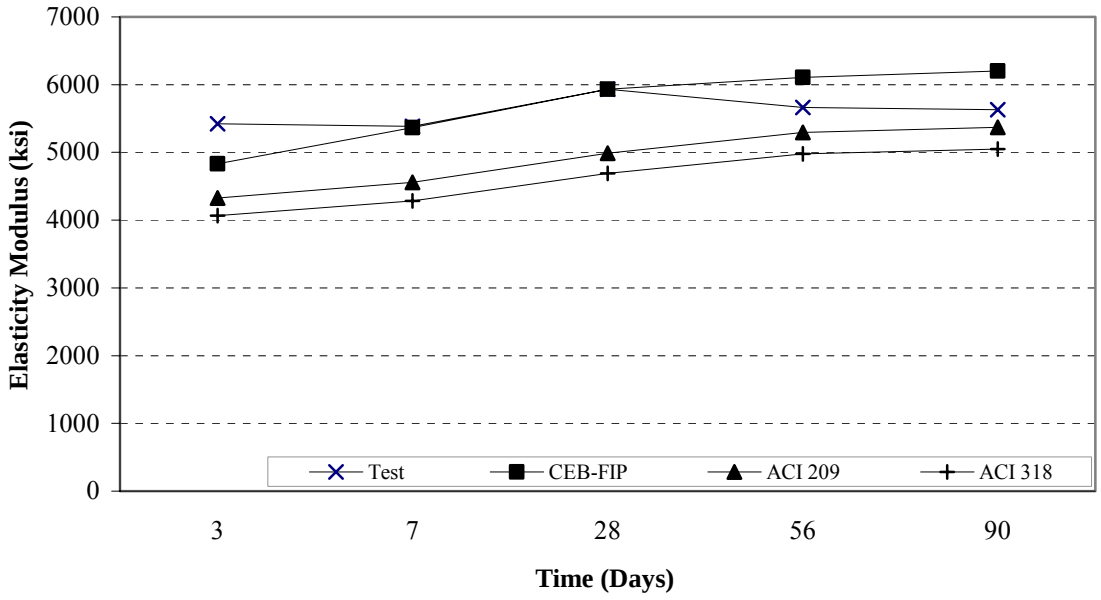

Figure 7-7. Variation of elasticity modulus against time (S05 of 82025)

Another method for calculating the elasticity modulus is by the use of ultrasonic pulse velocity (UPV) measurements (ASTM C215-97 1998). From UPV measurement, a dynamic modulus of elasticity is calculated. A ratio of static to dynamic moduli (E_s/E_d) is proposed by Carino (1991).

$$E_s / E_d = 0.368 + 0.0871 \times 10^{-6} E_s \qquad (7\text{-}6)$$

This Eq. 7-6, which is referred to as the CRC model in this document, is empirical in nature. It is proposed that the acceptable range of results is within 10% of the mean.

Table 7-1 shows the E_s/E_d ratio calculated using the data generated in this research and Eq. 7-6. The variation of test results was also compared with the applicable range proposed using the CRC model (Figure 7-8).

After the evaluation of all the potential models, CEB-FIP model provided the best fit with the experimental results obtained in this study within the total time spectrum of interest.

Table 7-1. Ratio of Static to Dynamic Moduli

Bridge ID	E_s (ksi)	E_d (ksi)	Es/Ed	
			Test	Eq. (7-6)
S 05 of 82191	4213	6432	0.66	0.81
	4316	6569	0.66	0.83
	4177	6423	0.65	0.82
	4303	6387	0.67	0.83

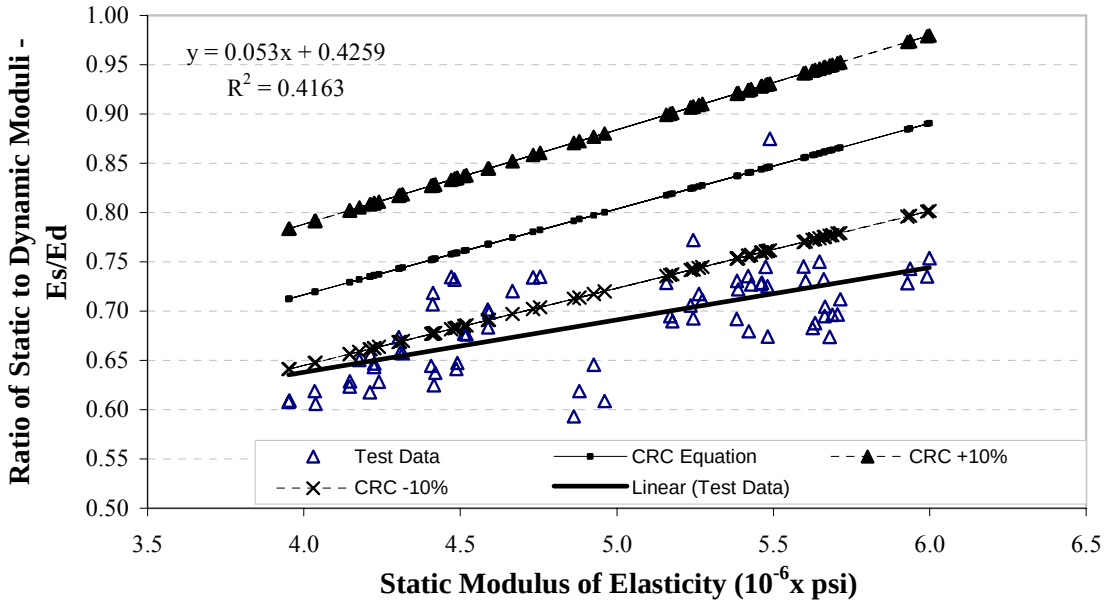

Figure 7-8. The comparison of CRC model predictions and the test data

7.2.3 Direct Tensile Strength

ACI Committee 209 recommends the following equation for computing average values for direct tensile strength ($f_t^{'}$).

$$f_t^{'} = g_t \left[w (f_c^{'})_t \right]^{1/2} \qquad (7\text{-}7)$$

where w is unit weight of concrete in *pcf*, and g_t is given as 1/3.

7.2.4 Concrete Strain

Assuming concrete behaves as an elastic brittle material in tension, concrete strain at cracking can be calculated using Hooke's law for tensile strength and elasticity modulus.

$$\varepsilon = f_t^{'} / E \qquad (7\text{-}8)$$

where ε is the strain, $f_t^{'}$ is the tensile stress, and E is the elasticity modulus.

Concrete will crack when strain due to volume change exceeds the concrete strain calculated using Eq. 7-8 and with sufficient accompanying stress due to restraint effects.

7.3 THERMAL STRAINS AND STRESSES

7.3.1 Overview

As demonstrated in Section 7.1, the stresses developed due to thermal load of 18°F may initiate deck cracking. In order to fully evaluate thermal effect, a rigorous analysis of the cracking potential of newly placed concrete decks is performed from the data collected during construction monitoring and the early-age mechanical properties established in Section 7.2.

7.3.2 Tensile Stress Development in Decks Under Thermal Loads

Krauss and Rogalla (1996) provided a system of equations to calculate the restraint in a composite reinforced concrete bridge deck subjected to uniform and linear temperature distributions. The girder and reinforcement restraints provide a means of calculation stresses at the top and bottom of the deck. The equations consider multiple layers of reinforcement in the deck to account for the restraint effects of longitudinal deck reinforcement and stay-in-place (metal) forms. These equations are based on basic mechanics principles, and only consider the decks with simply supported girders.

Eq. 7-9 to Eq. 7-13 given below are a means for calculating deck stresses under a uniform temperature distribution:

$$\varepsilon_{deckBot} = \frac{2(1-\mu^2)}{E_{deck}\, p\, t^2}\left[-3\left(Q + \sum_{i=1}^{nr}(dr_i Fr)_i\right) + t\left(2F + \sum_{i=1}^{nr}(Fr_i)\right)\right] + \alpha_{deck}(1+\mu)(T_1 - T_0) =$$

$$\frac{-1}{E_{beam}}\left(\frac{F}{A_{beam}} + \frac{d_1^2 F}{I_{beam}} + \frac{d_1 Q}{I_{beam}}\right) + \alpha_{beam}(T_2 - T_0) \qquad (7\text{-}9)$$

$$\frac{6(1-\mu^2)\left[-2(Q+\sum_{i=1}^{nr}(dr_i\,Fr)_i)+t(F+\sum_{i=1}^{nr}(Fr_i))\right]}{E_{deck}\,p\,t^3}=\frac{d_1F+Q}{E_{beam}\,I_{beam}} \tag{7-10}$$

$$\frac{1-\mu^2}{E_{deck}\,p}\left[\left(\frac{6}{t^2}-\frac{12\,dr_i}{t^3}\right)\cdot\left(Q+\sum_{i=1}^{nr}(Fr_i\,dr_i)\right)+\left(\sum_{i=1}^{nr}(Fr_i)\right)\cdot\left(\frac{6\,dr_i}{t^2}-\frac{4}{t}\right)+F\left(\frac{6\,dr_i}{t^2}-\frac{2}{t}\right)\right]$$

$$+\alpha_{beam}(1+\mu)(T_1-T_0)=\frac{Fr_i}{Ar_i\,E_{re\,inf}}+\alpha_{re\,inf}(Tr_1-T_0) \tag{7-11}$$

Eq. 7-9 to Eq. 7-11 are for determining the restraint forces. The stresses at top and bottom fibers of the deck are calculated from Eq. 7-12 and Eq. 7-13 upon calculating the restraint forces.

$$f_{deckTop}=\frac{F-\sum_{i=1}^{nr}Fr_i}{A_{deck}}-\frac{Fa-Q+\sum_{i=1}^{nr}[Fr_i(a-dr_i)]}{S_{deck}} \tag{7-12}$$

$$f_{deckBot}=\frac{F-\sum_{i=1}^{nr}Fr_i}{A_{deck}}+\frac{Fa-Q+\sum_{i=1}^{nr}[Fr_i(a-dr_i)]}{S_{deck}} \tag{7-13}$$

where:

α_{beam} = Coefficient of thermal expansion of the beam

α_{deck} = Coefficient of thermal expansion of the deck concrete

α_{reinf} = Coefficient of thermal expansion of the reinforcement

ε_i = Strain in direction i, elongation positive

μ = Poisson's ratio of the deck

f_i = Stress in direction i, tensile stresses positive

a = Half of the deck thickness, = t/2

A_{beam} = Area of the beam

A_{deck} = Area of the concrete deck, = pt

Ar_i = Reinforcement area of layer i

d_1 = Distance to girder centroid from deck soffit

dr_i = Depth of deck reinforcement layer i, from upper surface of the deck

E_{beam} = Effective modulus of elasticity of the beam

E_{deck} = Effective modulus of elasticity of the deck

E_{reinf} = Effective modulus of elasticity of the deck reinforcement

F = Interface shear

Fr_i = Force in reinforcement layer i, positive denotes tensile force

i = Reinforcement layer number

I_{beam} = Moment of inertia of beam

I_{deck} = Moment of inertia of the deck, = $pt^3/12$

nr = Number of reinforcement layers in the deck

Q = Interface moment (force couple)

S_{deck} = Section modulus of deck, = $pt^2/6$

t = Deck thickness

T_0 = Initial temperature of bridge

T_1 = Later temperature at upper surface of deck

T_2 = Later temperature of beam

Tr_i = Later temperature of reinforcement layer i

7.3.3 Thermal Stresses on a Typical Michigan Deck

Concrete deck reaches peak temperature at sometime during hydration. As the cooling process starts, tensile stresses develop at the bottom of the deck where the highest restraint exists. The ACI 207.2R (2001) procedure (described in Chapter 2) is used for determining the peak temperature and the time at which the peak temperature forms.

The time required for concrete to achieve peak temperature is determined from the volume to exposed-surface ratio of the bridge deck and the concrete temperature at the time of placement. The concrete temperature at the time of placement is assumed to be equal to the ambient temperature. According to ACI 207.2R (2001), the temperature of concrete placed during hot weather may exceed the mean daily ambient air temperature by 5 to 10 ^{0}F unless measures are taken to cool the concrete or the coarse aggregate. An analysis is performed considering ranges of ambient temperature as well as cement fineness. For night casting during summer months, the time to peak temperature is calculated as 12 hours within the placement temperature range that is assumed based on the ACI 207.2R (2001) requirements and the ambient temperature (Table 7-2). During late season daytime construction, the time to peak temperature is calculated to be

between 18 - 36 hours corresponding to upper and lower limits of placement temperature. Often retarders are used in the concrete mix in late season deck placement projects. It is assumed that the time to peak temperature with retarders is delayed for six hours beyond the time calculated using the ACI procedure. With the use of retarders, during late season daytime construction, the time to peak temperature is assumed to be between 24 – 42 hours (Table 7-2).

In this analysis a typical 9-inch concrete deck supported on Michigan 1800 girder is used to investigate the development of thermal stresses at the deck bottom under temperature loads. The cement content of 7 sacks/yd^3 and other parameters required in the thermal load calculation are given below in Table 7-2, Table 7-3, and Table 7-4.

Table 7-2. Parameters used for Calculating Peak Differential Temperature in Deck Concrete

Parameters	Summer (Night Casting)	Late Season (Daytime Casting)
Cement (Type 1) (lb/yd^3)	658	658
Ambient Temperature Range at Placement (F)	65 - 75	40 - 55
Relative Humidity (%)	60	45
Concrete Temperature at Placement (F)	70 – 80	45 – 60
Cement Fineness (ft^2/lb) (Assumed)	1173 - 1466 (2400 - 3000 cm^2/g)	
Volume/Exposed-surface ratio (ft)	0.75 (for 9 in. deck)	

Table 7-3. Mechanical Properties and Ambient Temperature at the Time of Peak Temperature

Parameters	Summer (Night Casting)	Late Season (Daytime Casting)	
Time to Peak Temperature (hours)	12	42	24
Ambient Temperature during Concrete Peak Temperature (F)	75 - 85	30	55
Compressive Strength (psi)	1400 (at 12 hours)	3500 (at 42 hours)	2750 (at 24 hours)
Elasticity Modulus E_{deck} (ksi)	2300 (at 12 hours)	4200 (at 42 hours)	3750 (at 24 hours)
Tensile Strength (psi)	153	242	214

Table 7-4. Differential Deck Temperature for Construction Season and Cement Fineness

Parameters	Summer (Night Casting)		Late Season (Daytime Casting)	
Cement Fineness (ft^2/lb)	1173	1466	1173	1466
Ambient Air and Deck Concrete Temperature Differential ΔT_{deck} (F)	28 - 37	39 - 49	24 - 26	28 - 30

The additional parameters used in the thermal load calculations are (Figure 7-1 and Figure 7-2):

α_{beam} = 6.0×10^{-6} in./in./^{0}F (Coefficient of thermal expansion of the concrete beam) (AASHTO 1998)

α_{deck} = 8.33×10^{-6} in./in./^{0}F (Coefficient of thermal expansion of the deck concrete) (RILEM-42-CEA 1981)

α_{reinf} = 6.7×10^{-6} in./in./^{0}F (Coefficient of thermal expansion of the reinforcement) (Krauss and Rogalla 1996)

μ = 0.25 (Poisson's ratio of the deck)

a = t/2 = 4.5 in. (Half the deck thickness)

A_{beam} = 875 in^2 (Area of the beam)

A_{deck} = pt = 1080 in^2 (Area of the concrete deck)

Ar_1 = 1.32 in^2 (Reinforcement area of layer 1)

Ar_2 = 1.86 in^2 (Reinforcement area of layer 2)

d_1 = 37.6 in. (Distance to girder centroid from deck soffit)

dr_1 = 2.76 in. (Depth of top longitudinal reinforcement from upper surface of the deck)

dr_2 = 7 in. (Depth of bottom longitudinal reinforcement from upper surface of the deck)

E_{beam} = 4000 ksi (Effective modulus of elasticity of the concrete beam)

E_{reinf} = 29,000 ksi (Effective modulus of elasticity of the deck reinforcement)

I_{beam} = 624,700 in^4 (Moment of inertia of beam)

I_{deck} = $pt^3/12$ = 7290 in^4 (Moment of inertia of the deck)

p = 120 in. (Effective deck width)

S_{deck} = $pt^2/6$ = 1620 in^3 (Section modulus of deck)

t = 9 in. (Deck thickness)

During the period of rising concrete temperature, stay-in-place or wooden forms keep the deck edges and the bottom insulated. Thus, it is reasonable to assume that the increase in deck temperature will not affect the girder temperature. Hence, the girder temperature will be same as the ambient temperature. In addition, a uniform temperature distribution within the deck can be assumed since the deck thickness is small compared to the length and width (Figure 7-2). Based on these assumptions thermal load calculations, Eq. 7-9 – Eq. 7-11 are first solved to calculate the restraint forces. For a standard Michigan bridge deck Eq. 7-11 is solved for each reinforcement layer. Finally, Eq. 7-13 is used to calculate the stress at bottom of the deck due to the thermal load.

Assuming uniform deck temperature (Figure 7-2), Eq. 7-9 is simplified as given below:

$$\left(\frac{4(1-\mu^2)}{E_{deck}\,pt}+\frac{1}{E_{beam}\,A_{beam}}+\frac{d_1^2}{E_{beam}\,I_{beam}}\right)F+\left(\frac{-6(1-\mu^2)}{E_{deck}\,pt^2}+\frac{d_1}{E_{beam}\,I_{beam}}\right)Q$$

$$+\frac{2(1-\mu^2)}{E_{deck}\,pt^2}(-3\,dr_1+t)\,Fr_1+\frac{2(1-\mu^2)}{E_{deck}\,pt^2}(-3\,dr_2+t)\,Fr_2+$$

$$\alpha_{deck}(1+\mu)(-\Delta T_{deck})=0 \qquad (7\text{-}14)$$

The top fiber strain of the beam is due to the force (F) and the moment (Q) developed at the deck-girder interface from the uniform thermal load (Figure 7-9). Assuming compatibility, the strain at the bottom of the deck and the top of the girder will be equal. With decreasing temperature, deck shrinkage generates tensile stresses at the deck bottom from the restraint imposed by the girder.

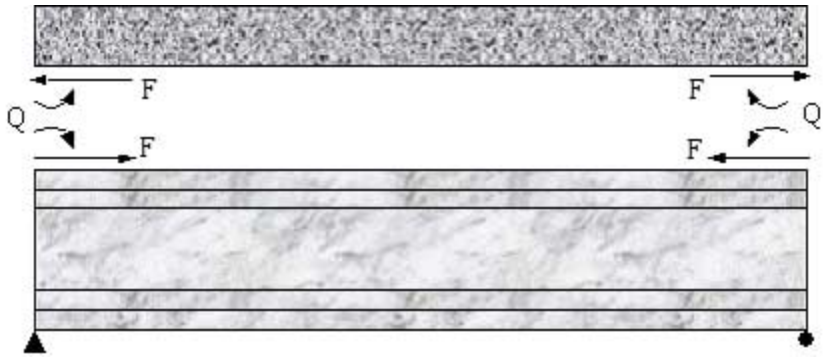

Figure 7-9. Compatibility shear force and moment at deck-girder interface

The Eq. 7-10 is also simplified using the Michigan deck parameters as follows:

$$\left(\frac{6(1-\mu^2)}{E_{deck}\,p\,t^2}-\frac{d_1}{E_{beam}I_{beam}}\right)F+\left(\frac{-12(1-\mu^2)}{E_{deck}\,p\,t^3}-\frac{1}{E_{beam}I_{beam}}\right)Q+$$

$$\frac{6(1-\mu^2)}{E_{deck}\,p\,t^3}(-2dr_1+t)Fr_1+\frac{6(1-\mu^2)}{E_{deck}\,p\,t^3}(-2dr_2+t)Fr_2=0 \qquad (7\text{-}15)$$

The equation is developed from the beam curvature under a uniform thermal load on the deck (i.e., M/EI; where M is the moment, E is the elasticity modulus, and I is the moment of inertia).

There are multiple (two) reinforcement layers and, Eq. 7-11 is solved independently for each layer. For the top layer Eq. 7-11 is written as;

$$\frac{1-\mu^2}{E_{deck}\,p}\left(\frac{6dr_1}{t^2}-\frac{2}{t}\right)F+\frac{1-\mu^2}{E_{deck}\,p}\left(\frac{6}{t^2}-\frac{12dr_1}{t^3}\right)Q+$$

$$\left[\frac{1-\mu^2}{E_{deck}\,p}\left(\left(\frac{6}{t^2}-\frac{12dr_1}{t^3}\right)dr_1+\left(\frac{6dr_1}{t^2}-\frac{4}{t}\right)\right)-\frac{1}{Ar_1E_{re\,\inf}}\right]Fr_1+$$

$$\frac{1-\mu^2}{E_{deck}\,p}\left(\left(\frac{6}{t^2}-\frac{12dr_1}{t^3}\right)dr_2+\left(\frac{6dr_1}{t^2}-\frac{4}{t}\right)\right)Fr_2+$$

$$\left[\alpha_{deck}(1+\mu)-\alpha_{re\,\inf}\right](\Delta T_{deck})=0 \qquad (7\text{-}16)$$

The uniform thermal load assumption suggests that the two layers of reinforcement and concrete deck are subjected to equal thermal load. Substituting the deck and thermal parameters in Eq. 7-11 for the top reinforcement layer, Eq. 7-16 is developed. Similarly, Eq. 7-17 is developed by substituting the parameters for the bottom reinforcement layer.

$$\frac{1-\mu^2}{E_{deck}\,p}\left(\frac{6dr_2}{t^2}-\frac{2}{t}\right)F+\frac{1-\mu^2}{E_{deck}\,p}\left(\frac{6}{t^2}-\frac{12dr_2}{t^3}\right)Q+$$

$$\frac{1-\mu^2}{E_{deck}\,p}\left(\left(\frac{6}{t^2}-\frac{12dr_2}{t^3}\right)dr_1+\left(\frac{6dr_2}{t^2}-\frac{4}{t}\right)\right)Fr_1+$$

$$\left[\frac{1-\mu^2}{E_{deck}\,p}\left(\left(\frac{6}{t^2}-\frac{12dr_2}{t^3}\right)dr_2+\left(\frac{6dr_2}{t^2}-\frac{4}{t}\right)\right)-\frac{1}{Ar_2E_{re\,\inf}}\right]Fr_2+$$

$$\left[\alpha_{deck}(1+\mu)-\alpha_{re\,\inf}\right](\Delta T_{deck})=0 \qquad (7\text{-}17)$$

Equations 7-14, 7-15, 7-16 and 7-17 can now be solved simultaneously for F, Q, Fr_1, and Fr_2. These parameters are then substituted in Eq. 7-13 to calculate the stress at the bottom of the deck. The results of the thermal load analysis are summarized below in Table 7-5.

In Table 7-5 two cement different fineness values (1173 ft^2/lb and 1466 ft^2/lb) are used in the calculations. The lower fineness value leads to lower heat of hydration thus defined on the lower bound solution and vice versa. Different ambient temperature bounds were assumed for night casting in the summer and daytime casting in late-season construction. The deck placement projects that are carried out during late October and November are defined as late season construction. The time required for concrete to reach peak temperature is calculated based on cement type, volume to exposed-surface ratio of the deck, and the concrete temperature at the time of placement. ACI 207.2R (2001) requirements and the assumed ambient temperature range are used to establish the concrete temperature at the time of placement. For night casting, the time to peak temperature is calculated as 12 hours within the concrete temperature range of 65-75 ^{0}F at the time of placement, whereas for daytime casting, the peak temperature is achieved between 18 - 36 hours corresponding to upper and lower limits of concrete temperature during

the time of placement. Retarders are more commonly used in the concrete mix during late season construction. For late season construction, six hours are added to the time values calculated from the ACI procedure to account for the effects of retarders.

The calculated thermal load for a cement fineness of 1173 ft^2/lb and ambient temperature of 65 ^{0}F is 28 ^{0}F. For the same cement fineness and ambient temperature of 75 ^{0}F, the thermal load is 37 ^{0}F. This range of thermal load (28 – 37 ^{0}F) develops a tensile stress range in the deck of 237-313 psi as shown in Table 7-5. The tensile stress developed in the bridge deck is greater than the concrete tensile strength (refer column 2 of Table 7-5). Similar interpretations can be drawn for the data shown in the other columns of Table 7-5.

When cement fineness increases, rate and amount of strength and elasticity modulus gain as well as heat generated during hydration process increase. The effect of fineness on heat of hydration is accounted in the models given in ACI 207.2R (2001). However, the models used to predict the strength and elasticity modulus of concrete against time do not account this factor, hence, same values are used under different cement fineness values.

Table 7-5. Stress Developed at the Bottom of the Deck due to Thermal Effects (7 Sacks of Cement)

Parameters	Summer (Night Casting)		Late Season (Daytime Casting)	
	Lower Bound	Upper Bound	Lower Bound	Upper Bound
(1)	(2)	(3)	(4)	(5)
Cement Fineness (ft^2/lb)	1173	1466	1173	1466
Ambient Temperature Range (F)	65 - 75	65 - 75	40 - 55	40 - 55
Time to Peak Temperature (hours)	12	12	42	24
Difference in Ambient and Deck Concrete Temperature ΔT_{deck} (F)	28 - 37	39 - 49	24 - 26	28 - 30
Tensile Stress (psi)	**237 - 313**	**329 - 414**	**263 - 285**	**292 - 313**
Tensile Strength (psi)	***153***	***153***	***242***	***214***

7.3.3.1 Effect of Cement Content on Thermal Stresses

The effects of reducing the cement content are investigated for contents of 6 sacks (564 lb/yd^3) and 4 sacks (376 lb/yd^3) under constant water/cement ratio. Mechanical properties of concrete for 4 and 6 sacks of cement are given in Table 7-6 and Table 7-7.

Table 7-6. Mechanical Properties of Concrete with 6 Sacks of Cement

Parameters	Summer (Night Casting)	Late Season (Daytime Casting)	
Time to Peak Temperature (hours)	12	42	24
Compressive Strength (psi)	1215	3033	2383
Elasticity Modulus (ksi)	2131	3758	3348
Tensile Strength (psi)	142	225	199

Table 7-7. Mechanical Properties of Concrete with 4 Sacks of Cement

Parameters	Summer (Night Casting)	Late Season (Daytime Casting)	
Time to Peak Temperature (hours)	12	42	24
Compressive Strength (psi)	795	1983	1558
Elasticity Modulus (ksi)	1724	2538	2250
Tensile Strength (psi)	115	182	161

When 6 sacks of cement are used, the calculated thermal load is 24 ^{0}F, for a cement fineness of 1173 ft^2/lb and an ambient temperature of 65 ^{0}F. For the same cement fineness, if ambient temperature is increased to 75 ^{0}F, the thermal load is increased to 31 ^{0}F. At this thermal load range (24 – 31 ^{0}F), the range of tensile stress developed in the deck is calculated to be 196-253 psi. The tensile stress in the bridge deck is greater than the tensile strength of 142 psi. Under similar exposure conditions and cement fineness, if 4 sacks of cement are used, the range is reduced to 14 – 19 ^{0}F and the range of tensile stress developed in the deck is 104-141 psi (refer column 2 of Table 7-8). The stresses due to thermal load are about equal to the tensile strength of 115 psi. Similar interpretation can be drawn for the data shown in the other columns of Table 7-8.

Table 7-8. Stress Developed at the Bottom of the Deck due to Thermal Effects (6 Sacks & 4 Sacks of Cement)

Parameters	Summer (Night Casting)		Late Season (Daytime Casting)	
	Lower Bound	Upper Bound	Lower Bound	Upper Bound
(1)	(2)	(3)	(4)	(5)
Cement Fineness (ft^2/lb)	1173	1466	1173	1466
Ambient Temperature Range (F)	65 - 75	65 - 75	40 - 55	40 - 55
Time to Peak Temperature (hours)	12	12	42	24
6 sacks of cement				
Difference in Ambient and Deck Concrete Temperature ΔT_{deck} (F)	24 - 31	33 - 42	22 - 25	26
Tensile Stress (psi)	**196 - 253**	**270 - 343**	**230 -261**	**258**
Tensile Strength (psi)	***142***	***142***	***225***	***199***
4 sacks of cement				
Difference in Ambient and Deck Concrete Temperature ΔT_{deck} (F)	14 - 19	20 - 26	16 - 22	23
Tensile Stress (psi)	**104 - 141**	**149 - 193**	**141 - 194**	**192**
Tensile Strength (psi)	***115***	***115***	***182***	***161***

Analysis results given in Table 7-8 show that the use of lower cement content lowers the thermal load significantly but the tensile stresses are still in excess of tensile strength. Tensile strength and modulus of elasticity are also lower for concrete with 4 and 6 sacks of cement. It is possible to achieve lower tensile stress using coarse cements. The highest fineness used for these calculations is 1466 ft^2/lb (3000 cm^2/g). Use of the fineness value of cement is limited to 1466 ft^2/lb by the graphs provided in ACI 207.2R (2001) for calculation of the peak temperature and the age of concrete at peak temperature. The cement mill reports (see Appendix C) obtained from the concrete supplier indicate the fineness of cement of 1774 ft^2/lb (3630 cm^2/g). An increase in the cement fineness further increases the level of heat generated within the concrete mass, resulting in a greater thermal load. Though not accounted in the analysis, increase in cement fineness results higher rate and amount of strength and elasticity modulus gain.

7.3.3.2 Effect of Girder Type on Thermal Stresses

The analysis performed on a typical 9-inch deck supported on Michigan 1800 girder showed that the thermal stresses at bottom of the deck is sufficiently high enough to cause early-age deck

cracking. Generally, three types of girders are used in Michigan with 9-inch concrete decks – PCI, PC spread box, and steel. Further analysis on thermal stress development is performed in order to investigate the effects of girder types on deck cracking due to thermal loading. Figure 7-1, Figure 7-10, and Figure 7-11 show the geometric properties and the reinforcement arrangements within the bridge decks. Table 7-9 Summarizes the geometric properties of bridge decks supported on various girder types.

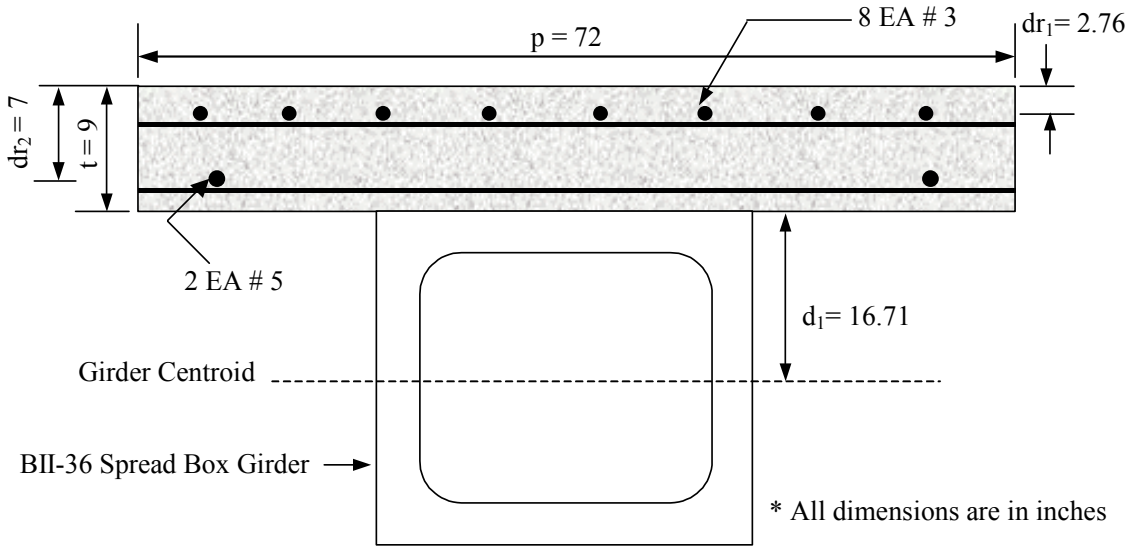

Figure 7-10. Geometry and reinforcement arrangement of the deck section supported on PC spread box girders

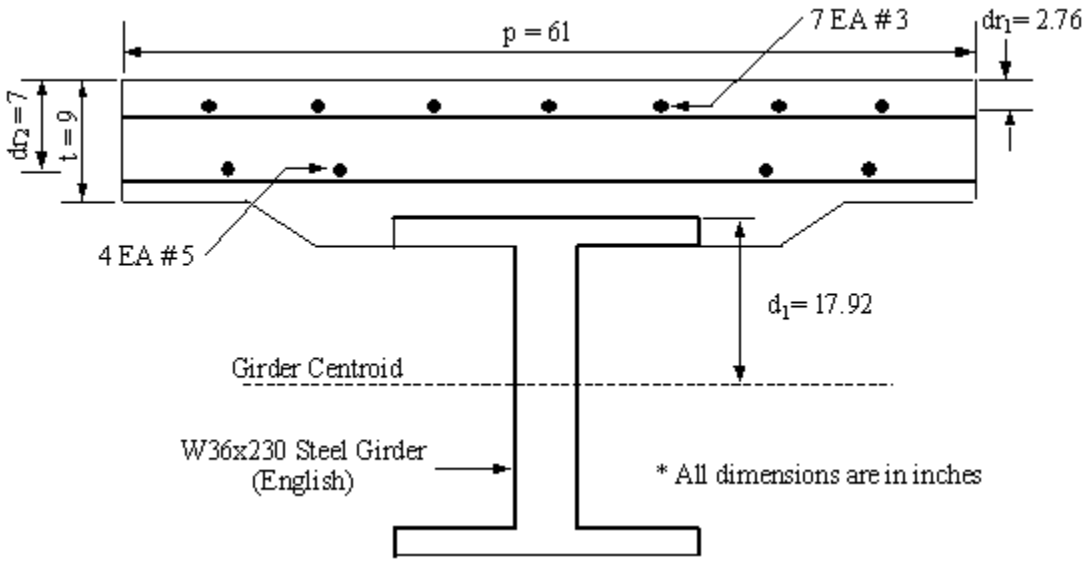

Figure 7-11. Geometry and reinforcement arrangement of the deck section supported on steel girders

Table 7-9. Summary of Geometric Properties of Bridge Decks

Girder Type	t (in)	p (in)	A_{beam} (in^2)	A_{deck} (in^2)	A_{r1} (in^2)	A_{r2} (in^2)	d_1 (in)	d_{r1} (in)	d_{r2} (in)	I_{beam} (in^4)	I_{deck} (in^4)	S_{deck} (in^3)
PCI	9	120	875	1080	1.32	1.86	37.6	2.76	7	624,700	7290	1620
Spread Box	9	72	620.5	648	0.88	0.62	16.71	2.76	7	85,153	4374	972
Steel	9	61	67.6	549	0.77	1.24	17.95	2.76	7	15,000	3706	824

With the given geometric properties and early-age mechanical properties of concrete (compressive strength of 1400 psi and elasticity modulus of 2300 ksi), and a 25 ^{0}F uniform thermal load on the deck, tensile stress magnitudes at the deck-girder interface are calculated and given in Table 7-10 below.

Table 7-10. Tensile Stress Developed at Girder-Deck Interface

Girder Type	Tensile Stress at Girder-Deck Interface (psi)
PCI	211
Spread Box	249
Steel	260

According to this analysis, the bridge decks supported on PCI girders have the least potential to crack under thermal loading while decks with steel girders show the highest potential.

7.3.3.3 Effect of Girder Spacing on Thermal Stresses

The analysis is performed on a typical 9-inch deck supported on W36x230 girders. Three different girder spacings were considered - 61-, 71-, and 91-inches. Summary of bridge deck geometric properties are given in Table 7-11.

Table 7-11. Summary of Geometric Properties of Bridge Decks

Girder Spacing (in)	t (in)	p (in)	A_{beam} (in^2)	A_{deck} (in^2)	A_{r1} (in^2)	A_{r2} (in^2)	d_1 (in)	d_{r1} (in)	d_{r2} (in)	I_{beam} (in^4)	I_{deck} (in^4)	S_{deck} (in^3)
61	9	61	67.6	549	0.77	1.24	17.95	2.76	7	15,000	3706	824
71	9	71	67.6	639	0.88	1.55	17.95	2.76	7	15,000	3706	824
91	9	91	67.6	819	1.10	1.86	17.95	2.76	7	15,000	3706	824

With the given geometric properties and early-age mechanical properties of concrete (compressive strength of 1400 psi and elasticity modulus of 2300 ksi), and a 25 ^{0}F uniform thermal load on the deck, tensile stress magnitudes at the deck-girder interface are calculated and given in Table 7-12 below.

Table 7-12. Tensile Stress Developed at Girder-Deck Interface

Girder Spacing (in)	**Tensile Stress at Girder-Deck Interface** (psi)
61	260
71	253
91	249

According to the analysis, increased girder spacing reduces the restraint effects on the deck and reduces the tensile stress at deck-girder interface due to volume change loads.

7.4 METHODS FOR ESTIMATING SHRINKAGE STRAIN

7.4.1 Overview

To improve the design of bridge decks, the material behavior under drying has to be characterized more accurately. Even though predictions of humidity may not be very accurate, the shrinkage strains that develop is dependent on the humidity of the environment (Bissonette 1999). Performance-based specifications, on shrinkage limits, will be useful for control of deck cracking (Mokarem et al. 2003).

The shrinkage predictions of concrete are based on ACI 209 and CEB-FIP models. Other models reported in the literature are derived from these two (Hani et al. 2003). Some researchers tried to evaluate shrinkage under different curing procedures. Mokarem et al. (2003) used crushed limestone gravel and diabase in concrete mixes in order to see the effects of aggregate type. For all types of aggregate, CEB-FIP model was found to be a better predictor than ACI 209. Although, ACI 209 is considered poor in overall prediction of drying shrinkage, Hani et al. (2003) suggested it is a good predictor for 28-day shrinkage. On the other hand, the CEB-FIP is a good prediction model for early ages.

The mathematical formulations of prediction models are similar. Each model has an ultimate shrinkage calculation that predicts total long-term shrinkage for given strength and cement type.

For different cement types and mix designs, ultimate shrinkage is a constant only in ACI 209. The shrinkage is a time-dependent function with its value based on drying time of concrete. The drying time of concrete is the difference between its age (t) and duration of wet curing (t_c). The shape of the concrete element is incorporated in shrinkage models as volume to exposed-surface ratio. The relative humidity component is represented as the average humidity of the environment. There are several limitations to the various shrinkage prediction models that are described in Table 7-13.

Table 7-13. Limitations of Shrinkage Prediction Models

Parameter (1)	ACI 209 (2)	CEB-FIP 90 (3)	Bazant B3 (4)	GL 2000 (5)
Mean 28-day compressive strength f_c' psi	NA*	2,900 – 13,000	2,500 – 10,000	2,900 – 10,000
Aggregate/Cement	NA	NA	2.5 – 13.5	NA
Cement lbs/ft^3	NA	NA	10 – 45	NA
Water/cement ratio	NA	NA	0.3 - 0.85	NA
Relative Humidity (%)	40-100	40-100	40-100	40-100
Cement Type	I or III	R, SL, or RS	I, II, or III	I, II, or III
Age of concrete at which the shrinkage strain is interested (t) or age at which concrete starts drying (t_c) (Moist cured)	≥ 7 days	$t_c \leq 14$ days	$t_c \leq t$	≥ 2 days
t or tc (Steam cured)	≥ 1-3 days	$t_c \leq 14$ days	$t_c \leq t$	≥ 2 days
Additional Notes				Aggregate stiffness is considered

* Model does not account for the parameter

7.4.1.1 ACI 209 Prediction Model

ACI 209 is an empirical approach to calculate total free shrinkage of concrete:

$$\varepsilon_{sh}(t) = \left[\frac{t - t_c}{35 + (t - t_c)}\right] \cdot \varepsilon_u \qquad (7\text{-}18)$$

where t is the age of concrete, t_c is the duration of wet cure, and ε_u is the ultimate shrinkage.

The value of ultimate shrinkage (ε_u) is a constant (780 μ strain) for all types of concrete and curing conditions. Ultimate shrinkage is corrected only by a humidity factor as given below in Table 7-14:

Table 7-14. The Relationship Between Humidity Range and Correction Formula

Humidity Range	Correction Formula γ_{RH}
40% < RH < 80%	1.40 – RH/100
80% < RH < 100%	3.00 – 3xRH/100

$$\varepsilon_u = 780x10^{-6} \times \gamma_{RH}$$

ACI formulation is based on a 7-day wet curing duration and no correction is provided for different curing durations. Practically speaking, it is difficult to undertake long-term field curing of concrete.

7.4.1.2 Bazant B3 Model

The Bazant B3 formulation was developed from analytical statistical evaluation (Bazant 1995). Ultimate shrinkage has been calculated based on the type of cement, curing, water content, and 28-day standard strength:

$$\varepsilon_{sh}(t) = \varepsilon_u \cdot k_h \cdot S(t) \qquad (7\text{-}19)$$

Ultimate shrinkage is formulated as follows:

$$\varepsilon_u = \alpha_1 \cdot \alpha_2 \, [26 \, w^{2.1} \cdot \, (f'_c)^{-0.28} + 270] \text{ (in } 10^{-6}) \qquad (7\text{-}20)$$

Shrinkage is a function of cement type (α_1), curing conditions (α_2), water content (w), and 28-day strength (f'_c).

Table 7-15. Coefficients α_1 and α_2 used in Bazant B3 Model

ASTM C 150 type cements	α_1
Type I	1
Type II	0.85
Type III	1.1

Curing coefficient	α_2
Steam cured concretes	0.75
Water cured or RH 100 %	1.0
Sealed specimens	1.2

The component k_h is related to the humidity of the environment, and calculated as follows:

$$k_h = 1 - h^3 \quad (7\text{-}21)$$

The humidity correction is made when the humidity is less than 0.98. For determining swelling of concrete in a relative humidity of 100%, k_h is given as 0.2.

The time function of shrinkage S(t) is a function of concrete age (t), duration of wet cure (t_c), and shrinkage time coefficient (γ_{sh}).

$$S(t) = \tanh\left(\sqrt{\frac{t - t_c}{\gamma_{sh}}}\right) \quad (7\text{-}22)$$

Shrinkage time coefficient γ_{sh} is size dependent as given below:

$$\gamma_{sh} = (k_s \cdot D)^2 \quad (7\text{-}23)$$

where D is the square of two times the volume to exposed-surface ratio as formulated below, and k_s is a cross-section shape factor. For simple members similar to slabs, k_s can be assumed to be 1.

$$D = 4\,(v/s)^2 \quad (7\text{-}24)$$

The formulation incorporates almost all factors affecting shrinkage, but is not suggested for early-age predictions since mathematical approximation includes an intrinsic error for early ages (Bazant 2001).

7.4.1.3 CEB-FIP 90 Model

The European Concrete Committee formulation is one of the most powerful shrinkage prediction formulas (Shah et al. 1996). The formulation of CEB-FIP 90 is as follows:

$$\varepsilon_{sh}(t) = \varepsilon_u \cdot \beta_{RH} \cdot \beta_s(t) \quad (7\text{-}25)$$

This formulation is similar to the Bazant B3 prediction formula. It incorporates an ultimate shrinkage (ε_u) and humidity coefficient (β_{RH}) as well as a time dependent shrinkage function $\beta_s(t)$. In this formulation, ultimate shrinkage is given as follows:

$$\varepsilon_u = \left[160 + 10\,\beta_{sc} \cdot \left(9 - \frac{f'_c}{1450} \right) \right] \cdot 10^{-6} \qquad (7\text{-}26)$$

where β_{sc} is the cement type factor and f'_c is the 28-day strength of concrete.

The cement type factor is established for European cement standards. It is transformed for the ASTM designated cement types as given below:

Table 7-16. Cement Type Coefficient used in CEB-FIP 90 Model

Type of cement	βsc
Low heat development cements (Type II and Type V)	4
Rapid heat development cements Type I and Type III	5

Relative humidity factor is calculated as follows:

$$\beta_{RH} = 1 - \left(\frac{RH}{100} \right)^3 \qquad (7\text{-}27)$$

The time dependent shrinkage function is given as follows:

$$\beta_s(t) = \left[\frac{t - t_c}{350 \left(\frac{h}{3.937} \right)^2 + (t - t_c)} \right]^{0.5} \qquad (7\text{-}28)$$

where t is age of concrete, t_c is duration of wet cure and h is volume to exposed-surface ratio dependent coefficient:

$$h = 2\ v/s \qquad (7\text{-}29)$$

The CEB-FIP formulation is a very accurate method for predicting shrinkage, since the formulation covers almost all factors that may affect shrinkage. The results of this formulation are in close agreement with the Bazant B3 formulation in the long term (Mokarem et al. 2003 and Hani et al. 2003). In addition, the CEB-FIP 90 model is quite accurate for early-age predictions of shrinkage (Hani et al. 2003).

7.4.1.4 Gardner – Lockman Model

The Gardner –Lockman model was proposed in 2001 (Gardner et al. 2001). This prediction model is also known as the Gardner model. Formulation is as follows:

$$\varepsilon_{sh}(t) = \varepsilon_u \, \beta(h) \, \beta_s(t) \tag{7-30}$$

The ultimate shrinkage coefficient (ε_u) is calculated as:

$$\varepsilon_u = 1000 \, K \sqrt{\frac{4350}{f'_c}} \cdot 10^{-6} \tag{7-31}$$

where K is cement type coefficient and f'_c is the concrete mean compressive strength at 28-day, (psi). Cement type coefficient (K) is given in the table below:

Table 7-17. Cement Type Coefficient used in Gardner-Lockman Model

Type of cement	K
Type I	1.00
Type II	0.70
Type III	1.15

Other components are humidity and time coefficients and are formulated below:

$$\beta_h = 1 - 1.18 \left(\frac{h}{100} \right)^4 \tag{7-32}$$

$$\beta_s(t) = \sqrt{\frac{t - t_c}{(t - t_c) + 97 \, (vs)^2}} \tag{7-33}$$

where h is relative humidity, vs is volume to exposed-surface ratio, t is age of concrete, and t_c is duration of wet cure. Recent research on this model indicates that this formulation is useful in estimating shrinkage of concrete containing low heat pozzolans (fly ash, slag, etc) (Mokarem et al. 2003).

7.4.2 Shrinkage and Cracking Relationship

Recent research done by the Virginia DOT on performance of concrete mixes tries to correlate restraint shrinkage and free shrinkage. The concrete mixes were subjected to the same curing conditions and they were measured for restraint and free shrinkage. After the free shrinkage amount exceeded 200 microstrain, the probability of cracking in the restraint shrinkage sample increased. Concrete designs were suggested to limit free shrinkage to reduce the cracking probability (Mokarem et al. 2003).

In order to evaluate effects of curing periods on 28 days of shrinkage for a 9-inch deck concrete, shrinkage calculations were performed as shown in Table 7-18, assuming that 28-day concrete strength is 5000 psi with Type 1 cement and wet cured 2 days, 7 days, and 14 days. The MDOT structural concrete design requires 7 days wet cure. In shrinkage calculations, a relative humidity of 60 % is assumed.

Table 7-18. Predicted Shrinkages for Different Curing Periods

ACI 209 (Microstrain)	**CEB-FIP 90** (Microstrain)	**Bazant B3** (Microstrain)	**Gardner & Lockman** (Microstrain)	**Curing duration (days)**
266	32	27	45	2
234	29	26	41	7
178	23	22	33	14

Using ACI 209 as a benchmark, a free shrinkage of 266 microstrain for 2 day wet cure and 178 microstrain for 7 day wet cure can be calculated. The additional free shrinkage will generate additional stresses due to restraints of girders and/or deck forms. This increase at an early-age is more significant since concrete is immature and has low tensile strength.

The influence of wet curing duration on shrinkage is also shown in Figure 7-12. As seen in Figure 7-12, the duration of wet cure reduces the early-age shrinkage without any change in ultimate shrinkage. The reason for increase in duration of wet curing to help reducing shrinkage cracking is because the tensile strength of concrete will develop with increased concrete maturity; therefore, the stress developed due to shrinkage and associated restraint will not cause cracking.

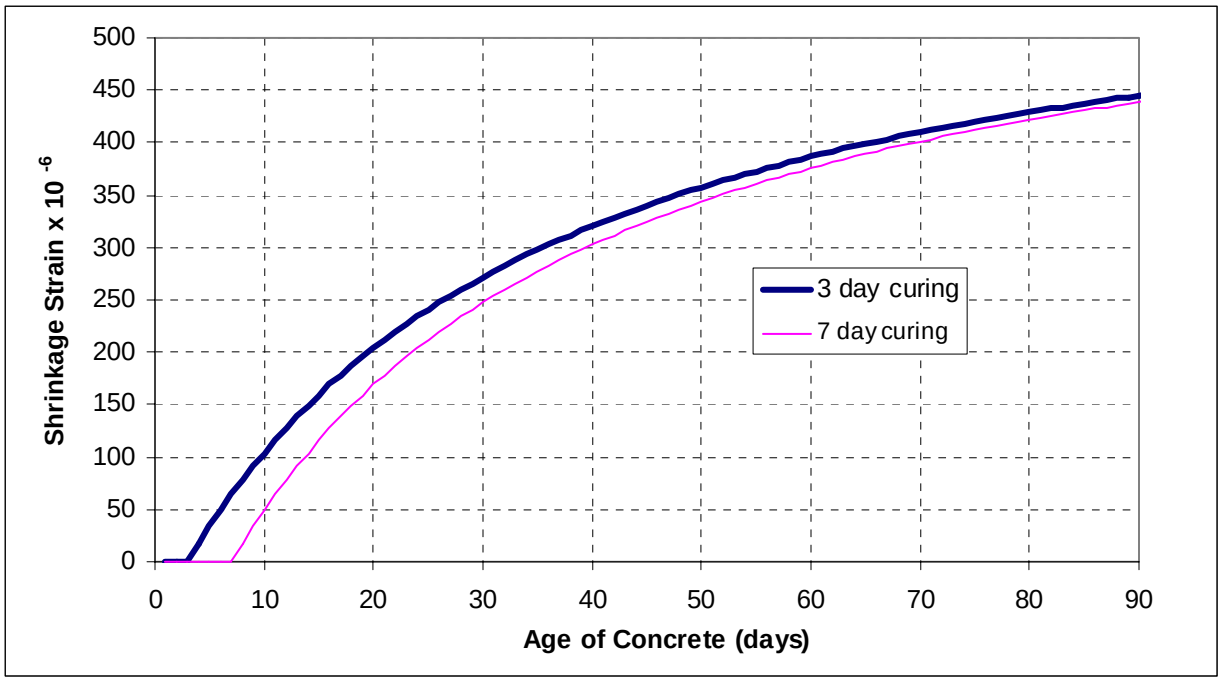

Figure 7-12. Effects of wet curing duration – shrinkage predicted by ACI model

7.5 CONCLUSIONS

The summaries of previous chapters – Literature Review, Multi-State Survey, and Construction Monitoring, point towards a factor that influences early-age cracking of reinforced concrete bridge decks. The primary cause of early-age deck cracking is identified as the volume change due to shrinkage and thermal effects. Volume change in concrete under restraint induces tensile stress. Early-age cracking is identified as the leading cause of other types of distress, and the reduction or prevention of this type of cracking will improve bridge deck service life.

The analysis presented in this research demonstrated that the tensile stress due to early-age thermal load alone can cause deck cracking. Volume change of concrete due to temperature and shrinkage occurs simultaneously. An increase in drying shrinkage due to construction errors and delays in wet cure can increase the tensile stresses. Drying shrinkage, beyond the very early ages, will increase with crack widths that have formed due to thermal loads.

The time concrete reaches peak temperature during hydration depends, among other parameters, on the volume to exposed-surface ratio and the concrete temperature at the time of placement. Volume to exposed-surface ratio of concrete is very small for bridge decks. For small volume to

exposed-surface ratio, the percent absorbed or dissipated heat between concrete and ambient temperatures at the time of placement is very high. In that case, the concrete temperature at the time of placement quickly reaches the ambient temperature. Consequently, the measured concrete temperature before placement does not play a major role in predicting early-age concrete properties. The ambient temperature at the time of concrete placement governs the early-age concrete thermal properties. Based on this finding, the concrete parameters controlling the thermal load are the cement type, content, and fineness, ambient temperature at the time of concrete placement, and the time of inception of curing. These parameters govern the temperature rise in bridge deck concrete during the hydration process. The temperature difference between peak temperature within the concrete mass and the ambient temperature establishes the thermal load on the deck. The thermal load controls the magnitude of the tensile stress developed at the deck. The thermal load depends on the maximum temperature developed within the concrete mass and the ambient temperature at the time of concrete achieving peak temperature. Use of retarders in the concrete mix delays the hydration process. Use of retarders may be an advantage or a drawback depending on the ambient temperature at the time of peak hydration temperature. Today's weather prediction technology can be utilized as a decision tool in using admixtures that can refine the hydration process in order to minimize the thermal load.

Analysis performed with lower cement amounts of 4 and 6 sacks shows that this reduction will reduce thermal load. However, the stresses developed under the reduced thermal load can still exceed the tensile strength of concrete. Further analysis is performed to find out the vulnerability of different girder-deck combinations to early-age bridge deck cracking due to volume change. When standard mix design (grade D) is used, the PCI girder-deck combination has the lowest potential for deck cracking, while the steel girder-deck combination has the highest. Further, increased girder spacing reduces the stress developed at the deck-girder interface due to volume change loads.

8 SUMMARY & CONCLUSIONS

8.1 SUMMARY

The need for this research was based on the observed deck deterioration mechanism that is accelerated by the presence of cracks. The primary objective of this research was to identify the major parameters influencing the cracking of the reinforced concrete (RC) deck. The second objective was to state recommendations to manage these parameters that are within the control of the bridge designer, the materials engineer, the contractor, and/or the maintenance engineer in order to maximize deck life. The project tasks consisted of literature review, nationwide survey on the subject of RC deck cracking, field inspection and data collection of existing RC bridge decks that were replaced within the last five years, monitoring the construction of new decks, laboratory and field testing of concrete samples, and establishing the parameters influencing deck cracking.

8.2 CONCLUSIONS

The results of this research first of all confirmed the observations of the Michigan Department of Transportation engineers that the deck cracks become visible within the first few months of construction. This research established the mechanism by which these cracks form as thermal stresses that develop during the cement hydration process and, in most cases, during the first 12 to 24 hours upon concrete placement. The research recommendations focused on the means of reducing the thermal stresses in order to control deck cracking by development of a project specific concrete mix design that accounts not only for the current ambient temperature but also incorporates the temperature predictions during the next 12 to 24 hours. Thermal effects and its adverse impact are already recognized and certain requirements of current practice like the night placement during summer months are useful practices and should be continued. Naturally, these recommendations will only be effective by full compliance with the Michigan Department of Transportation – Standard Specifications for Construction, especially the requirements related to curing.

A nationwide survey conducted in this research revealed that, transverse cracking is the most prevalent type of cracking observed on the deck. Most of the responding State DOTs emphasized changing the mix design in order to reduce cracking. Of the respondent states, 45%

have been using fly ash and 29% GGBS in their mix design. The most popular type of chemical admixture among the responding State DOTs is air entrainment, which is similar to Michigan's practice. The predominant causes of early-age deck cracking identified by the responding states in the order of significance are as substandard curing, construction practices, and mix design.

The field inspection data generated in this research showed that most bridge decks are cracked. In most cases, the crack widths and density are high enough to dramatically increase the ingress of the aggressive agents into the deck interior, initiate deterioration, and reduce its service life. However, the field inspection data could not identify any operational and design parameters that influence RC deck cracking. These parameters included average daily truck traffic (ADTT) volume, span type (simple or continuous), span length, structure type (steel or prestressed concrete beams), deck thickness, and skew angle.

During the monitoring of construction of decks, it was observed that the Michigan Department of Transportation – Standard Specifications for Construction are often not adhered to. The observed violations that significantly impact the cracking potential of the deck are, in the order of frequency of violation: delays in the start of the wet curing process, lack of sufficient moisture in the burlap during the curing process, and delays in application of the curing compound.

Concrete placement near the construction or expansion joint boundaries was observed to be quite problematic. During the floating process excess concrete overflows the joints, loses its plasticity and is scraped off and thrown in with the deck concrete near the joint. This creates a substandard concrete quality near the joint, which is where deterioration often starts. Continuous concrete placement without construction and expansion joints should be investigated. Joints can be opened by saw cutting upon concrete hardening.

The testing of the concrete samples prepared during the monitoring of the deck construction showed that the concrete properties are approaching high strength with rapid early strength gain. This is a concern because these mixtures generate higher heat of hydration, and increased drying shrinkage. The 28-day concrete strength was measured to be in excess of 6,000 psi, which is considered to be high-strength concrete, and needs to comply with special construction and curing procedures.

It is recommended that the following steps be taken based on these findings:

1. Education of project consultants to ensure the enforcement of the current Michigan Department of Transportation – Standard Specifications for Construction related to RC bridge deck placement. Portions of the Michigan Department of Transportation – Standard Specifications for Construction related to concrete placement, finishing, and curing may be reorganized as describing the requirements in an order starting from the most significant to least significant in terms of its impact on the quality of the hardened concrete.

2. Implementation of measures to control thermal stresses and shrinkage stresses in RC decks. These measures should be decided based upon a comprehensive review of all benefits and drawbacks. The measures should include the reduction and/or substitution of cement with mineral admixtures; re-grading coarse aggregates for reducing mortar volume; and use of current and forecast weather data in optimizing the mix design and placement time. Also, limitations to set-retarding chemical admixtures need to be established so that wet curing can practically be initiated before build-up of thermal load.

3. A further inspection study to cover a large number of existing decks to identify the relative importance of operational parameters influencing deck cracking. This study should use a sample on the order of hundreds to cover the entire state.

9 SUGGESTIONS FOR FUTURE RESEARCH

There are two major recommendations for research that should follow this study. The first recommendation is to undertake an immediate project to develop mix parameters optimized for the reduction of thermal and shrinkage loads. This new study should also include the development of tools that will utilize the current and forecasted climatic data, as well as cement and aggregate properties in order to determine an optimized, project-specific mix design.

The field inspection of twenty bridges could not provide sufficient data to understand the relationship between crack density and bridge skew, span length, and ADTT. It is suggested that a continuation research project be undertaken to investigate these parameters on a much larger sample space, as many as 100 bridge decks.

10 REFERENCES

Abdun-Nur, E.A. (1982). “Incentive specifications for concrete.” *Concrete International*, Vol. 4, No.9, pages 20-24.

Abdun-Nur, E.A. (1982). ”Inspection and quality assurance.” *Concrete International*, Vol. 4, No.9, pages 58-62.

Abel, J., and Hover, K. (1998). “Effect of Water-Cement Ratio on the Early Age Tensile Strength of Concrete.” *TRB Annual Meeting practical papers*.

ACI Committee 211, 211.1-97. (2001). “Standard Practice for Selecting Proportions for Normal, Heavyweight and Mass Concrete.” *ACI Manual of Concrete Practice*, American Concrete Institute, Detroit, Michigan.

ACI Committee 212, 212.3R-91. (2001). “Chemical Admixtures for Concrete.” *ACI Manual of Concrete Practice*, American Concrete Institute, Detroit, Michigan.

ACI Committee 221, 221R-96, (2001). “Guide for Use of Normal Weight and Heavyweight Aggregates in Concrete.” *ACI Manual of Concrete Practice*, American Concrete Institute, Detroit, Michigan.

ACI Committee 223, 223-98. (2001). “Standard Practice for the Use of Shrinkage-Compensating Concrete.” *ACI Manual of Concrete Practice*, American Concrete Institute, Detroit, Michigan.

ACI Committee 224, 224.IR-84. (2001). "Causes, Evaluation and Repair of Cracks in Concrete." *ACI Manual of Concrete Practice*, American Concrete Institute, Detroit, Michigan.

ACI Committee 224, 224.R-01, (2001). “Control of Cracking in Concrete Structures.” *ACI Manual of Concrete Practice*, American Concrete Institute, Detroit, Michigan.

ACI Committee 225, 225R-99. (2001). “Guide to Selection and Use of Hydraulic Cements.” *ACI Manual of Concrete Practice*, American Concrete Institute, Detroit, Michigan.

ACI Committee 226, 226.1R-87. (2001). “Ground Granulated Blast Furnace Slag as a Cementitious Constituent in Concrete.” *ACI Manual of Concrete Practice*, American Concrete Institute, Detroit, Michigan.

ACI Committee 232, 232.2R-96. (2001). “Use of Fly Ash in Concrete.” *ACI Manual of Concrete Practice*, American Concrete Institute, Detroit, Michigan.

ACI Committee 233, 233R-03. (2003). “Slag Cement in Concrete Mortar.” *ACI Manual of Concrete Practice*, American Concrete Institute, Detroit, Michigan.

ACI Committee 234, 234R-96. (2001). “Guide for the Use of Silica Fume in Concrete.” *ACI Manual of Concrete Practice*, American Concrete Institute, Detroit, Michigan.

ACI Committee 308, 308.1-98. (1986). "Standard Specification for Curing Concrete." *ACI Manual of Concrete Practice*, American Concrete Institute, Detroit, Michigan.

Adkins, D. F., and Christiansen, V. T. (1989). "Freeze-Thaw Deterioration of Concrete Pavements." *Journal of Materials in Civil Engineering*, Vol. 1, No. 2, pp. 97-104.

Adkins, D. F., and Merkley, G. P. (1990). "Mathematical Model of Temperature Changes in Concrete Pavements." *Journal of Transportation Engineering*, Vol. 116, Issue 3, pp. 349-358.

Adkins, D. F., Merkley, G. P., and Brito, G. P. (1993). "Mathematics of Concrete Scaling." *Journal of Materials in Civil Engineering*, Vol. 5, Issue 2, pp. 280-288.

Aïtcin, P. C. (2000). "Cements of yesterday and today concrete of tomorrow." *Cement and Concrete Research*, Vol. 30, Issue 9, pp. 1349-1359.

Aitcin, P.C. (2003). “The durability characteristics of high performance concrete: a review.” *Cement and Concrete Composites*, Vol. 25, pp. 409-420.

Akhras, N. M. (1998). "Detecting freezing and thawing damage in concrete using signal energy." *Cement and Concrete Research*, Vol. 28, Issue 9, pp. 1275-1280.

Alampalli, S., and Owens, F. (2000). "Increasing Durability of Concrete Decks Using Class HP Concrete.” *Concrete International*, Vol. 22, Issue 7.

Al-Khaja, W. A. (1997). “Influence of temperature, cement type and level of concrete consolidation on chloride ingress in conventional and high-strength concretes.” *Construction and Building Materials*, Vol. 11, Issue 1, pp. 9-13.

Allan, M.L. (1995). "Probability of corrosion induced cracking in reinforced concrete." *Cement and Concrete Research*, Vol. 25, Issue 6, pp. 1179-1190.

Almusallam, A. A. (2001). "Effect of environmental conditions on the properties of fresh and hardened concrete." *Cement and Concrete Composites*, Vol. 23, Issues 4-5, pp. 353-361.

Almusallam, A. A. (2001). “Effect of environmental conditions on the properties of fresh and hardened concrete.” *Cement and Concrete Composites*, Vol. 23, pp. 353.

Alsayed, S.H. (1998). “Influence of superplasticizer, plasticizers, and silica fume on the drying shrinkage of high strength concrete subjected to hot-dry field conditions.” *Cement and Concrete Research*, Vol. 28, No. 10, pp. 1405–1415.

Altoubat, S. A., and Lange, D. A. (2001). "Creep, Shrinkage, and Cracking of Restrained Concrete at Early Age.” *ACI Materials Journal*, Vol. 98, Issue 4.

Anguelov, P. (1995). “Roller form technology for concrete construction.” *Concrete International*, Vol. 17, Issue 10, pp. 50-54.

ASHRAE Handbook of Fundamentals. Atlanta: American Society of Heating Refrigerating and Air Conditioning Engineers, Inc. 1992.

ASTM C215-97. (1998). “Standard Test Method for Fundamental Transverse, Longitudinal, and Torsional Frequencies of Concrete Specimens.” ASTM International, 100 Barr Harbor Drive, P.O.Box C700, West Conshohocken, Pennsylvania, USA

Babaei, K., and Fouladgar, A. M. (1997). “Solutions to Concrete Bridge Deck Cracking.” *Concrete International*, Vol. 19, No. 7, pp. 34.

Babaei, K., and Hawkins, N. M. (1987). "Evaluation of Bridge Deck Protective Strategies." *NCHRP Report 297*, Transportation Research Board, National Research Council, Washington, D.C.

Banthia, N., Yan, C., and Mindess, S. (1996). "Restrained shrinkage cracking in fiber reinforced concrete: a novel test technique." *Cement and Concrete Research*, Vol. 26, Issue 1, pp. 9-14.

Basheer, P. A. M., Chidiact, S. E., and Long, A. E. (1996). "Predictive model for deterioration of concrete structures." *Construction and Building*, Vol. 10, pp. 27-37.

Bazant, Z. (1995). "Creep and shrinkage prediction model for analysis and design of concrete structures – Model B3." *Materials and Structures*, Vol. 28, pp. 357-365.

Bazant, Z. (2001). "Prediction of creep and shrinkage: past, present and future." *Nuclear Engineering and Design*, Vol. 203, pp. 27-38.

Bentz, D. P., Garbaczi, E. J., Haecker, C. J., and Jensen, O.U.M. (1999). " Effects of cement particle size distribution on performance properties of portland cement based materials." *Cement and Concrete Research*, Vol. 29, pp. 1663-1671.

Bentz, D. P., and Snyder, K. A. (1999). "Protected paste volume in concrete extension to internal curing using saturated lightweight fine aggregate." *Cement and Concrete Research*, Vol. 29, Issue 11, pp. 1863-1867.

Berke, N. S., and Roberts, L. R. (1989). "Use of Concrete Admixtures to Provide Long-Term Durability from Steel Corrosion." *ACI Special Publication (SP-119-20)*, pp.384-403.

Bhal, N.S., and Mital, N.K. (1996). "Effect of relative humidity on creep and shrinkage of concrete." *Indian Concrete Journal*, Vol. 70, pp. 21-27.

Bissonnette, B., Pierre, P., and Pigeon, M. (1999). "Influence of key parameters on drying of cementitious materials." *Cement and Concrete Research*, Vol. 29, pp. 1655-1662.

Bolander, J.E. Jr., and Le, B.D. (1999). "Modeling crack development in reinforced concrete structures under service loading." *Journal of Construction and Building Materials,* Vol. 13, pp. 23-31.

Borrowman, P. E., Seeber, K. E., and Kesler, C. E. (1977). "Behavior of Shrinkage-Compensating Concretes Suitable for use in Bridge Decks." *Department of Theoretical and Applied Mechanics*, University of Illinois, Urbana, Illinois, T. and A.M. Report No. 416.

Boulware, B. L., and Nelson, B. H. (1979). *Factors Affecting the Durability of Concrete Bridge Decks: Shrinkage Compensated Cement Concrete in Bridge Deck.* Interim Report No. 5. California Department of Transportation, FHWA/CA/SD-79/18.

Brozzetti, J. (2000). "Design development of steel-concrete composite bridges in France." *Journal of Constructional Steel Research*, Vol. 55, Issues 1-3, pp. 229-243.

Burke, M. P. Jr. (1999). "Cracking of concrete decks and other problems with integral-type bridges." *Transportation Research Record*, pp. 131.

Cady, P. D., and Carrier, R. E. (1971). *Durability of Bridge Deck-concrete-Part 2: Moisture Content of Bridge Decks*. Final Report. Department of Civil Engineering, Pennsylvania State University.

Cady, P.D., Carrier, R.E., Bakr, T., and Theisen, J. (1971). *Durability of Bridge Decks-Part 1: Effect of Construction Practices on Durability*. Final Report. *Department of Civil Engineering*, Pennsylvania State University.

Cai, H., and Liu, X. (1998). "Freeze-thaw durability of concrete: ice formation process in pores." *Cement and Concrete Research*, Vol. 28, Issue 9, pp. 1281-1287.

Campbell-Allen, D., and Lau, B. (1978). *Cracks in Concrete Bridge Decks*. Research Report R313, Department of Civil Engineering, University of Sydney.

Carlson, R. W. (1940). "Attempts to Measure the Cracking Tendency of Concrete." *Journal of the ACI*, Vol. 36, No. 6, pp.533-540.

Chapman, R. A., and Shah, S. P. (1987). "Early-age bond strength in reinforced concrete." *ACI Materials Journal*, Vol. 84, Issue 6.

Chatterji, S. (1999). "Aspects of freezing process in porous material-water system (Part 2. Freezing and properties of frozen porous materials)." *Cement and Concrete Research*, Vol. 29, Issue 5, pp. 781-784.

Cheng, T. T., and Johnston, D. W. (1985). *Incidence Assessment of Transverse Cracking in Bridge Decks: Construction and Material Considerations*. North Carolina State University, Department of Civil Engineering, Raleigh, North Carolina, FHWA/NC/85-002 Vol. 1.

Committee on the Comparative Costs of Rock Salt and Calcium Magnesium Acetate (CMA) for Highway Deicing, (1991). *Highway Deicing Comparing Salt and Calcium Magnesium Acetate*. NCHRP Special Report 235, Transportation Research Board.

"Concrete Network", (2003). http://woncretenetwork.com/concrete/concreteadmixtures/crack_control.htm.

Costa, A., and Appleton, C. J. (2002). "Case studies of concrete deterioration in a marine environment in Portugal." *Cement and Concrete Composites*, Vol. 24, Issue 1, pp. 169-179.

Coutinho, A. de S. (1959). "The Influence of the Type of Cement on its Cracking Tendency." *RILEM Journal*, New Series No. 5.

Cusick, R.W., and Kesler, C. E. (1980). "Behavior of Shrinkage Compensating Concretes Suitable for Use in Bridge Decks." *ACI Special Publication (SP-64-15)*. American Concrete Institute, Detroit, Michigan, pp.293-310.

Cusson, D., and Repette, W. (2000). "Early-Age Cracking in Reconstructed Concrete Bridge Barrier Walls." *ACI Materials Journal.* Vol. 97, Issue 4.

Cusson, D., and Mailvaganam, N.P. (1999). "Corrosion-inhibiting systems." *Concrete International* , Vol. 21, Issue 8, pp. 41-47.

Dakhil, F. H., Cady, P. D., and Carrier, R. E. (1975). "Cracking of Fresh Concrete as Related to Reinforcement." *Journal of the ACI*, pp. 421-428.

De Schutter, G., and Taerwe, L. (1996). "Estimation of Early-Age Thermal Cracking Tendency of Massive Concrete Elements By Means of Equivalent Thickness." *ACI Materials Journal*, Vol. 93, Issue 5.

Dhir, R.K., Hewlett, P.C., and Dyer, T.D. (1995). " Durability of 'self-cure' concrete." *Cement and Concrete Research*, Vol.25, pp. 1153-1158.

Ding, Y., Kusterle, W. (1999). "Comparative study of steel fiber-reinforced and steel mesh reinforced concrete at early ages panel tests." *Cement and Concrete Research*, Vol.29, issue 11, pp. 1827-1834.

Dry, C. M. (1999). "Repair and prevention of damage due to transverse shrinkage cracks in bridge decks." *Proceedings of SPIE - The International Society for Optical Engineering*, Vol. 3671, pp. 253.

Edwards, D.L. (2000). "HPC on bridges: The Florida experience." *Concrete International*, Vol. 22, Issue 2, pp. 63-65.

EN Committee, prEN 206-1: 2000E. (2000). "Concrete: Specification, performance, production and conformity." European Committee for Standardization, Brussels.

Engelund, S., and Sorensen, J.D. (1998) "A probabilistic model for chloride ingress and initiation of corrosion in reinforced concrete structures." *Structural Safety*, Issue 20, pp. 69-89.

Enright, M. P., and Frangopol, D. M. (1998). "Probabilistic analysis of resistance degradation of reinforced concrete bridge beams under corrosion." *Engineering Structures*, Vol. 20, Issue 11, pp. 960-971.

Forster, S. W. (2000). "HIPERPAV-Guidance to Avoid Early-Age Cracking in Concrete Pavements." *ACI Special Publication*, Vol. 192.

Fouad, F. H., and Furr, H. L. (1986). "Behavior of Portland Cement Mortar in Flexure at Early Ages." *ACI Special Publication (SP-9-5-6)*, American Concrete Institute, Detroit, Michigan, pp. 93-113.

Fowler, D.W. (1999). " Polymers in concrete a vision for the 21st century." *Cement and Concrete Composites*, Vol. 21, pp. 449-452.

Fraczek, J. (1979). "ACI survey of concrete structure errors." *Concrete International*, Vol. 1, Issue 12.

Freidin, C. (1999). "Hydration and strength development of binder on high calcium oil fly ash Part II: Influence of curing conditions on long term stability." *Cement and Concrete Research*, Vol. 29, Issue 11, pp. 1713-1719.

Freidin, C. (2001). "Effect of aggregate on shrinkage crack-resistance of steam cured concrete." *Magazine of Concrete Research*, Vol. 53, pp. 85.

French, C., Eppers, L., Le, Q., and Hajjar, J. (1999). "Transverse Cracking in Bridge Decks." *TRB Annual Meeting practical papers.*

Fu, Z. (1998). "Slipform pavement construction in China." *Concrete International.* Vol. 20, Issue 5, pp. 36-38.

Furr, H. L., and Fouad, F. H. (1982)."Effect of Moving Traffic on Fresh Concrete During Bridge-Deck Widening." *Transportation Research Record 860*, pp. 28-36.

Furtak, K. (1999). "Assessment of crack state in RC slabs of composite bridges." *Archives of Civil Engineering*, Vol. 45, pp. 59.

Gardner, N.J., and Lockman, M.J. (2001). "Design provisions for drying shrinkage and creep of normal strength concrete. " *ACI Materials Journal*, Vol. 98, No.2, pp. 159-167.

Ghaffori, N., and Mathis, R. (1998). "Prediction of Freezing and Thawing Durability of Concrete Paving Blocks." *Journal of Materials in Civil Engineering*, Vol. 10, Issue 1, pp. 45-51.

Gilbert, R. I. (2001). "Shrinkage, Cracking and Deflection- The Serviceability of Concrete Structures." *Electronic Journal of Structural Engineering*, Vol. 1, No. 1, pp. 2-14.

Gilbert, R. I. (1992). "Shrinkage Cracking in Fully Restrained Concrete Members." *ACI Structural Journal*, Vol. 89, No. 2, pp. 141-149.

Gowripalan, N. V., Sirivivatnanon, C., and Lim, C. (2000). "Chloride diffusivity of concrete cracked in flexure." *Cement and Concrete Research*, Vol. 30, Issue 5, pp. 725-730.

Gratton-Bellew, P.E. (1996). "Microstructural investigation of deteriorated Portland Cement concretes." *Construction and Building Materials*, Vol.10, No. 1, pp. 3-16.

Guenot, L., Torrenti, J. M., and Laplante, P. (1996). "Stresses in Early-Age Concrete: Comparison of Different Creep Models." *ACI Materials Journal*, Vol. 93, Issue 3.

Hani, N., Suksawang, N., and Mohammed, M. (2003). "Effects of curing methods on early age and drying shrinkage of high performance concrete." *TRB 2003 Annual meeting CD-Rom*.

Hansen, T. C., and Mattock, A. H. (1966). "Influence of Size and Shape of Member on the Shrinkage and Creep of Concrete." *Journal of the ACI*, Vol. 63. [Also *PCA Development Department Bulletin D103*, Portland Cement Association].

Hanson, J. A., Elstner, R. C., and Clore, R. H. (1973). "The Role of Shrinkage Compensating Cement in Reduction of Cracking of Concrete." *ACI Special Publication (SP-38-12)* American Concrete Institute, Detroit, Michigan, pp. 251-271.

Haque, M.N. (1996). "Strength development and drying shrinkage of high strength concretes." Cement and Concrete Composites, Vol.18, pp. 333-342.

Hawks, N.F., Teng, T.P., Bellinger, W.Y., and Rogers, R.B. (1993). *Distress identification manual for the long term pavement performance project*, Strategic Highway Research Program, SHRP-P-338.

Healy, R. J., and Lawrie, R. A. (1998). "Bridge Cracking: A Dot Experience and Perspective." *Concrete International*, Vol. 20, No. 9, pp. 37-40.

Ho, D. W. S., and Chirgwin, G. J. (1996). "A performance specification for durable concrete." Construction and Building Materials, Volume 10, Issue 5, Pages 375-379.

Ho, D. W. S., and Chirgwin, G. J., and Mak, L.S. (1997). "Water sorptivity of heat cured concrete for bridge structures." *ACI Special Publication (SP-171)*, Paper 3, pp. 97-108.

Hoff, G.C., Bilodeau, A., and Malhotra, M. (2000). "Elevated temperature effects on HSC residual strength." *Concrete International*, Vol. 22, Issue 2, pp. 41-47.

Holley, J.J., Thomas, M.D.A., Hopkins, D.S., Cail, K.M., and Lanctot, M. C. (1999). "Custom HPC mixtures for challenging bridge design." *Concrete International*, Vol. 21, No. 9, pp. 43-48.

Holt, E.E., and Janssen, D. J. (1998). "Influence of Early Age Volume Changes on Long-Term Concrete Shrinkage." *TRB Annual Meeting practical papers*.

Hong, K., and Hooton, R. D. (1999). "Effects of cyclic chloride exposure on penetration of concrete cover." *Cement and Concrete Research*, Vol. 29, Issue 9, pp. 1379-1386.

Hong, K., and Hooton, R. D. (2000). " Effects of fresh water exposure on chloride contaminated concrete." *Cement and Concrete Research*, Vol. 30, pp. 1199-1207.

Horn, M. W., Stewart, C. F., and Boulware, R. L. (1975). *Factors Affecting the Durability of Concrete Bridge Decks*. Construction Practices-Interim Report No. 4. Bridge Department, California Division of Highways, CA-DOT-ST-4104-4-75-3.

Horn, M. W., Stewart, C. F., and Boulware, R. L. (1972). *Webber Creek Deck Crack Study-Final Report*. State of California, Business and Transportation Agency, Department of Public Works, in Cooperation with the FHWA, Research Report CA-HWY-BD-624102 (2)-72-2.

Horn, M. W., Stewart, C. F., and Boulware, R. L. (1972). *Factors Affecting the Durability of Concrete Bridge Decks: Normal vs. Thickened Deck*-Interim Report No. 3. Bridge Department, California Division of Highways, CA-HY-4101-3-72-11.

Hue, F., Serrano, G., and Bolaño, J. A. (2000). "Öresund Bridge. Temperature and cracking control of the deck slab concrete at early ages." *Automation in Construction*, Vol. 9, Issues 5-6, pp. 437-445.

Hughes, B. P., and Mahmood, A. T. (1988). "Laboratory investigation of early thermal cracking of concrete." *ACI Materials Journal*, Vol. 85, Issue 3.

Igarashi, S., Kubo, H.R., and Kawamura, M. (2000). "Long-term volume changes and microcracks formation in high strength mortars." *Cement and Concrete Research*, Vol. 30, pp. 943-951.

Irwin, R. J., and Chamberlin, W. P. (1981). *Performance of Bridge Decks with 3-inch Design Cover*. New York State Dept. of Transportation, Report No. FHWA/NY/RR-81/93.

Issa, M. A. (1999). "Investigation of cracking in concrete bridge decks at early ages." *Journal of Bridge Engineering*, pp. 116.

Issa, M.A., Yousif, A.A., and Issa, M.A. (2000). "Effect of construction loads and vibrations on new concrete bridge decks." *Journal of Bridge Engineering*.

Jacobsen, S., and Sellevold, E.J. (1996). "Self healing of high strength concrete after deterioration by freeze/thaw." *Cement and Concrete Research*, Vol. 26, Issue 1, pp. 55-62.

Jauregui, D.V. (2001). "A field-testing system for experimental bridge evaluation." *Experimental Techniques*, Vol. 25, pp.37.

Jaycox, C.E. (1982). "Guidance in the establishment of an inspection program." *Concrete International*, Vol. 4, No. 9, pp. 79-83.

Jeknavorian, A., and Barry, E. F. (1999). "Determination of durability-enhancing admixtures in concrete by thermal desorption and pyrolysis gas chromatography-mass spectrometry." *Cement and Concrete Research*, Vol. 29, Issue 6, pp. 899-907.

Jensen, O. M., and Hansen, P. F. (1999). "Influence of temperature on autogenous deformation and relative humidity change in hardening cement paste." *Cement and Concrete Research*, Vol. 29, Issue 4, pp. 567-575.

Jones, M. R., Dhir, R. K., and Gill, J. P. (1995). "Concrete surface treatment: effect of exposure temperature on chloride diffusion resistance." *Cement and Concrete Research*, Vol. 25, Issue 1, pp. 197-208.

Jovall, O. (2001). "Avoiding early age cracking." *Concrete Engineering International*, Vol. 5, pp. 41.

Kawamura, M. K., and Nakamura, H. (2001). "Development of a bridge management system for existing bridges." *Advances in Engineering Software*, Vol. 32, Issues 10-11, pp. 821-833.

Khan, M. S. (1991). "Corrosion state of reinforcing steel in concrete at early ages." *ACI Materials Journal*, Vol. 88, Issue 1.

Kheder, G. F., Al Rawi, R. S., and Al Dhahi, J. K. (1994). "Study of the behavior of volume change cracking in base-restraint concrete walls." *ACI Materials Journal*, Vol. 91, Issue 2.

Kim, J. K., and Lee, C. S. (1998). "Prediction of differential drying shrinkage in concrete." *Cement and Concrete Research*, Vol. 28, Issue 7, pp. 985-994.

Kmita, A. (2000). "A new generation of concrete in civil engineering." *Journal of Materials Processing Technology*, Vol.106, pp. 80-86.

Kosel, H. C., and Michois, K. A. (1985). "Evaluation of Concrete Deck Cracking for Selected Bridge Deck Structures of the Ohio Turnpike, Report to Ohio Turnpike Commission." *Construction Technology Laboratories (CTL)*.

Kovler, K. (1995). "Shock of evaporative cooling of concrete in hot dry climates." *Concrete International*, Vol. 17, Issue 10, pp. 65-69.

Kraii, P. (1985). "A Proposed Test to Determine the Cracking Potential Due to Drying Shrinkage of Concrete." *Concrete Construction*, Vol. 30, No. 9, pp. 775-779.

Krauss, P.D. (2003). "Practical considerations for materials selection for cracking avoidance." Presentation in meeting # 113, TRB 2003, Washington.

Krauss, P. D., and Rogalla, E.A. (1996). *Transverse Cracking in Newly Constructed Bridge Decks.* NCHRP Report No. 380. Washington, D.C.

Ksomatka, S. H., and Panarese, W. C. (1990). *Design and Control of Concrete Mixtures*. Edition 13, *Portland Cement Association*.

Kumaat, E., and Lorrain, M. (1996). "Cracking of plain or reinforced high performance concrete slabs." *International Journal of Structures*, Vol. 16, pp. 1.

Kwak, H. G., and Seo, Y. J. (2002). "Shrinkage cracking at interior supports of continuous pre-cast pre-stressed concrete girder bridges." *Construction and Building Materials*, Vol. 16, pp. 35.

Kwak, H. G., Seo, Y. J., and Jung, C. M. (2000). "Effects of the slab casting sequences and the drying shrinkage of concrete slabs on the short-term and long-term behavior of composite steel box girder bridges, Part 2." *Engineering Structures*, Vol. 22, pp. 1467.

La Fraugh, R. W., and Perenchio, W. F. (1989). *Phase I Report of Bridge Deck Cracking Study West Seattle Bridge.* Wiss, Janney, Elstner Associates, Report No. 890716.

Lebet, J. P., and Ducret, J.M. (1998). "Experimental and theoretical study of the behavior of composite bridges during construction." *Proceedings of the 1998 2nd World Conference on Steel in Construction*, Journal of Constructional Steel Research.

Lerch, W. (1957). "Plastic Shrinkage." *Journal of the ACI*, Vol. 53, No. 2, pp. 803-802.

Li, Z., Qi, M., and Ma, B. (1999). "Crack Width of High-Performance Concrete Due to Restrained Shrinkage." *Journal of Materials in Civil Engineering*, Vol. 11, Issue 3, pp. 214-223.

Liang, M. T., Wang, K. L., and Liang, C. H. (1999). "Service life prediction of reinforced concrete structures." *Cement and Concrete Research*, Vol. 29, Issue 9, pp. 1411-1418.

Long, E., Henderson, G. D., and Montgomery, F. R. (2001). "Why assess the properties of near-surface concrete?." *Construction and Building Materials*, Vol. 15, Issues 2-3, pp. 65-79.

Lou, Z., Gunaratne, M., Lu, J. J., and Dietrich, B. (2001). "Application of a Neural Network Model to Forecast Short-Term Pavement Crack Condition: Florida Case Study." *Journal of Infrastructure Systems*, Vol. 7, Issue 4, pp. 166-171.

Lower, D. O. (1980). "Summary Report on Type K Shrinkage-Compensating Concrete Bridge Deck Installations in the State of Ohio." *ACI Special Publication (SP-64-10*), American Concrete Institute, Detroit, Michigan, pp. 181-192.

Lykke, S., Skotting, E., and Kjaer, U. (2000). "Prediction and Control of Early-Age Cracking: Experiences From the Oresund Tunnel." *Concrete International*, Vol. 22, Issue 9.

Malhotra, V.M., and Hemmings, R.T. (1995). "Blended Cements in North America – A Review." *Cement and Concrete Research*, Issue 17, pp. 23-35.

Manning, D. G. (1981). "Effect of Traffic-induced Vibrations on Bridge Deck Repairs." *NCHRP Synthesis 86*, Transportation Research Board, National Research Council. Washington, D.C.

Mayer, C.W. (1982). "Quality control by the contractor." *Concrete International*, Vol. 4, No. 9, pp. 72-74.

Mc Connell, V. (1999). "Composites make progress in reinforcing concrete." Reinforced Plastics, July/August, pp. 40-46.

McDonald, J. E. (1992). "The Potential for Cracking of Silica-Fume Concrete." *Concrete Construction*.

Mehta, P. K. (1986). *Concrete Structure, Properties, and materials.* Prentice Hall, New Jersey.

Meyers, C. (1982). "Survey of Cracking on Underside of Classes B-1 and B-2 Concrete Bridge Decks in District 4." Investigation 82-2, Missouri Highway and Transportation Department, Division of Materials and Research.

Mietz, J., and Isecke, B. (1996). "Monitoring of concrete structures with respect to rebar corrosion." *Construction and Building Materials*, Vol. 10, Issue 5, pp. 367-373.

Mohamed, O. A., Rens, K. L., and Stalnaker, J. J. (2000). "Factors Affecting Resistance of Concrete to Freezing and Thawing Damage." *Journal of Materials in Civil Engineering*, Vol. 12, Issue 1, pp. 26-32.

Mokarem, D.W. (2002). *Development of concrete shrinkage performance specifications*. Ph. D. Dissertation, Virginia Polytechnic Institute and State University.

Mokarem, D.W., Weyers, R.E., and Lane, D.S. (2003). "Development of Portland cement concrete shrinkage performance specifications." *TRB 2003 Annual meeting CD-Rom.*

Montemor, M.F., Cunha, M.P., Ferreira, M.G., and Simoes, A.M. (2002). "Corrosion behavior of rebars in fly ash mortar exposed to carbon dioxide and chlorides." *Cement and Concrete Composites*, Vol. 24, pp. 45-53.

Nagi, M., Janssen, D., and Whiting, D. (1994). "Durability of concrete for early opening of repaired highways--Field evaluation." *ACI Special Publication (SP-145)*, Volume 145.

Naik, T. R., Shiw, S. S., and Hossain, M. M. (1995). "Properties of high performance concrete systems incorporating large amounts of high-lime fly ash." *Construction and Building Materials*, Vol. 9, Issue 4, pp. 195-204.

Nehdi, M. (2001). "Ternary and Quaternary Cements for Sustainable Development." *Concrete International*, Vol. 23, Issue 04.

Neville, A.M. (2000). "The question of concrete durability: We can make good concrete today." *Concrete International*, Vol. 22, Issue 7, pp. 21-26.

Neville, A.M. (1999). "Specifying concrete for slipforming." *Concrete International,* Vol. 21, Issue 11, pp. 61-63.

Neville, A.M. (1995*). Properties of concrete*. Longman Group, 4th edition.

Nishida, N., Ushioda, K., Dobashi, Y., and Matsui, K. (1995). "Evaluation of thermal cracking index in slab-concrete under uncertain parameters." *Transactions of the Japan Concrete Institute*, Vol. 17, pp. 127.

Nmai, C. K. (1998). "Cold Weather Concreting Admixtures." *Cement and Concrete Composites*, Vol. 20, Issues 2-3, pp. 121-128.

Nmai, C., Tomita, R., Hondo, F., and Buffenbarger, J. (1998). "Shrinkage-Reducing Admixtures." *Concrete International*, Vol. 20, Issue 4.

Ohama, Y., Demura, K., Satoh, Y., Tachibana, K., and Miyazaki, Y. (1989). "Development of Admixtures for Highly Durable Concrete." *ACI Special Publication (SP-119-17)*, pp. 321-342.

Osretgoard, L., Lange, D.A., Altaubat, S.A., and Stang, H. (2001). "Tensile basic creep of early-age concrete under constant load." *Cement and Concrete Research*, Vol. 31, Issue 12, pp. 1895-1899.

Ozyildirim, C., and, Lane, D.S. "Investigation of self leveling concrete." TRB 2003 Annual meeting Proceedings.

"PCA-concrete basics." (2003). http://www.portcement.org/cb/concretebasics_concretebasics.asp, (June 12, 2003).

Pedeferri, P. (1996). "Cathodic protection and cathodic prevention." *Construction and Building Materials*, Vol. 10, No. 5, pp. 391-402.

Perfetti, G. R., Johnson, D. W., and Bingham, W. L. (1985). "Incidence Assessment of Transverse Cracking in Concrete Bridge Decks." *Structural Consideration*, FHWA/NC/85-002 Vol. 2.

Perragaux, G. R., and Brewster, D. R. (1992). *In-Service Performance of Epoxy-Coated Steel Reinforcement in Bridge Decks-Final Repor*t. New York State Dept. of Transportation Technical Report 92-3.

Pettersson, D., and Thelandersson, S. (2001). "Crack development in concrete structures due to imposed strains - Part I: Modelling." *Materials and Structures/Material Constructions*, Vol. 34, pp. 7.

Pheeraphan, T., and Leung, C. K. Y. (1997). "Freeze-thaw durability of microwave cured air-entrained concrete." *Cement and Concrete Research*, Vol. 27, Issue 3, pp. 427-435.

Phelan, W.S. (2000). "Admixtures and aggregates: Key elements of athletic concrete." *Concrete International*, Vol. 22, Issue 4, pp. 35-39.

Phillips, M.V., Ramey, G.E., and Pittman, D.W. (1997). "Bridge deck construction using Type K cement." *Journal of Bridge engineering*.

Popovic, P., Rewerts, T. L., and Sheahen, D. J. (1988). "Deck Cracking Investigation of the Hope Memorial Bridge." *Ohio Department of Transportation*.

Portland Cement Association, (1970). *Final Report-Durability of Concrete Bridge Deck--A Co-operative Study*.

Purvis, R. L. (1989). "Prevention of Cracks in Concrete Bridge Decks." *Wilbur Smith Associates,* Report on Work in Progress.

Ramakrishnan, V., and Mc Donald, C.N. (1997). "Durability evaluations and performance histories of projects using polyolefin fiber reinforced concrete." *ACI Special Publication 170*, paper 35, pp. 665-680.

Ramey, G. E., Stallings, J. M., and Oliver, R. S. (1999). "Cracking damage/deterioration and rehabilitation considerations of some Birmingham, Alabama, Interstate bridge decks." *Transportation Research Record,* pp. 33.

Randall, F. A. (1980). "Field Study of Shrinkage Compensating Cement Concrete." *ACI Special Publication (SP-64-13),* American Concrete Institute, Detroit, Michigan, pp. 239-257.

Rawi, R. S. A., and Kheder, G. F. (1990). "Control of Cracking Due to Volume Change in Base-Restrained Concrete Members." *ACI Structural Journal*, Vol. 87, No. 4, pp. 397-405.

Razek, M. M. A., and Enein, S. A. A. (1999). "Moisture performance through fresh concrete at different environmental conditions." *Cement and Concrete Research*. 29, 1819-1825.

Redston, J. (1999). “Canada’s infrastructure benefits from FRP.” Reinforced Plastics, July/August, pp. 33-34.

Reed, R. C. (1993). "Cracking--An early warning of structural problems." *Concrete International*, Vol. 15, Issue 9.

Reis, E. E. Jr., Mozer, J. D., Bianchini, A. C., and Kesler, C.E. (1964). “Causes and Control of Cracking in Concrete Reinforced with High Strength Steel Bars-A Review of Research.” *T. & A.M.* Report No. 261, Department of Theoretical and Applied Mechanics, University of Illinois, Urbana, Illinois.

Rhodes, C. C. (1950). “Curing Concrete Pavements with Membranes.” *Journal of the ACI*, Vol. 57, No. 12, pp. 277-295.

Rhodes, J.A., and Carreira, D. (1997). “Prediction of creep, shrinkage, and temperature effects in concrete structures.” *ACI Manual of Concrete Practice*, Vol. 1, Report 209-R.

Rixom, R., and Mailvaganam, N. (1999). *Chemical admixtures for concrete*, Third Edition, E & FN Spon, London, England.

Rixom, R., and Mailvaganam, N. (1999). *Chemical admixtures for concrete*, Routledge, Newyork.

Ronneberg, H, (1989). “Use of chemical admixtures in concrete platforms.” *ACI Special Publication 119*, paper 27, pp. 517-533.

Rostam, S. (1996). "High performance concrete cover--why it is needed, and how to achieve it in practice." Construction and Building Materials, Volume 10, Issue 5, Pages 407-421.

Russell, H. G. (1980). "Performance of Shrinkage-Compensating Concretes in Slabs." *ACI Special Publication (SP-65-6),* American Concrete Institute, Detroit, Michigan, pp. 81-114.

Sabir, B. B. (1997). "Mechanical Properties and Frost Resistance of Silica Fume Concrete." *Cement and Concrete Composites*, Vol. 19, Issue 4, pp. 285-294.

Samman, T.A., Mirza, W.H., and Wafa, F.F. (1996). “Plastic shrinkage cracking of normal and high strength concrete: a comparative study.” *ACI Material Journal*, Vol. 93, pp. 36-40.

Samples, L.M., and Ramirez, J.A. (2000). “Field investigation of concrete bridge decks in Indiana.” *Concrete International*, Vol. 22, Issue 2, pp. 53-56.

Schiessl, P. (1996). "Durability of reinforced concrete structures." *Construction and Building Materials*, Vol. 10, Issue 5, pp. 289-292.

Schmitt, T.R., and Dawin, D. (1999). “Effect of material properties on cracking in bridge decks.” *Journal of Bridge Engineering*.

Sellevlod, E. J. (1996). "High-performance concrete: early age cracking, pore structure, and durability." *ACI Special Publication (SP-159),* Vol. 159.

Shaeles, C.A. (1988). “Influence of mix proportions and construction operations on plastic shrinkage cracking in thin slabs.” *ACI Material Journal*, Vol. 85, pp. 495-504.

Shah, S. P., Marikunte, S., Yang, W., and Aldea, C. (1996). “Control of cracking with shrinkage-reducing admixtures.” *Transportation Research Record*, pp. 25.

Shah, S. P., Weiss, W. J,. and Yang, W. (1998). “Shrinkage cracking - can it be prevented?” *Concrete International*, Vol. 20, pp. 51.

Shah S.P., and Ahmad S.H. (1994). *High performance concretes and applications*, Great Britain.

Shi, Z., and Nakano, M. (2001). “Application of a 3-D crack analysis model to RC cantilever decks of excessive cracking.” *Structural Engineering and Mechanics*, Vol. 12, pp.377.

Shihata, S. A., and Baghdadi, Z. A. (2001). "Simplified Method to Assess Freeze-Thaw Durability of Soil Cement." *Journal of Materials in Civil Engineering*, Vol. 13, Issue 4, pp. 243-247.

Shilstone, J. M. Jr., and Shilstone, J. M. (2002). “Performance based concrete mixtures and specifications for today.” *Concrete International*, Vol. 24, Issue 2, pp. 80-83.

Siebel, E. (1989). “Air-void characteristics and freezing and thawing resistance of superplasticized air entrained concrete with high workability.” *ACI Special Publication 119*, paper 16, pp. 297-319.

Simonsen, E., Janoo, V. C., and Isacsson, U. (1997). "Prediction of Pavement Response during Freezing and Thawing Using Finite Element Approach." *Journal of Cold Regions Engineering*, Vol. 11, Issue 4, pp. 308-324.

Smith, J.L., and Virmani, Y.P. (2000). *Materials and methods for corrosion control of reinforced and prestressed concrete structures in new construction*, LTTP publication No: 00-091.

Spellman, D. L., Woodstrom, J. H., and Baily, S. N. (1973). “Evaluation of Shrinkage Compensated Cement.” Materials and Research Department, California Division of Highways, CA-HY-MR-5216-1-73-15.

Stewart, M.G., and Rosowsky, D.V. (1998). “ Time dependent reliability of deteriorating reinforced concrete bridge decks.” *Structural Safety*, Vol. 20, pp. 91-109.

Stewart, C. F., and Gunderson, B. J. (1969). “ Factors Affecting the Durability of Concrete Bridge Decks-Interim Report #2.” Report by the Research and Development Section of the Bridge Department, State of California.

Suh, Y., and McCullough, B. F. (1994). “Factors affecting crack width of continuously reinforced concrete pavement.” *Transportation Research Record*, pp. 134.

Sun, W., Zhang, Y. M., Yan, H. D., and Mu, R. (1999). "Damage and damage resistance of high strength concrete under the action of load and freeze-thaw cycles." *Cement and Concrete Research*, Vol. 29, Issue 9, pp. 1519-1523.

Swamy, R.N. (1997). ”Design for durability and strength through the use of fly ash and slag in concrete.” *ACI Special Publication 171*, paper 1, pages 1-72.

Swamy, R.N. (1989). “Super plasticizers and concrete durability.” *ACI Special Publication 119*, article 19, pages 363-382.

Tamtsia, B.T., and Beaudain, J.J. (2000). “Basic tensile creep of hardened cement paste, a reexamination of the role of the water.” *Cement and Concrete Research*, Vol. 30, pp. 1465-1475.

Tang, T., Zollinger, D. G., and Yoo, R. H. (1993). "Fracture toughness of concrete at early ages." *ACI Materials Journal*, Vol. 90, Issue 5.

Tay, D. C. K., and Tam, C. T. (1996). "In situ investigation of the strength of deteriorated concrete." *Construction and Building Materials*, Vol. 10, Issue 1, pp. 17-26.

Taylor, H.F.W. (1990). *Cement Chemistry*, Academic Press Ltd, London, England.

Toutanji, H. A. (1999). “Durability characteristics of concrete columns confined with advanced composite materials.” *Composite Structures*, Vol. 44, pp 155-161.

Ulm, F. J., and Coussy, O. (2001). "What is a 'Massive' Concrete Structure at Early Ages? Some Dimensional Arguments." *Journal of Engineering Mechanics*, Vol. 127, Issue 5, pp. 512-522.

Uzzafar, R. (1992). "Influence of cement composition on concrete durability." *ACI Materials Journal*, Vol. 89, Issue 6.

Van der Veen, C., Koenders, E. A. B., and Kaptijn, N. (1996). “Thermal cracking in a cantilever bridge made of HSC.” *Computing in Civil Engineering (New York)*, pp. 892.

Wang K., Jansen D., and Shah, S.P. (1997), “Permeability of cracked concrete.” *Cement and Concrete Research*, Vol.27, No.3, pp. 381-393.

Wang, Q., Zhang, T., and Zhao, G. (2001). “Analysis of biaxial bending of reinforced concrete slabs with simply support under concentrated loads.” *Journal of Dalian University of Technology*, Dalian Ligong Daxue Xuebao, Vol. 41, pp. 481.

Weiss, W. J., Yang, W., and Shah, S. P. (2000). "Factors Influencing Durability and Early-Age Cracking in High-Strength Concrete Structures." *ACI Special Publication*, Vol. 189.

Whiting, D., and Schmitt, J. (1989). “A model for deicer scaling resistance of field concretes containing high-range water reducers.” *ACI Special Publication 119*, paper 18, pp. 343-359.

Wiegrink, K., Marikunte, S., and Shah, S. (1996). "Shrinkage cracking of high strength concrete." *ACI Materials Journal*, Vol. 93, Issue 5, pp. 409-415.

Wong, G.S., Alexander, A.M., Haskins, R., Poole, T.S., Malone, P.G., and Wakeley, L. (2001). *Portland Cement concrete rheology and workability – Final report*, FHWA report (FHWA-RD-00-025).

Wood, J. G. M., and Crerar, J. (1997). "Tay road bridge: analysis of chloride ingress variability & prediction of long-term deterioration." *Construction and Building Materials*, Vol. 11, Issue 4, pp. 249-254.

Xu, Y., and Chung, D.D.L. (2000), "Reducing the drying shrinkage of cement paste by admixture surface treatments." *Cement and Concrete researches*, Vol. 30, pp. 241-245.

Xu, Y., and Chung, D.D.L. (2000), "Improving silica fume cement by Silane." Cement and Concrete Research, Vol. 25, pp1305-1311.

Zhou, Y., Cohen, M. D., and Dolch, W. L. (1995). "Effect of external loads on the frost-resistant properties of mortar with and without silica fume." *ACI Materials Journal*, Vol. 91, Issue 6.